Dexterous Mechanical Systems for Intuitive Telemanipulation in Minimally Invasive Surgery

THÈSE Nº 5689 (2013)

PRÉSENTÉE LE

À L'ÉCOLE POLYTECHNIQUE FÉDÉRALE DE LAUSANNE

FACULTÉ DES SCIENCES ET TECHNIQUES DE L'INGÉNIEUR

LABORATOIRE DE SYSTÈMES ROBOTIQUES 1

À L'INSTITUTO SUPERIOR TECNICO (IST) DA UNIVERSIDADE TÉCNICA DE LISBOA

INSTITUTO DE SISTEMAS E ROBÓTICA

PROGRAMME DOCTORAL EN SYSTÈMES DE PRODUCTION ET ROBOTIQUE

POUR L'OBTENTION DU GRADE DE DOCTEUR ÈS SCIENCES

PAR

Ricardo Daniel Rita Beira

EPFL
ÉCOLE POLYTECHNIQUE
FÉDÉRALE DE LAUSANNE

Contents

Abstract

Major progress in abdominal surgery has occurred over the last decades with the introduction of laparoscopic and minimally invasive techniques in the operating room. These innovative procedures attracted much attention due to several advantages: the need for smaller abdominal incisions, resulting in faster recovery of the patient, improved cosmetics, shorter hospitalization and a significant reduction of costs. However, surgical instrumentation for this type of intervention remains still non-intuitive and much more difficult to use than tools for open surgical procedures. As a consequence, these minimally invasive techniques are limited to fairly simple procedures.

Due to the landscape of medical reimbursement, there is a substantial push by insurance companies, health care organizations and hospitals to extend minimally invasive techniques to a wider range of surgical procedures in order to reduce hospital stays and therefore costs. In order to respond to these demands, a strong research effort has been made over the past years on the development of enabling minimally invasive technologies, mainly through the introduction and development of robotic systems. Surgical robots significantly contribute to the improvement of the surgical performance by increasing the dexterity and user-friendliness of surgical procedures through the use of robotic telemanipulation. However, despite years of research, the field of surgical robotics is still only at the beginning of a very promising large scale development. Although a large number of systems have been developed, several issues are not yet addressed, limiting the adoption of surgical robots by a broader range of hospitals.

A major limitation is related to the lack of internal dexterity, caused by the mobility constraints imposed by the small entry port. On one hand, it is important to increase the dexterity of the end-effectors inside the body, overcoming the issues of limited manoeuvrability in the abdominal cavity. On the other hand, the system must be introduced through conventional trocars. The management of this trade-off is extremely challenging, making the development of dexterous micro-manipulators one of the most important issues in the field of robotic systems for surgery.

Another limitation is that the current surgical robots are voluminous, competing for precious space within the operating room and significantly increasing the complexity of operating room logistics. Access to the patient is thus impaired, which raises safety concerns. Furthermore, due to the physical separation from the operating area and lack of force-feedback on the existing surgical systems, surgeons cannot feel the contact forces between instruments and tissue. This limitation may cause long operating times and unintentional damage of tissue and suturing material.

Although bringing several technical advantages for surgeons, current robotic systems are extremely expensive in acquisition, maintenance, disposable tools and training, representing much higher direct costs compared with open surgery and laparoscopic instrumentation. For this reason, access to robotic surgery is limited to a minority of hospitals that can afford to

purchase it and have enough patient volume to justify the acquisition. This tendency towards centralisation of complex minimally invasive surgeries draws patients from hospitals without surgical robots and places a significant burden on the health care system.

This thesis investigates novel mechanical systems to be used in different surgical telemanipulators, solving the limitations of existing robotic and manual surgical equipment. Firstly, in the area of patient safety, by providing the surgeon with more compact systems, secondly, in the area of surgical dexterity, by providing new multi-DOF micro-manipulators, which can deliver complex kinematics to remote and narrow places, and finally, in the area of health care cost, by providing a new telemanipulator that is able to deliver dexterous manipulations, as current robotic systems, but through a more affordable technology.

These objectives implied not only an investigation of technical aspects such as the performance requirements of surgical tools, but also the investigation of the different medical procedures and surgical tasks used by doctors during minimally invasive interventions.

Although, the solutions studied in this thesis have been applied in the context of surgical systems for MIS, the outcome of this research can be extended to several other application fields. From a general perspective, the ultimate goal of this thesis is to propose a document which may be useful and inspiring for machine designers, developers, or scientists who wish to create efficient remotely controlled manipulators for several applications involving multi-DOF manipulations.

Keywords– minimally invasive surgery, surgical robotics, telemanipulator, mechanical system, cable-driven system

1 Introduction

1.1 Medical Background

The field of abdominal surgery has been progressing strongly over the last thirty years with the continuous introduction of new techniques and tools. Conventional open surgery has been the reference technique, requiring the use of a fairly large incision to allow an effective access to the operating field, Figure 1-1. This large incision, which can go up to 300 mm (Delaney et al., 2005), enables the surgeon to have a direct view of the patient anatomy as well as a direct contact with the tissue. The introduction of simple surgical instruments, such as knives, scissors, graspers and retractors, is also permitted, making possible a precise performance of the different surgical tasks. Surgeons are able to use their hands, working together in the most natural area of their manual workspace, allowing natural hand-eye coordination (Sung and Gill, 2001). For delicate surgical actions, it is even possible to increase the stability and precision of the task by supporting the wrists and elbows on the patient body or on an armrest designed for this purpose (Rosen et al., 2010).
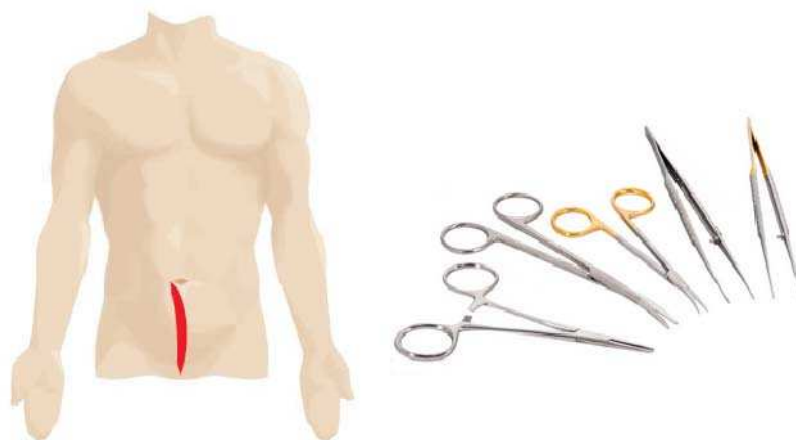
Figure 1-1: Example of an open surgical procedure: a large abdominal incision for the patient but a straightforward and intuitive access for the surgeon. (image from Intuitive Surgical Inc.(2012))

However, with open surgery, and due to the extremely large dimensions of the incision, the post operatory effects of the wound are often considerable. Bleeding, discomfort, long recovery time and high costs are some of the consequences of this highly invasive surgical approach (Williams et al., 1993). Besides these clinical disadvantages, open surgery also generate inferior cosmetically outcomes, characterized by long visible scars.

In order to reduce the invasiveness of open surgical procedures, Minimally Invasive Surgery (MIS) has been introduced in a variety of procedures (Moorthy et al., 2004). One of these MIS procedures is the so called Laparoscopic Surgery (LS) that is performed in the abdominal

cavity. It requires three to six small incisions of about 5 to 15 mm, for the insertion of different surgical instruments and endoscopic miniature cameras into the abdominal cavity (Jacobs et al., 1991). The surgeon and the assistants look at an external monitor where a picture of the internal abdomen is displayed while rigid surgical instruments are inserted through the other incisions, Fig. 1.2. These instruments differ from conventional open surgery tools in that the working end is separated from its handle by an approximately 30 cm long and 5-13 larger diameter shaft (Berguer, 1998). Space for the surgery is obtained by inflating the abdomen with CO_2 gas (Jacobs et al., 1991). The endoscopic camera and the instruments are inserted through trocars (plastic or metal cannulas) with airtight sealing. This solution prevents leaking of the CO_2 gas through the incisions and protects the tissue in the incision area. Figure 1-2 shows the LS approach with the surgical tools operating.
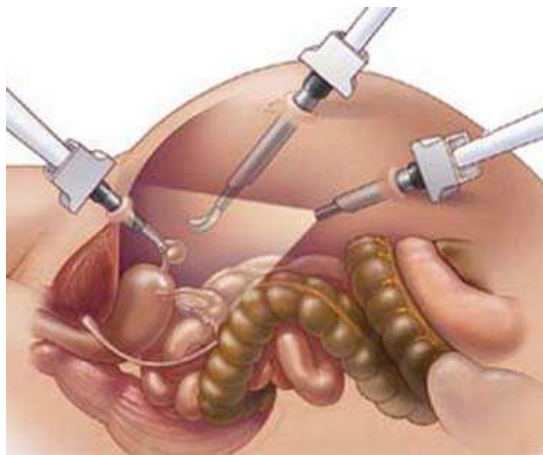
Figure 1-2: Example of a laparoscopic surgical procedure: multi small incisions for the patient but an indirect and not intuitive access for the surgeon. (image from Nucleus Medical Media, Inc.(2009))

The benefits of MIS are numerous. In comparison with traditional surgery, the patient's discomfort, surgical trauma, aesthetical outcomes, and potential complications occurring after surgery are dramatically reduced (Perissat et al., 1992). Moreover, the time a patient has to stay in the hospital and the rehabilitation period are shortened. Consequently, both direct health care costs and indirect costs, in lost worker productivity, can be lowered (Bailey et al., 1991).

Despite such advantages, there has recently been a request from patients asking for a further reduction in the invasiveness of laparoscopy (Hagen et al., 2010), which would result in a decrease in the number of incisions and consequently in the number of visible scars. One of the most recent trends to achieve this goal is called Single Incision Laparoscopic Surgery (SILS) (Chamberlain and Sakpal, 2009). This technique consists of getting access to the peritoneal cavity using a single skin incision, Figure 1-3. However, SILS introduces even more technical constraints than LS (Curcillo 2nd et al., 2009). For instance, surgeons are required to use adapted laparoscopic instruments which are not intuitive to use and lack of suitable dexterity. As a result, these issues make the implementation of this approach extremely difficult (Filipović Čugura et al., 2008).
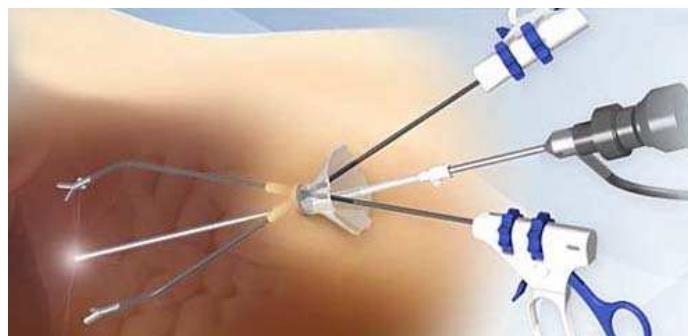
Figure 1-3: Current single-incision configuration of laparoscopic instruments (image from www.sw.org)

The great majority of SILS procedures currently performed is carried out through the umbilicus with penetration of the abdominal wall, by the umbilical midline. However, such an approach can lead to a deformed umbilicus, whose integrity and appearance is considered to be extremely important for many patients (Dini and Ferreira, 2007, Barbosa et al., 2008) and to an increased rate of incision hernias after the procedure (Montz et al., 1994).

Due to these presumed disadvantages, a novel approach to enter into the abdominal cavity for SILS has been developed. Subcutaneous surgical tunnelling (SST) disconnects the skin incision from the entrance of the peritoneal cavity through the abdominal wall (Hagen et al., 2010). Therefore, the skin incision can be placed in almost any cosmetically favourable location of the body such as the supra-pubic hair, groin, axillae or previous (Figure 1-4). Then, a subcutaneous tunnel is formed to enter the peritoneal cavity through the abdominal wall at a mechanically favourable location, such as the rectal muscle to decrease the risk of incision hernias.
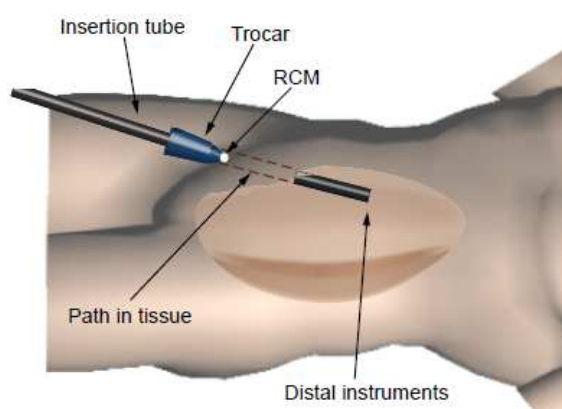
Figure 1-4: Subcutaneous Surgical Tunnelling, SST, procedure, where the surgical instrument reaches the peritoneal cavity, from the incision point, through the abdominal wall (Beira et al., 2011a)

The flexibility of this method of access makes it possible to theoretically customize each incision to the specifics of each patient, regarding existing scars, cosmetic preferences and individual weak areas of the abdominal wall. In addition, having the MIS instruments inserted close to a horizontal orientation allows an easy access to different quadrants of the abdomen, decreasing significantly the total operating time.

There are several theoretical benefits of the SST approach, including the potential for reducing pain, blood loss, recovery time, hospital stays and medical costs (Chamberlain and Sakpal, 2009). However, this technique hasn't yet demonstrated a clear economic or clinical benefit beyond improved cosmesis [Gettman2008]. The surgical community is questioning the safety of these procedures and whether an improved cosmetic deserves the cost of new equipment, extended operating room (OR) time, and added risk potential (Gettman et al., 2008).

In spite of the debate, a scarless approach continues to be the ultimate goal of surgery and there has been an increasing research effort to develop new rigid and flexible endoscopic technologies for SILS, SST and LS, trying to fill a technological gap that is evident for this kind of procedures.

1.2 Challenges of MIS

While MIS is now standard for simple procedures, the use of these techniques for complex surgeries is still being performed only in a few excellence centres worldwide (Gettman et al., 2008). Surgical equipment for this kind of operations remains non-ergonomic and much more difficult to use than tools for open surgery. In addition, the use of these techniques requires more skills from surgeons (Chamberlain and Sakpal, 2009). This fact becomes even more critical for SST where tools are basically adaptations of LS equipment (Filipović Čugura et al., 2008).

Due in part to the landscape of medical reimbursement, there is a substantial push by insurance companies, health maintenance organizations and hospitals to extend MIS to a wider range of surgical procedures (Canes et al., 2008). The major goal is to reduce hospital stays and therefore costs. In addition, recoveries are typically faster and less painful, which is an essential aspect to be considered for the patient (Canes et al., 2008).

In order to respond to these demands and technological challenges, medical device companies and research institutions have been racing over the past years to enable minimally invasive technologies for MIS, through the design of both manual and robotic systems.

1.3 Manual Surgical Equipment

MIS procedures demand a notorious technological investment in terms of engineering. Regular equipment do not respond to the requirements for complex surgeries. In order to propose alternatives and solutions, it is important to mention some of the existing limitations in the current manual equipment for MIS, which are pointed out beneath (Canes et al., 2008, Gettman et al., 2008, Guo et al., 2008, Kaouk et al., 2008, Rao et al., 2008, Chamberlain and Sakpal, 2009, Hong et al., 2009):

- A single access point creates problems with clashing of instruments inside the patient as well as crowding and clashing of cords, scopes, and instruments outside the patient.
- A fixed port also means a potentially longer distance to the surgical site requiring longer endoscopes and adapted instrumentation to perform surgery.
- Long instruments make it difficult to achieve angles to reach certain areas in the abdominal cavity, such as the lower abdomen and pelvis.
- Limited range of motion and triangulating difficulties due to multiple trocars location result in difficult grasping, cutting, dissecting, and suturing tissues.
- The insertion line of the camera is usually not aligned with the natural axis of the surgeon's eyes, which causes the operation area and the instruments tips to be seen from a different direction, Figure 1-5.
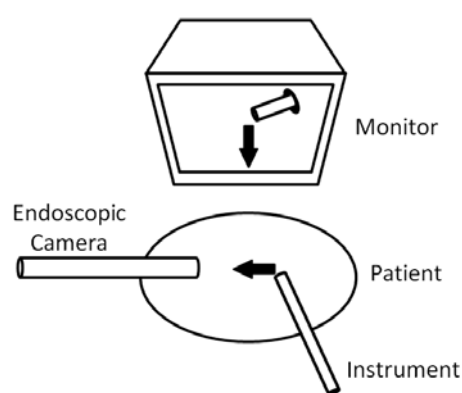
Figure 1-5: Disturbed hand-eye coordination due to misalignment of the natural view axis of the surgeon's eye and the view direction of the endoscopic camera

- The monitor on which the images are presented is usually not positioned in the surgeon's natural direction of view but on a trolley next to the patient, so that the surgeon has to look up and to the side to view the monitor, Figure 1-6.

6

Figure 1-6: Disturbed hand-eye coordination due to misalignment of the natural view axis of the surgeon's eye and the view direction of the monitor. (image from World Laparoscopy Hospital (2012))

- The long and straight endoscopic instruments force the surgeons to work in a non-ergonomic posture for hands, arms and body.
- The entry incision acts as a point of rotation - the fulcrum effect. Consequently, the freedom of positioning the instruments is reduced from 6 DOF, to 4 DOF and the movements of the surgeon's hand about this incision are mirrored and scaled relative to the instrument tip, Figure 1-7.
- Surgeon's ability to feel the interaction with the tissue is lost because there is no contact between hands and tissue anymore.
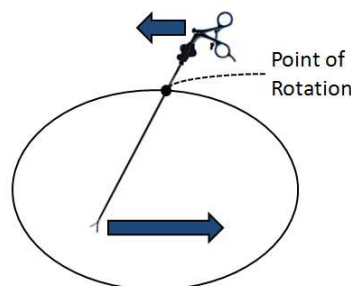
Figure 1-7: Disturbed hand-eye coordination because hand movements are mirrored and scaled relatively to the point of rotation

These equipment limitations significantly disturb the hand-eye coordination and complicate the surgical procedure, increasing the learning curve required to use MIS. Despite surgeons' considerable skill and ability to work within those constraints, the expansion of MIS remains limited due to the indirect way of instrument manipulation (Canes et al., 2008). One of the most effective ways to give back to surgeons the intuitive manipulation is through robotic solutions, due to their increased dexterity and ergonomy (Sackier and Wang, 1994).

1.4   Robotic Surgical Equipment

Over the last years, surgeons have been provided with robotic solutions to overcome some of the disadvantages of manual instrumentation for MIS [Kaouk2009]. The robotic approach significantly contributes to the improvement of the surgical performance by improving the dexterity and user-friendliness in the surgical procedures through the use of robotic telemanipulators. Although a wide range of surgical robotic devices have been developed (Sackier and Wang, 1994, Zemiti et al., 2004) the only commercial systems that have already been used in human surgery are the *da Vinci System*, by Intuitive Surgical (Madhani et al., 1998) and *ZEUS*, by Computer Motion.

Surgical robotic systems consist of three main components: (1) a computer controller, (2) a surgeon's interface device (master) and (3) specially designed instruments attached to robotic arms, with extra degrees of freedom (slave) (Madhani et al., 1998).

In order to visualize this surgical frame, surgeons can sit before the console looking at the surgical field in a right ergonomic position. The surgeon fingers engage the master controls in such a way that hands and wrists are in a natural position relative to the eyes and in line with the surgeon's point of view. The surgeon looks virtually at his own hands holding the instruments, like controlling instruments for open surgery, Figure 1-8. As a result, these systems can provide to surgeons several advantages like an ergonomic position, natural hand-eye coordination, wrist dexterity and stereoscopic visual feedback, making feasible the execution of complex surgical tasks by minimally invasive techniques (Madhani et al., 1998).

Figure 1-8: The Da Vinci Robotic System (image from Intuitive Surgical Inc.(2010))

However, despite years of research and the high potential of some systems, the field of surgical robotics is still only at the beginning of a very promising large scale development. Although a large number of robotic manipulators have been developed (Taylor and Jayne, 2007), some issues are not yet addressed, limiting a broader adoption of robotic systems by the majority of the hospitals. In this way, five major lines for improvements can be identified:

1. Surgical instruments should be provided with additional endoscopic degrees of freedom to increase their internal dexterity and facilitate the execution of precise surgical tasks inside the abdominal cavity;

2. The slave units should be more compact, enabling the patient to be easily reached in case of a surgical emergency and the platform to be easily moved and stored within the operating room;

3. Force feedback should be provided to surgeons, restoring their sense of touch to improve safety, reduce cognitive load and speed-up the procedure;

4. The time required to set-up such systems should be reduced;

5. The costs of acquisition, maintenance, disposable tools and training should be reduced.

While the nature of the three first points is essentially technical, the two last limitations have a significant economic impact in today's surgical landscape.

Although bringing several technical advantages for surgeons, current robotic surgical systems are extremely expensive in acquisition, maintenance, disposable tools and training, representing much higher direct costs compared with open surgery and laparoscopic instrumentation (Camberlin et al., 2009). For this reason, access to Robotic Surgery is limited to a minority of hospitals that (a) can afford to purchase it and (b) have enough patient volume to justify its acquisition. This tendency towards centralisation of complex minimally invasive surgeries draws patients from hospitals without the da Vinci robot and places an additional burden on the health care system. In addition, these systems require a considerable amount of OR time for the setting-up procedures. However, due to the presence of costly personnel and equipment, it is extremely important to reduce OR time to reduce costs.

1.5 Objectives and Approach

The research work developed on this thesis was motivated by the study of new mechanical systems to be used in different surgical telemanipulators, solving the limitations of existing surgical robots, analyzed on the previous section. These objectives implied not only an investigation of technical aspects such as the performance requirements of surgical tools, but also the investigation of the different medical procedures and surgical tasks used by doctors during minimally invasive operations.

This work have been applied and demonstrated in the design of three different surgical systems for minimally invasive procedures: (1) a positioning manipulator for surgical instruments, (2) a high dexterity endoscopic micro-manipulator and (3) a mechanical telemanipulator for the remote control of surgical tools. While the two first show superior performances in terms of dexterity and compactness, the third mechanical system is able to increase the force feedback of new surgical devices while decreasing their cost.

The systems (1) and (2) were integrated in the design of a new surgical platform for SST, consisting in one of the first attempts to develop a robotic device to perform surgical procedures by this recent minimally invasive technique. As shown in Figure 1-9, this SST Platform consists on a robotic telemanipulator, where the user can control an endoscopic slave manipulator by using a remotely located master manipulator. The goal is to bring bi-manual manipulation and standard surgical procedures inside the abdominal cavity, creating the illusion to surgeons that they are directly performing open surgery inside the body of the

patient. By reaching this goal, this platform is able to overcome some of the most critical limitations of existing surgical robots, being extremely compact (due to the use of system (1)), having increased internal dexterity (due to the use of system (2)) and being able to provide force-feedback to the surgeon ((due to the use of system (2)).
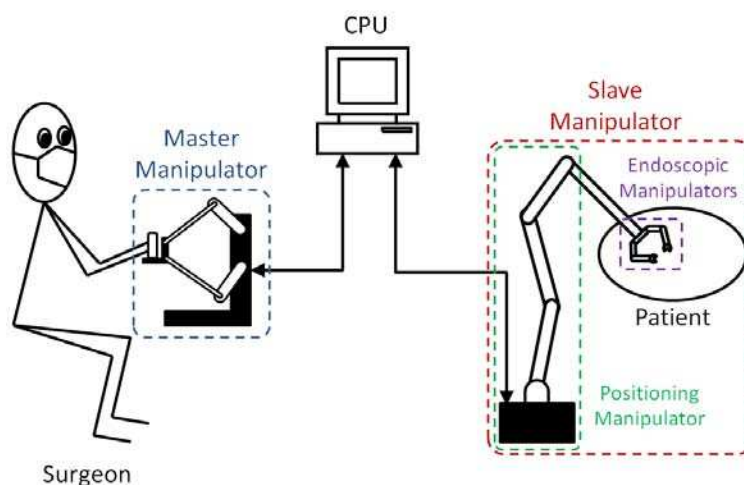
Figure 1-9: Architecture of the SST Platform, where the movements of the surgeon, applied on a master manipulator, are replicated by two endoscopic manipulators, inside the patient's abdominal cavity

The Slave Manipulator of this SST Platform is mainly composed by systems (1) and (2). The endoscopic unit (system (2)) is composed by two Endoscopic Manipulators, conceived to increase the dexterity of the Slave Manipulator inside the patient's body. Their requirements in terms of size, dexterity, force and precision, are beyond the existing state of the art. The external positioning unit (system (1)) consists in a Positioning Manipulator, whose purpose is to move the Endoscopic Manipulators inside the abdominal cavity of the patient, whose new kinematics respects the constraints imposed by the incision point.

System (3) enabled the development of a new surgical platform for laparoscopic surgery, with improved technical and medical performances (Figure 1-10). It consists of fully mechanical teleoperated device, whose kinematics allows surgeons to reach high dexterity levels inside the abdominal cavity of the patient, while respecting the constraints imposed by the incision point. In addition, the low inertia of its moving elements and the low-friction of its mechanical transmission are able to provide backlash and ripple-free movements, with force-feedback and motion scaling, giving to the surgeon a realistic rendering of the forces at the distal instruments. The use of a fully mechanical technology makes it considerably more affordable to produce than existing robotic platforms. It will also allow a reduction in the operating room time by being faster to set-up. These cost-reduction features increase the relevance of this system in today's surgical devices landscape.
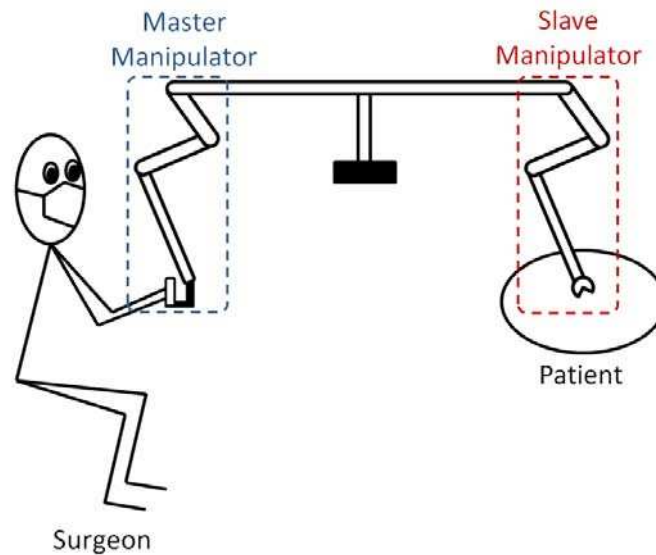
Figure 1-10: Architecture of the new laparoscopic platform, composed by a fully mechanical telemanipulator, composed by a master and a slave units

Although, the solutions studied on this thesis have been applied in the context of three surgical systems for MIS, the outcome of this research can be extended to several other application fields. From a general perspective, the ultimate goal of this thesis is to propose a document which may be useful and inspiring for machine designers, developers, or scientists who wish to create efficient and adapted remotely controlled manipulators for several applications involving multi-dof operations.

In the frame of this work, two journal papers have been published (Beira et al., 2011a, Beira et al., 2011b) and four patent applications filed, covering the technical solutions studied in this thesis. A new start-up company, DistalMotion Sàrl (www.distalmotion.com), has also been created to further develop and commercialize a novel surgical device using the mechanical systems developed here.

1.6 Thesis Outline

This thesis is structured as follows:

Chapter 1 introduces the context in which the present work was developed. A short survey on current trends in the MIS field is presented and the different types of existing surgical tools and devices are presented together with the main challenges. The aims of the thesis, its originalities and the scientific contributions are also stated.

Chapter 2 presents a state of the art of existing surgical robotic systems. Their technical features are analyzed and their key limitations are identified.

Chapter 3 presents the most important medical and technical requirements for a surgical device, being subsequently used to provide guidelines for the design of high performance

surgical systems. Then, the general concepts of the surgical platforms in which the thesis work is applied are presented.

Chapter 4 presents the development and analysis of a new external positioning manipulator, to be used on SST platforms. The description of the related geometry and constraints is presented, manipulator's mobility is analyzed and both inverse and direct kinematics are solved. A symbolic form for the Jacobian matrix is derived, the workspace is studied and the singular configurations are identified. A dynamic analysis is performed and the required maximum speed and maximum torque of the actuators are obtained for a set of typical trajectories to choose the most appropriate actuators. Finally, a working prototype of the system is presented.

Chapter 5 introduces the new micro-mechanical manipulator that will enable the design of high performance miniature endoscopic manipulators. The advantages and disadvantages of several different design possibilities are enumerated and the conceptual development of the system is shown. The geometrical modeling of the system is derived, taking into account the cable topology of the system, and the definition of several dimensional values of extreme importance for the realization of this specific kind of systems. The relationships between applied actuator torques and exerted forces are also analyzed, having in mind the coupling effect of the multi-DOF cable driven transmission. This chapter also presents the developed and realization of a three-DOF-prototype that serves as a case study to validate the novel manipulator concept.

Chapter 6 presents the design considerations and concept generation of a new fully mechanical telemanipulator system that is able to deliver dexterous manipulations to remote and narrow places, like the human abdominal cavity. The development of its mechanical transmission is analyzed and its specific kinematic model is discussed. The realization of a working prototype is presented, which is used to validate the system concept.

Chapter 7 concludes this work, summarizes the results and presents future work directions.

2 State of the Art

2.1 Master-Slave Telemanipulators

Over the last decades, robotic technology has been progressively employed, as a mean to overcome the difficult working conditions during MIS procedures, caused by the non-intuitive and non-ergonomic instrumentation. Currently, the majority of the robotic systems for surgery do not have any kind of autonomy, being controlled by surgeons as a surgical instrument. Most of the surgical robotic systems share the same general concept, providing a continuous exchange of movements between the user and the surgical instruments inside the body. This kind of systems, where a manipulator has the control over other manipulator is often referred as a master-slave system (Cui et al., 2003). Telemanipulation is a scheme in which a slave manipulator, which is usually in a remote environment, tracks the motion of a master manipulator (Cui et al., 2003).

Surgical telemanipulation is developing along a similar path to robotic telemanipulation. In the 1940s and 1950s, Goertz (Goertz, 1952) developed mechanical telemanipulators for the manipulation of highly radioactive materials (Figure 2-1). Goertz's remote manipulators, at first purely mechanical devices, restored the full six degrees of motion freedom to the operator and provided force feedback through the steel ribbon links.
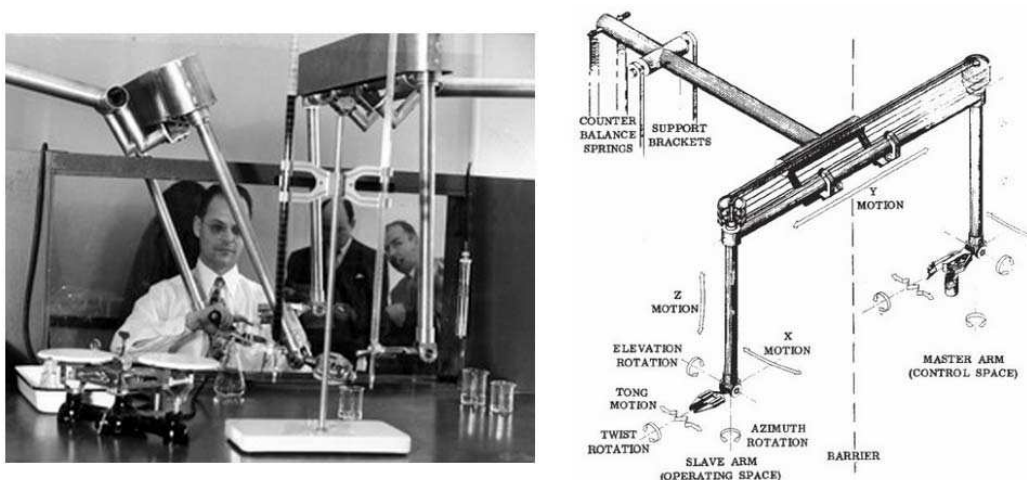
Figure 2-1: Mechanical telemanipulators for radioactive materials (Goertz, 1952)

Goertz's manipulators were soon made electronic (Goertz and Thompson, 1954), and in the 1980s Bejczy and others (Bejczy and Salisbury Jr, 1983) used emerging minicomputer technology to generalize the control system to enable kinematically different devices to be

used for master and slave. These systems were the direct precursors of today's telesurgery systems.

2.2 Surgical Robotic Systems

The first surgical telerobot system was developed at SRI International under the *DARPA Advanced Combat Casualty Care Program* in the early 1990s (Green et al., 1991). This system was designed for open surgery with two 6-DOF manipulators coupled with a stereo vision system.

Nowadays, the most famous system for robotic surgery is the da Vinci, by *Intuitive Surgical* (Guthart and Salisbury Jr, 2000). The device includes a master, a computer controller and four robotic arms: one for the camera; and three (hand driven), carrying surgical tools, Figure .The surgical platform adopts cable drives to actuate tools, providing overall 6 DOF inside the body and 1 DOF for the tool actuation. The overall performances of the system are fairly good, enabling the performance of several minimally invasive surgical procedures worldwide.

Figure 2-2: The Da Vinci Robotic System from Intuitive Surgical Inc.(2010) (image from Intuitive Surgical Inc.(2010))

However, despite all these advantages, some issues are not yet addressed, limiting the wide adoption of robotic systems in by the majority of the hospitals. In an attempt to solve these limitations, several research groups and producers are developing robotic systems for a wide variety of surgical interventions. In this section, some of the most relevant teleoperated surgical robotic systems are presented.

The Amadeus Composer™, shown in Figure 2-3, from the Canadian company Titan Medical Inc. (2011) is about to enter the market, being a potential competitor to the da Vinci system. Little is known about this system as the new-born company is putting huge efforts to protect its intellectual property. The robot has four slave arms with seven DOF each, including the distal instrument, and its master console, is composed of two haptic devices that are very similar to Quanser's five-DOF Haptic Wand (Quanser, 2011). The company is putting huge

efforts to protect its intellectual property and claims that the system will provide force feedback and more dexterity than the da Vinci system.

Figure 2-3: The Amadeus Composer™ from Titan Medical Inc. (2011)

The *Zeus System*, by *Computer Motion*, is also a dual-handed teleoperated surgical system for MIS (Ghodoussi et al., 2002). Its multi-axis positioning system moves an endoscopic tool and also actuates grasping and tool-roll motions. Three DOFs of translation are provided to the tool by a relatively compact positioning manipulator, which positions the proximal end of the tool module for both manipulation and adaptation to the entry port location, Figure 2-4. Its "MicroWrist" robotic instruments have fewer DOF than Da Vinci with only 1 DOF moving the grasper by a cable drive mechanism (Faust et al., 2007). The wrist yaw actuator is located in a small cylindrical module at the proximal end of the tool. Grasping actuation is applied to an internal pushrod via a tool interface at the end of the external positioning arm through a movable tongue on the tool shaft. Following the fusion between *Computer Motion* and *Intuitive Surgical*, the ZEUS robot is no longer produced.

Figure 2-4: The Zeus Surgical System (Faust et al., 2007)

The Raven Surgical Robot is a cable actuated surgical manipulator designed to perform both MIS and open surgery, developed by a multidisciplinary team of engineers from the University of Washington and the University of California-Santa Cruz (Lum et al., 2009). As

shown in Figure 2-5, the slave robot is composed by manipulators with seven DOF, being teleoperated by a remotely located surgeon's console, with two master-input devices. An upgrade of this system, the RAVEN II, was developed to be an open source platform and is now used by several American laboratories for research purposes.

Figure 2-5: The Raven Surgical Robot from the University of Washington and the University of California-Santa Cruz (Lum et al., 2009)

The Miro Surge Robot was developed at the German Aerospace Research Establishment (DLR) (Seibold et al., 2005). The end-effectors of its slave robot, called Mica instruments, can provide 3 degrees of freedom inside the patient body (Kübler et al., 2005) and integrate a six-DOF force sensor in the wrist, Figure 2-6. The surgeon's console features two sigma.7 haptic devices able to provide force feedback in seven DOF (Force Dimension, 2011).

Figure 2-6: Miro Surge Robot with Sigma7 Haptic Interface (Hagn et al., 2010)

The Sofie Surgical Robot was developed at Technische Universiteit Eindhoven (TU/e) for abdominal and thoracic minimally invasive applications. As shown in Figure 2-7, it is much more compact than the da Vinci System and can render the instrument-organ interaction forces to the surgeon (van den Bedem, 2010). Its surgeon's console is bimanual and can render four DOF of force feedback.

Figure 2-7: The Sofie Surgical Robot from TU/e (van den Bedem, 2010)

At Technische Universiteit Eindhoven (TU/e), another system was developed for vitreo-retinal eye surgery, Figure 2-8. It is called Eye-Robot and is composed by two compact and lightweight slave manipulators, which are directly attached to the patient's bed (Hendrix, 2011). The interchangeable surgical instruments can be easily clipped on the slave manipulators that integrate six-DOF force sensors (Nano 17, ATI Industrial Automation Inc., NC, USA) to measure the forces that will then be rendered to the surgeon. The surgeon's console is the same as the previously described Sofie Surgical Robot.

Figure 2-8: The Eye-robot from TU/e (Hendrix, 2011)

The *RAMS System* (Robot-Assisted Micro-Surgery) has been developed to exploit NASA telerobotics technology in a beneficial commercial application, Figure 2-9. At the *Jet Porpolsion Lab*, a precision cable-driven master-and-slave telerobotic system has been developed for eye surgery (Schenker et al., 1995). The system provides scaled-down human-input motions, tremor filtering to improve precision, amplified force-feedback to the human operator, and programmable constrained motion of the instrument in the eye to minimize surgical impacts. The slave robot, which manipulates a tool in the eye, has 6 actuated degrees of freedom (DOFs), 6-DOF tip-force sensing, and 15-micron positioning accuracy (Schenker et al., 1995). However, there is a major drawback in term of dexterity, since the used cable transmission can only be applied to actuate joints with parallel axis, which limits its use for complex kinematics.
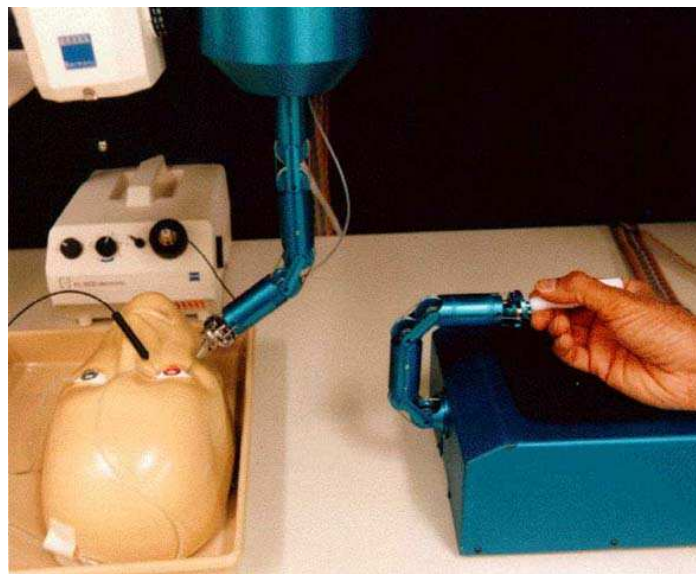
Figure 2-9: RAMS master and slave manipulators (Schenker et al., 1995)

A system to perform endonasal skull surgery was developed at the University of Vanderbilt, Figure 2-10. This system uses tentacle-like concentric-tube continuum robots as tool shafts (Burgner et al., 2011). These tentacles have diameters comparable to surgical needles and are made of precurved concentric tubes made of superelastic nitinol. The path of the tubes inside the patient can be controlled by axially rotating and translating each tube at its proximal base. In total, this system is able to provide six DOF to position and orientate the instrument introduced through the tubes. The master console is composed of two Phantom Omni devices (Sensable Technologies, 2011).

Figure 2-10: Surgical Robot from Vanderbilt University (Burgner et al., 2011)

The NeuroArm Robot (Figure 2-11) was one of the first attempts to perform the first image-guided robotic neurosurgery to remove a brain tumor (Neuroarm Project, 2008). It was developed at University of Calgary and is the world's first MRI-compatible, image-guided surgical robot. It is composed by two manipulators, whose kinematics are similar to the SCARA-Arm. and by a surgeon's console that can provide force feedback in three DOF (Sutherland et al., 2003).
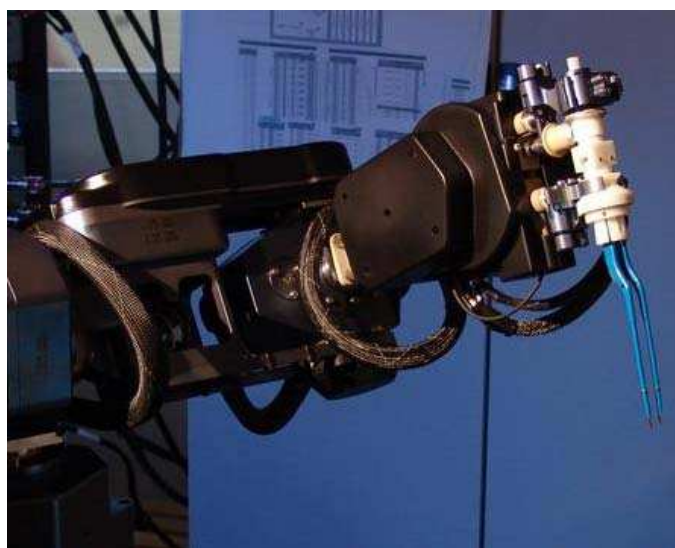
Figure 2-11: The NeuroArm Robot from the University of Calgary (Sutherland et al., 2003)

The Sensei Robotic Catheter is a surgical robot developed to enhance a surgeon's ability to perform complex operations using a small flexible tube called a catheter, Figure 2-12. It is FDA-approved and commercially produced and distributed by Hansen Medical Inc. This system was designed for cardiovascular procedures, having a master-slave architecture in which a slave robotic catheter is teleoperated by the surgeon through a haptic interface called Instinctive Motion Controller. The distal extremity of the catheter is able to measure the forces of contact with the tissue.

Figure 2-12: The Sensei Robotic Catheter from Hansen Medical Inc with Sigma7 Haptic Interface

The main features of the surgical robotic systems presented in this chapter are summarized in Table 2.1.

Table 2.1: Summary of current Teleoperated Surgical Robotic Systems

Surgical System	Slave Manipulator			Target Surgery	Ref.
	DOF (per arm)	Kinematics	Transmission		
daVinci Surgical System	7 (3 internal)	Serial	Cable-driven	MIS Abdominal, thoracic and urologic surgery	(Intuitive Surgical Inc., 2010)
ZEUS	6 (2 internal)	Serial (SCARA-like)	Direct actuation + Cable-driven	MIS Abdominal, thoracic and urologic surgery	(Faust et al., 2007)
Sensei Robotic Catheter	7	Continuum	Cable-driven	Catheter based cardiovascular procedures	(Hansen Medical Inc., 2011)
NeuroArm	8 (including instrument)	Serial (SCARA-like)	Direct actuation	Microneurosurgery and stereotaxy	(Sutherland et al., 2003)
Amadeus Composer	8 (including instrument)	Serial	Direct actuation + Cable-driven	MIS Abdominal and thoracic surgery	(Titan Medical Inc., 2011)

RAMS	6 (external)	Serial	Cable-driven	Brain, eye, ear, face and hand microsurgery	(NASA, 2011)
Miro Surge	7 (3 internal)	Serial	Direct actuation + Cable-driven	MIS Abdominal and thoracic surgery	(Hagn et al., 2010)
Eye-Robot	5 (1 internal)	Serial	Direct actuation	Vitreo-retinal eye surgery	(Hendrix, 2011)
Sofie-Robot	7	Serial	Direct actuation + Cable-driven	MIS Abdominal and thoracic surgery	(van den Bedem, 2010)
Endonasal Robot	7 (including instrument)	Continuum	Remote actuation with flexible tubes	MIS endonasal skull base surgery	(Burgner et al., 2011)
RAVEN	7 (3 internal)	Serial	Cable-driven	MIS Abdominal and thoracic surgery	(Lum et al., 2009)

2.3 Conclusions

All these robotic systems for minimally invasive surgery can provide to surgeons several advantages like an ergonomic position, natural hand-eye coordination, wrist dexterity and stereoscopic visual feedback. However, despite all those advantages, some issues are not yet addressed, limiting a broader adoption of robotic systems by the majority of the hospitals. In this way, some major lines for improvements can be identified:

1. Surgical instruments should be provided with additional degrees of freedom to increase their internal dexterity and facilitate the execution of precise surgical tasks, as well as, extend the access to different organs;
2. The slave unit should more compact, enabling the patient to be easily reached if something goes wrong and the platform to be easily moved and stored within the operating room;
3. Force feedback should be provided, restoring the surgeon's sense of touch to improve safety and increase telepresence during surgery;
4. The time required to set-up the device should be reduced;
5. The costs of acquisition, maintenance, disposable tools and training should be reduced.

In the next chapter, the most important medical and technical requirements for high performance surgical telemanipulators will be presented. They will be used to provide

guidelines for the development of new mechanical systems able to overcome the limitations of current minimally invasive surgical equipment.

3 Requirements for MIS Manipulators

3.1 Introduction

Based on a review of the literature, validated by the collaboration with the *Visceral Surgical Department* of the *University Hospital of Geneva*, HUG, this chapter aims to formulate the design goals for general MIS manipulators, driving the design of new surgical systems to overcome the main limitations of existing surgical devices.

3.2 Kinematic Requirements

The mechanical design is a key phase in the development of MIS robotic manipulators. At this stage, a set of MIS concerns, e.g. safety, accuracy, ergonomics, and dexterity, has to be transformed into several design considerations, like mechanism kinematics, workspace, dimensions, etc, to satisfy the surgical requirements. Consequently, these mechanical design considerations will constitute a set of special design challenges for MIS robots.

3.2.1 Manipulation Mobility

Generally, an MIS instrument comprises a long and narrow tube that is operated on its proximal extremity by the surgeon's hand, in traditional MIS, or by a robotic manipulator, in robotically assisted MIS. The surgical instrument is then inserted in the patient's body through a small incision to perform different surgical operations at the instrument tip.

This arrangement thus constitutes a motion constraint to the MIS instrument, responsible for the "fulcrum effect" at the entry point. As a consequence, the instrument can have only four DOFs for manipulation, which are composed by pan–tilt–spin rotations centered at the entry point for angular orientation and axial translation for depth of penetration (Figure 1-1).
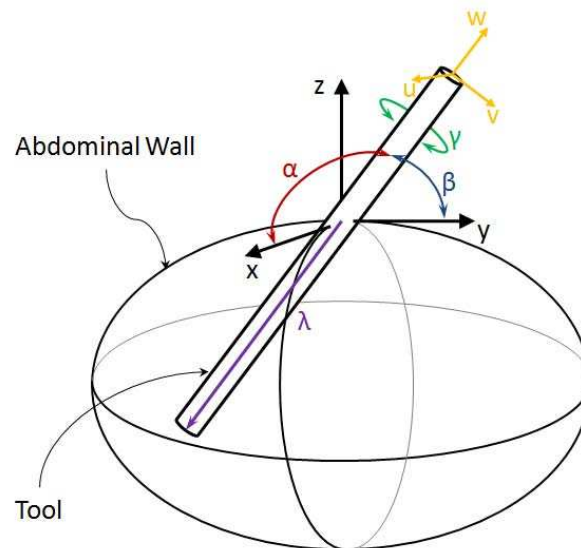
Figure 3-1: Four practical DOFs used in an MIS instrument

Accordingly, the motion DOFs of the surgical tool are described by four variables, α, β, γ, and λ, in which α and β imply rotations about the x- and y-axes of the incision coordinate system and γ and λ imply a rotation and a translation about and along the w-axis of the tool coordinate system.

To respect the kinematic constraint at the entry point, (1) the robotic manipulator should have four DOFs of motion, including three rotational DOF and one translational DOF, (2) the axes of the three rotational DOF should intersect at a single point, which should be located away from the manipulator, and (3) the translational DOF should always point at the direction along which the surgical instrument is being inserted or retracted.

3.2.2   Extracorporeal Workspace

Safety is one of the key concerns in robotic applications for surgery. Therefore, when designing a surgical robot, the safety issue is involved at many levels with various topics such as sterilization, control, sensing and programming. A number of safety issues for medical robots, in either software or hardware perspective, have been discussed by (Davies, 1995, Fei et al., 2001).

In terms of mechanical design, a fundamental safety requirement is related with the human-machine interaction. As opposed to industrial robots, surgical robots are highly human-interactive systems, so that this interaction should be taken into account when designing the robotic manipulator.

To avoid physical interference between the robotic system and the patient, the MIS robot should work outside the patient's body, being a pure extracorporeal mechanism, whose kinematic links and joints never touch the patient's body during the whole cycle of motion. In addition, the extracorporeal workspace of the manipulator should be as small as possible to prevent collisions with the operating room staff and equipment.

Moreover, a compact design of the surgical manipulator enables an easy access to the patient if something goes wrong with the surgical procedure. The platform can also be easily moved and stored within the operating room.

3.2.3 Precision

Precision is another important major design requirement for most robotic applications, since any position error might cause considerable risks to the patient.

Generally, the high precision of a surgical robot can be influenced in several ways, like tolerance sensitivity, feedback control, manufacturing quality, etc. In the mechanical design phase, the kinematic precision of an MIS robot depends mainly on the manipulator topology and dimensions.

Two major limitations that affect the precision in traditional minimally invasive operations can be improved by robotic systems: hand tremor amplification and scaled up surgical movements (Stylopoulos and Rattner, 2003). These are caused by the fact that, quite often, the length of the MIS instrument that is outside the patient's body, l_1, is smaller than the internal length, l_2, Figure 3-2. As a consequence, the input displacement, d_1, which can be a normal displacement or a hand tremor, is amplified inside the body, d_2.
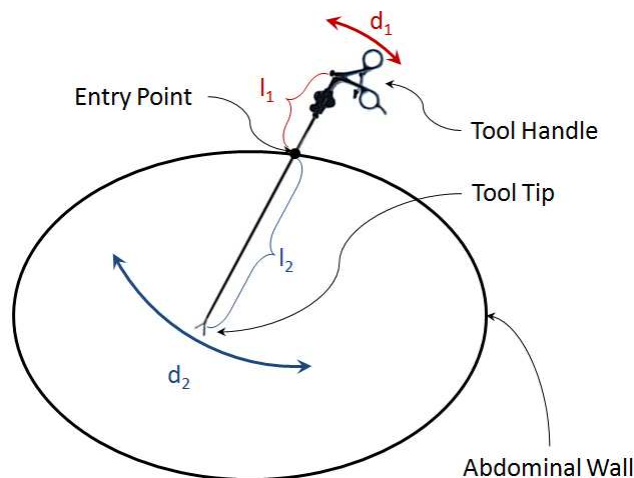
Figure 3-2: Movement scaling-up on an MIS instrument

Therefore, the precision of an MIS robot can be measured by the ability of the instrument tube to achieve a certain displacement at its tip, for the maximum displacement of the external actuators. For that reason, the higher the value of the input/output displacement ratio is, the better is the precision of the robot.

However, attention should be paid to the fact that while the input/output displacement ratio is increased, the extracorporeal workspace of the robotic structure may become larger, which can reduce the safety of the extracorporeal movements. This compromise between safety and precision should be considered carefully when designing an MIS robot. A possible solution

may be the use of gearbox transmission, which ensures a high input/output reduction ratio for increased precision, without any decrease in tool workspace.

3.2.4 Internal Dexterity

One of the most considerable advantages of introducing robotics in MIS is related to the significant increase of internal dexterity over traditional surgical operations. It is a consequence of the larger reachable workspace of the MIS manipulator (the volume of space within which every point can be reached by the end-effector in at least one orientation) and the dexterous workspace (the volume of space within which every point can be reached by the end-effector in all possible orientations).

According to (Lum et al., 2004), the reachable workspace volume generated by an MIS instrument is a cone with an apex located at the entry point. By analyzing a database of general surgical tasks performed on an animal model in vivo in an MIS environment, 95% of the time the MIS surgical tool orientations encompass a 60° cone (Lum et al., 2004). Since all the points within the workspace cone are expected to be approachable by the instrument at a range of angles, this cone-like workspace should be not only a reachable workspace but also a dexterous workspace.

However, due to the constraints imposed by the incision at the end-effector, it is impossible to generate an internal dexterous workspace by a kinematic structure without internal DOFs. A frequently used strategy for dealing with this limitation consists in enhancing the dexterity at the instrument tip, inside the body (Taylor and Jayne, 2007), which can be done by attaching a higher-DOF mechanism at the instrument tip. Depending on the surgical technique, these dexterous endoscopic mechanisms can be kinematically equivalent to mini-humanoid robotic hands or arms, Figure 3-3.

Figure 3-3: Multi-DOF endoscopic mechanisms attached to the distal extremity of an MIS instrument, increasing its internal dexterity

3.2.5 Redundancy

A redundant robotic manipulator is a mechanical system that has redundant actuations (actuation redundancy) or redundant degrees of freedom (kinematic redundancy) (Dasgupta and Mruthyunjaya, 1998, Wang and Gosselin, 2004). In general, both are employed to guarantee a larger workspace, increase the dexterity, and avoid configuration singularities. For the particular case of surgical robots, they can also be used to produce higher levels of safety, avoiding unwanted interferences with vital areas. The first situation occurs when the number of actuators is larger than the mobility of the mechanisms and is used to furnish more degrees of freedom for control flexibility. The second case is achieved by adding kinematic links and joints, to the mechanism such that the mobility is increased and the manipulator can be reconfigured without changing the position/orientation of the instrument to adapt to a more flexible OR set-up (Ortmaier et al., 2004).

3.2.6 Ergonomics

Ergonomics is a science that studies the suitable design of machines and tools that optimize the performance of the user, taking into account the limits of the user (Berguer, 1999, Kaya et al., 2008). In the field of MIS, the ergonomic problems include a broad range of concerns, which can be divided in visualization, manipulation, surgeon posture, mental and physical workload, and the OR environment ergonomics (Berguer, 1999).

In the mechanical design phase, ergonomic concerns for MIS robots are related to the ergonomy of the manipulation. For an MIS procedure, the surgical instrument is controlled by the surgeon's hand, outside the body. Due to the "fulcrum effect" at the incision point, the movements of the surgeon's hand result in an opposite movement of the instrument tip in the patient's body, creating an inversion between visual and kinesthetic preception, Figure 3-4.
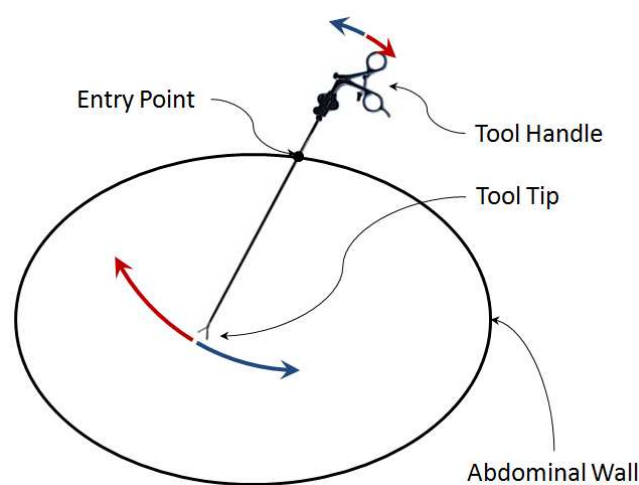
Figure 3-4: Movement inversion on an MIS instrument

In addition, as the MIS instrument is held by the surgeon's hand, manual operation will induce ergonomic problems in terms of excessive flexion, supination, and ulnar deviation of the surgeon's wrist (Kaya et al., 2008). Currently, this problem is solved by the MIS robots through the use of control rectification, where the coordinate system is mirrored from the instrument tip to the holding part of the surgical tool. However, an intrinsic solution from the viewpoint of manipulator kinematic design would be an ideal solution, requiring reduced computational efforts.

3.3 Medical and Health Care Requirements

3.3.1 Set-Up Time

Ideally, the medical team should be able to enter the operating room, tune the system, insert the instruments on the patient and start manipulating the device without spending too much time calibrating and setting-up procedures. This means that the system should provide an entirely ergonomic and user-friendly interface, with a realistic telepresence to the surgical field, and good contact with the staff at the room. Due to the presence of costly personnel and equipment, it is extremely important to reduce preparation, operating and change-over time per procedure.

3.3.2 Dimensional

The working volume of the surgical instruments in standard MIS procedures has to be respected. The axial translation of the instrument with respect to the incision point should allow a 200mm insertion of the end-effectors, with a range of motion of ±50mm (Baumann, 1997).

It should be possible to orientate the instrument with respect to the incision point within a vertically oriented conic workspace of 90° opening angle (Lum et al., 2004). Inside the conic workspace, the instrument should be able to rotate at least 270° about its longitudinal axis for driving the needle through tissue in a single movement (Cavusoglu, 2000). The volume of the total workspace should be consistent with this, obviously varying with different patient sizes and different procedures.

The diameter of the endoscopic unit must be such that it fits into a trocar smaller than the current single port incisions, which range from 25mm to 60mm.

The size of the end-effectors should be comparable with the current instruments for minimally invasive surgery, whose diameter can go up to 12mm (Baumann, 1997).

3.3.3   Force

The force that a surgical robotic system can apply at its end-effector should match the maximum forces applied by surgeon's manual tools during normal procedures. Several studies can be found in the literature, were surgeons are asked to perform numerous surgical tasks, using force sensors in the tools. The force requirements change from procedure to procedure and according to surgeon's experience. For surgical procedures in soft tissues, the maximum continuous value can reach 10N (Baumann, 1997) in x, y and z directions and 20N in the gripping elements (Cavusoglu, 2000).   However, in other surgical fields like Orthopaedic and Neurosurgery, the force requirements may be much higher.

3.3.4   Cost

The market of robotic systems is currently dominated by the da Vinci robot, developed and marketed by Intuitive Surgical. However, this system is extremely expensive in acquisition (close to CHF 2 million (Camberlin et al., 2009)), maintenance (about CHF 200'000 per year (Camberlin et al., 2009)), disposable tools (about CHF 3'500 per procedure (Camberlin et al., 2009)) and training, representing much higher direct costs compared with open surgery instrumentation (Camberlin et al., 2009). For this reason, access to Robotic Surgery is limited to a minority of hospitals that (a) can afford to purchase the Da Vinci System and (b) have enough patient volume to justify its acquisition. This tendency towards centralisation of complex minimally invasive surgeries draws patients from hospitals without the da Vinci and places an additional burden on the health care system (Camberlin et al., 2009).

3.4   Actuators

The specific requirements imposed by minimally invasive applications, namely in term of the reduced dimensions, pose some constraints in the selection of the most suitable actuators for a surgical robot. Besides the torque capacity, the torque-to-volume ratio is an important selection criterion that should be taken into account. In the following, an evaluation of today's most relevant actuator technologies for minimally invasive surgical applications will be presented.

3.4.1   Hydraulic Actuators

In what concerns the torque-to-weight ratio, hydraulic actuators can be considered ideal for MIS applications. They transform energy supplied by pressurized hydraulic fluid into rotary or linear motion. This hydraulic fluid flow over the hydraulic actuator is controlled typically by electromagnetic servo valves or by variable displacement pumps. However, the presence of fluids poses a few problems in terms of mechanical design, like increased friction and leakage. In addition, the valves often exhibit complex non-linear dynamics, and are therefore

more demanding for control (Hunter et al., 1991). Another major limitation of hydraulic actuation for a force-feedback surgical robot is the lack of backdriveability.

3.4.2   Pneumatic Actuators

Like in hydraulic actuators, pneumatic actuators involve a piston driven by a pressurized gas. However, due to the higher pressures used in hydraulic actuators, pneumatic actuators tend to have a lighter constitution, resulting in more compact structures (Hunter et al., 1991). Key advantages of pneumatic over hydraulic actuators are their simplicity and cleanliness. The main drawback of pneumatic actuator is gas compressibility, which makes tem inherently compliant and so, significantly more complex to control. Moreover, the velocity of the valve used to regulate the pressure and flow into the piston will limit the actuator's dynamic performance.

3.4.3   Shape Memory Actuators

After a mechanical deformation, the shape memory effect of certain alloys implies a return to the non-deformed state when heated. The main advantages of shape memory alloys (SMA) are their compactness and lightness. On the other hand, the main disadvantage is related with their long time required to cool back after heating. Another drawback is related with their low energy efficiency (Burdea and Burdea, 1996).

3.4.4   Electromagnetic Actuators

The electromagnetic actuators are comparatively clean, quiet and efficient, providing generally high linearity and high bandwidth, while being easy to control and maintain. For this reasons, and although high torque without the use of gearboxes is difficult to be achieved, they are the most suitable solution for MIS, being used in the majority of the current surgical robots. Moreover, it is possible to estimate the joint torques by using only the motor currents and specifications. This method eliminates the dependence of destabilizing force-torque-sensor schemes by making the slave manipulator able to sense directly the interaction force with the environment and feed them back to the master (Townsend, 1988). However, this approach forces the manipulators to be designed with mechanical properties that improve their transparency.

3.5   Transparency Requirements

The quality of a man-machine interface is often characterized by its degree of transparency. Transparent manipulators should therefore be able to appear mechanically invisible to the operator, not exerting any external forces on the user when moving through the free space. On the other hand, they should show high stiffness, being able to transmit a broad range of

external force interactions. In the following, some of the most important issues that have to be considered in the design of mechanically transparent systems are discussed.

3.5.1   Friction

In a teleoperated system, the ability to return forces back to the user may be decreased by friction in the slave manipulator. Consequently, friction will be reflected to the user not only during free-space motions, but also in contact actions. In this situation, small contact forces will risk to be covered up by frictional forces, limiting their ability of the user to distinguish the contact.

3.5.2   Ripple

Sensing high frequency vibrations represents a tight constraint on a telemanipulator design, requiring a careful attention to several aspects of hardware design and actuator selection. A significant level of vibration has a huge negative effect on the haptic fidelity and can really decrease the sense of telepresence. Sources of vibration such as ripple torques and noisy transmission elements should be avoided or minimized.

3.5.3   Inertia

In the case of a manipulator, the inertia is composed primarily by the mechanical structure of the links plus the motors. Inertial effects may be felt by the operator if the control scheme is not compensating them. Therefore, an ideal mechanical design should reduce inertial effects as far as possible, providing the user with more sensitivity at low force levels. However, for slow movement and small size applications, such as surgical tools, inertia is expected to play only a minor role on system's performance.

3.5.4   Backdrivability

Backdrivability is the ability of a mechanical system to interactively transmit forces between input and output actuations. However, there has been for years a controversial debate about the use of backdrivable versus non-backdrivable transmission in surgical robots. Both solutions have their advantages and disadvantages, when different design goals are considered. A backdrivable transmission increases the transparency of the system. On the other hand, a non-backdrivable transmission increases the level of safety since the manipulator will remain static following a power failure. When considering a compromise between backdrivable and non-backdrivable systems, using a careful combination of both transmissions may be adequate solutions to deal with the case of power loss.

3.5.5 Stiffness

A further parameter to analyse the performance of a force-reflecting manipulator consists in measuring its stiffness. Compliance in the links, joints and transmission reduces the precision of the manipulation, when forces are being applied on the device, and decreases the bandwidth of the system, which may cause control instabilities when force sensors are not being used (Millman et al., 1993).

Figure 3-5 shows the stiffness measurement performed on two commercially available minimally invasive tools: an *EndoWrist Instrument*® from *Intuitive Surgical*® and a *LigaSure*® from *Covidien*®. The force was applied at the instrument's end-effector, perpendicularly to the tool's axis. Then, it was increased gradually and registered by a force sensor. The deformations were measured by using a standard dial gauge.
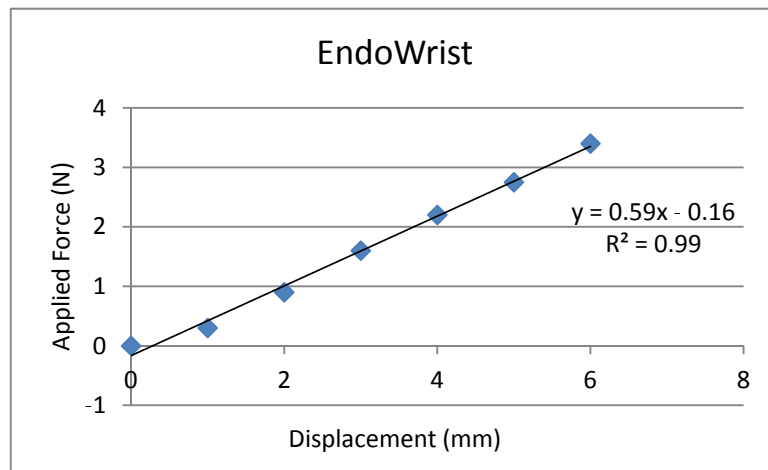
a)
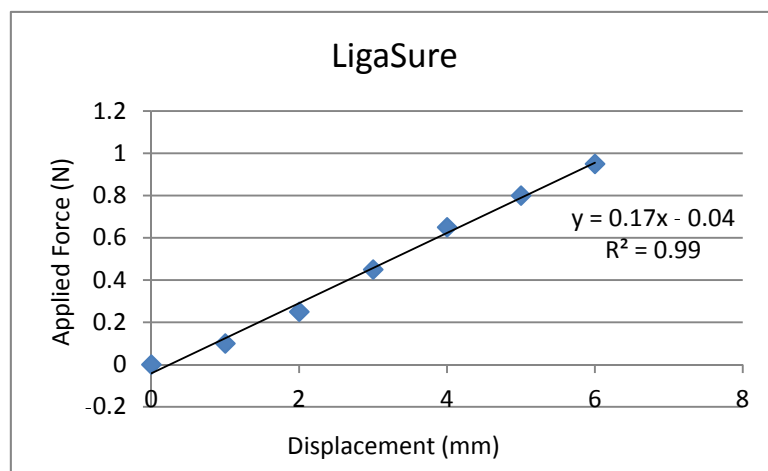
b)

Figure 3-5: Stiffness measurements for two standard MIS tools

As can be seen, the relationship between the applied force and the displacements on the end-effector, for both instruments, can be linearized within the measured range, resulting in of 590N/m (*EndoWrist Instrument*®) and 170N/m (*LigaSure*®).

3.5.6 Gravity Compensation

Static balance of the telemanipulator is a necessity, since a poorly balanced system may lead to greater operator fatigue and increase the likelihood of errors. In order to accurately reproduce force feelings, the weight of the mechanical structure must be compensated. The main decision relates to whether use mechanic or electronic counterbalancing. The first approach has the advantage of being passive and simple to implement but adds additional inertia to the system. The second solution brings more complexity to the control software.

3.6 Summary

To sum up, the key mechanical design requirements for a MIS manipulator are:

- The external positioning should have 4 DOF of motion, including 3 rotational DOF and 1 translational DOF.
- The axes of the 2 rotational DOF should always intersect at the same point (incision point) which should be located some distance away from the manipulator.
- The translational DOF must always move along a fixed line, which intersects the axes of the 2 rotational DOF at the incision point.
- The extracorporeal workspace of the manipulator should not collide with the patient, medical staff and operating room equipment.
- The overall system design should be compact, occupying little space above and around the operating table.
- The internal dexterity of the surgical manipulator, inside the body, should be increased by attaching additional DOFs to the distal extremity of the instrument's shaft.
- The multi-DOF dexterous endoscopic mechanism should have an anthropomorphic kinematics.
- The movements of the distal end-effector, inside the patient's body, should not be inverted, in relation to the surgeon's hand.
- The reachable workspace volume inside the patient's body should be, at least, a 90°cone with an apex located at the incision point.
- Inside the conic workspace, the instrument should be able to rotate at least 270° about its longitudinal axis.
- The system should allow a 200mm insertion of the end-effectors inside the patient's body, with a range of motion of ±50mm.
- In order to increase the level of safety in the case of a power failure, a non-backdrivable transmission should be applied in some system's DOFs or a gravitational balance should be provided to the system.

- Backdriveability should be applied on the DOFs of the dexterous endoscopic mechanism in order to increase the mechanical transparency.
- The instrument's diameter should be compatible with current trocars, with diameters up to 12 mm for laparoscopy and up to 30mm for single incision surgery.
- Inside the patient's body, the system should be able to apply 10N in the x, y, z directions.
- Electromagnetic actuators should be used in order to facilitate system's control.
- The system should have a low complexity, being fast and easy setup and transport from one place to the other within the hospital

4 Mechanical Positioning System for MIS Instruments

4.1 Introduction

This chapter presents the study and development of a new mechanical system for the external positioning on MIS surgical instruments. The proposed kinematic structure will contribute to increase the precision and compactness of MIS manipulators, increasing patient safety. We will concentrate essentially on abdominal surgery, although the principles of this system also can apply to other types of MIS surgery.

4.1.1 Surgical Technique

Recent developments in surgery show a clear trend toward less invasive methods of access over the past decades. While conventional laparoscopy is the standard treatment for various disorders at present, newer methods such as Single Incision Laparoscopic Surgery (SILS) and Natural Orifice Translumenal Endoscopic Surgery (NOTES) are gaining clinical significance worldwide (Gettman et al., 2008, Chamberlain and Sakpal, 2009). Besides hypothetical clinical advantages such as faster recovery, fewer pain medication and milder anaesthesia, surveys point out that potential patients actually favour cosmetically superior surgical approaches (Hagen et al., 2010). While pure NOTES will deliver cosmetically perfect outcomes with no external scars, this method is still under development and only performed at a few hospital centres world-wide (Zorrón et al., 2007, de Sousa et al., 2009). SILS, on the other hand, is a feasible technique that has gained large attention during the last few years, reporting many successful cases on medical publications (Filipović Čugura et al., 2008, Curcillo 2nd et al., 2009). The great majority of SILS techniques currently performed is carried out through the umbilicus, with penetration of the abdominal wall by the umbilical midline. However, such an approach might lead to a deformed umbilicus, whose integrity and appearance is considered to be extremely important for many patients (Dini and Ferreira, 2007, Barbosa et al., 2008) and to an increased rate of incision hernias after the procedure (Montz et al., 1994).

Due to these presumed disadvantages, a novel approach to enter into the abdominal cavity for SIL has been developed and may represent a bridge between the cosmetic advantages of NOTES with the technical feasibility of SIL. Subcutaneous surgical tunnelling (SST) disconnects the skin incision from the entrance of the peritoneal cavity through the abdominal wall (Hagen et al., 2010). Therefore, the skin incision can be placed in almost any cosmetically favourable location of the body such as the supra-pubic hair, groin, axillae or previous (Figure 4-1). Then, a subcutaneous tunnel is formed to enter the peritoneal cavity

through the abdominal wall at a mechanically favourable location, such as the rectal muscle to decrease the risk of incision hernias.
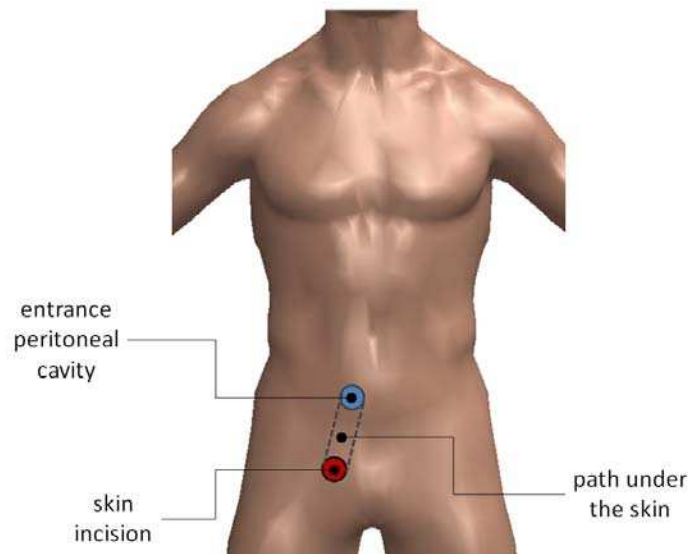
Figure 4-1: Subcutaneous surgical tunnelling technique

The flexibility of this method of access makes it possible to customize each incision to the specifics of each patient, regarding existing scars, cosmetic preferences and individual weak areas of the abdominal wall. In addition, having the MIS instruments inserted close to a horizontal orientation allows an easy access to different quadrants of the abdomen, avoiding the docking and disengagement of the robot and decreasing significantly the total operating time.

4.1.2   Platform Overview

The mechanical system studied in this chapter is applied in new a robotic manipulator for MIS. The idea is to bring highly dexterous manipulation and standard surgical procedures inside the abdominal cavity, with a micro-robotic system, stabilized by an external manipulator and inserted through an incision on the supra-pubic hair region, Figure 4-2.
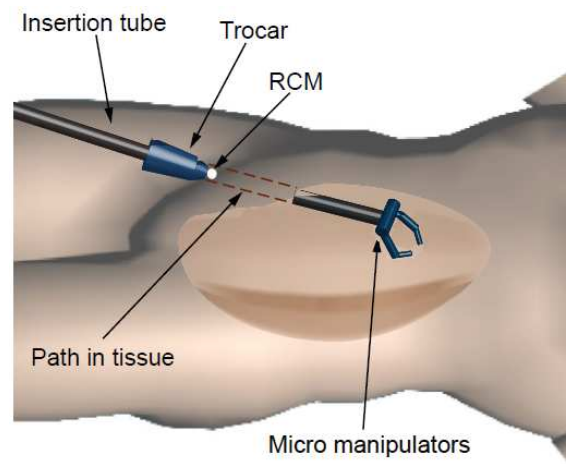
Figure 4-2: Conceptual representation of the Surgical Platform

This proposed surgical platform is mainly composed by two subsystems: (1) an external positioning manipulator, and (2) an endoscopic unit, designed to increase the degree of internal dexterity, inside the patient's body, Figure 4-3.
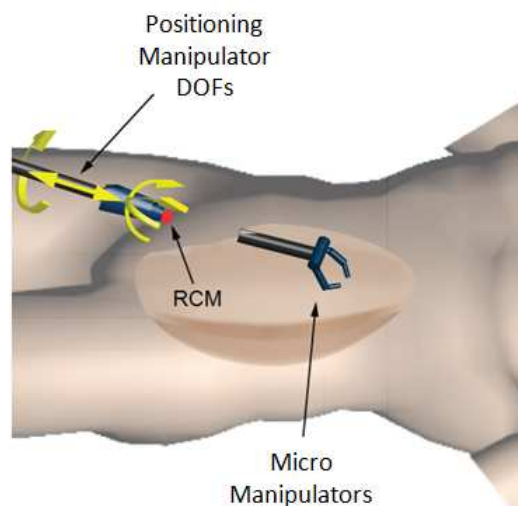
Figure 4-3: Conceptual design of the complete surgical platform

The purpose of the positioning manipulator is to place the micro-manipulators of the endoscopic unit inside the human body, without violating the constraints imposed by the fixed tissue incision point. The related kinematics gives to the insertion tube two rotating degrees of freedom about the incision port, placed around the supra-pubic-hair area, plus a linear movement in the direction of the same point, along the axis of the insertion tube. The fourth DOF is a rotation about the tube's axis, given by a fourth actuator of the external unit.

4.1.3 Remote-Center-of-Motion Manipulators

On Chapter 3, the design requirements for a MIS robot have been discussed. One of the key specifications for a surgical manipulator states that it should manipulate its surgical instruments moving along and rotating about the incision on the patient's body. Also, the extracorporeal workspace volume must ensure that the robotic manipulator does not collide with the patient during surgery. With a general multi-DOF manipulator, these goals can be achieved based on a specific control strategy (Ghafoor et al., 2000, Schneider and Troccaz, 2001, Dombre et al., 2004), which brings to such systems some advantages in terms of flexibility for pivot location. However, for surgical applications, a specially configured robot that accomplishes these required motions based on a physical constraint is considered to be more appropriate because the potential danger for surgeons and patients caused by any control failure can be avoided (Taylor and Jayne, 2007).

The above mentioned advantages have motivated researchers to develop mechanical systems with special kinematics that can produce a fixed rotational centre, located at a certain distance from its own structure. Based on this, the concept of remote centre-of-motion (RCM) was developed (Taylor et al., 1997). Geometrically, an RCM consists in a fixed virtual point, associated with a mechanical system, about which a link of the mechanical system rotates and translates. In addition, this virtual point should be located outside the workspace volume generated by all the other links belonging to the mechanical system, when it is in operation.

Owing to its superior advantages in control simplicity and safety confidence, using a special-purpose MIS robot with RCM design has become the norm, rather than using a general-purpose industrial robot for MIS tasks. The RCM function may be incorporated into robots by using different kind of kinematics. Some examples are listed below.

Spherical Systems

In terms of kinematic structure, a simple way to produce an RCM consists in using a Spherical Mechanical System. The idea is to provide a circular track as a movement base, having a member sliding on it (Figure 4-4a). The tracking arc is pivoted to the base by a revolute joint whose axis passes through the RCM and the sliding member is always pointing at the RCM. As a result, a 2-DOF RCM can be found in the curvature centre of the pathway. The system shown in Figure 4-4b is called UT-NEU and was developed for neurosurgery applications at the University of Tokyo (Ikuta et al., 2002). It uses a Spherical System as the RCM mechanism that, together with an additional prismatic joint at the end-effector, is able to provide two rotations and one translation to the instrument.

a)   b)
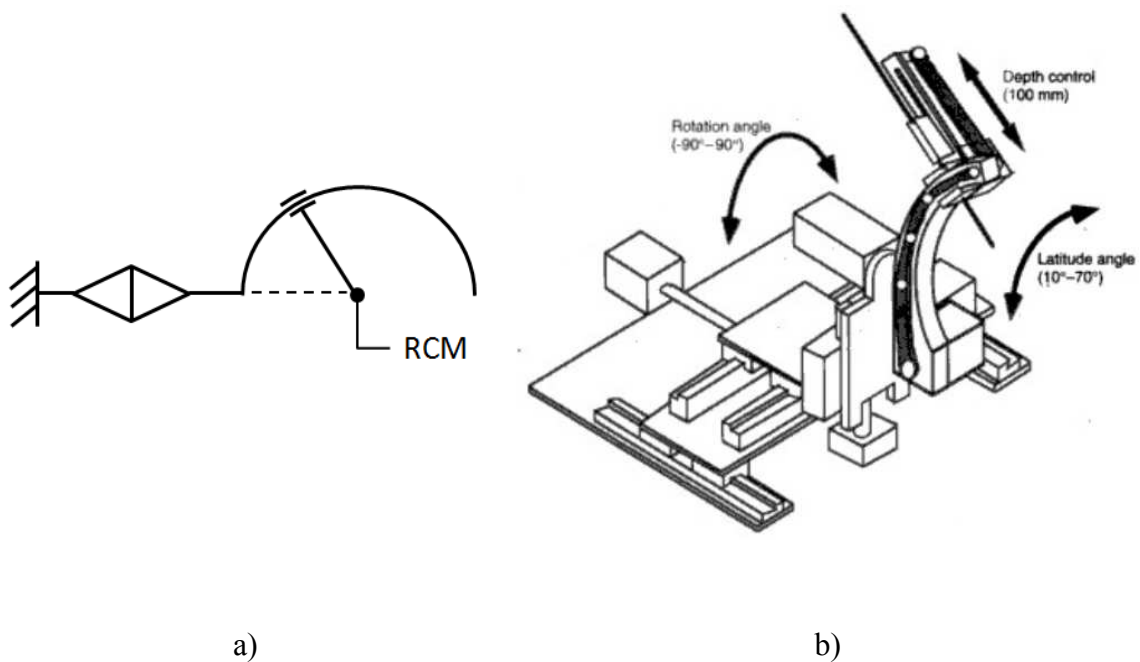
Figure 4-4: Spherical RCM a) Kinematic Sketch and b) Surgical Robot using it (Ikuta et al., 2002)

Double Parallelograms

The double parallelogram is one of the best known RCM mechanisms, well suited for MIS robots. Its kinematics concept, shown in Figure 4-5a, is based in the combination of two parallelograms, whose rotation at the base can produce an RCM at a remote location. Just like the concept of the Spherical Systems, the Double Parallelogram can be connected to the base by a revolute joint whose axis passes through the RCM point. The link pointing to the RCM may also have a coaxial or prismatic joint, providing two additional DOFS for the RCM.

There are several MIS manipulators using the Double Parallelograms (Taylor et al., 1997, Madhani et al., 1998), like the one of Figure 4-5b.
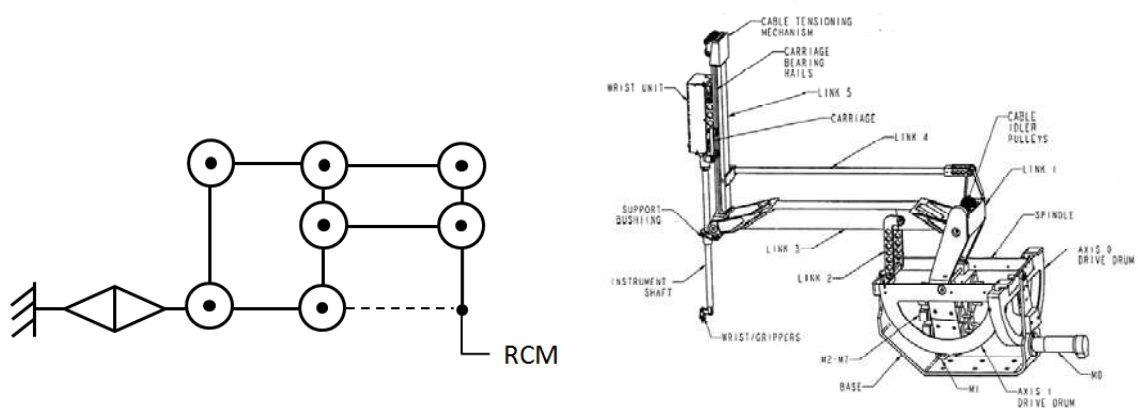
Figure 4-5: Double Parallelogram RCM a) Kinematic Sketch and b) Surgical Robot using it (Madhani et al., 1998)

Parallel Belt System

The Parallel Belt System is an alternative to obtain the same movement as the Double Parallelogram, where one of the parallelograms is replaced by a belt system, which keeps the parallel motion of the structure and consequently the RCM (Figure 4-6a). The system shown in Figure 4-6b uses a similar system comprising of a 2-DOF RCM mechanism.
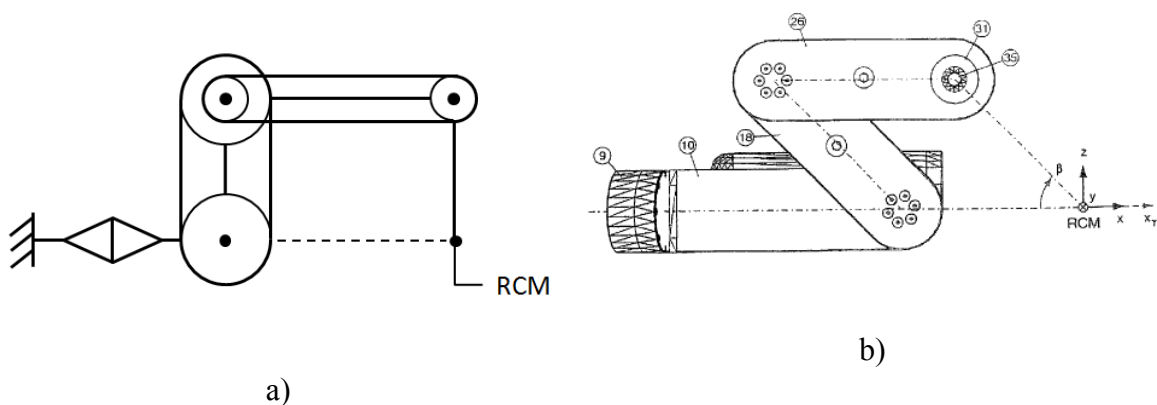
Figure 4-6: Parallel Belt System RCM a) Kinematic Sketch and b) Surgical Robot using it (Adhami and Coste-Manière, 2003)

Spherical Linkages

A spherical linkage is a mechanical system in which the RCM is achieved by three revolute joints whose axes intersect in a single point, Figure 4-7a. In this way, the moving bodies of the mechanism are forced to pivot around a virtual point that is stationary in space. The system shown in Figure 4-7b uses a spherical linkage to generate its RCM. The kinematic model consists on a 3R serial manipulator that can perform three decoupled rotations at the RCM point.

b)

a)
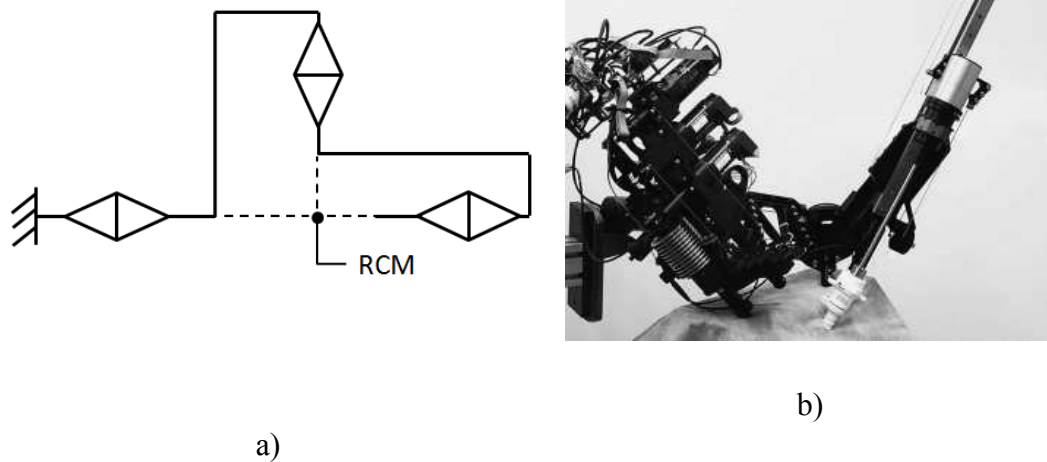
Figure 4-7: Spherical Linkage RCM a) Kinematic Sketch and b) Surgical Robot using it (Lum et al., 2009)

Parallel Manipulators

Another possibility of achieving an RCM consists in using a parallel or hybrid kinematics. The system shown Figure 4-8 has a parallel kinematics based on the Delta Kinematics (Clavel, 1988b). It is able to provide a fixed RCM, featuring two rotations and a translation along and about a virtual point (Pham et al., 2006). However, this RCM is placed within the workspace volume of the system's structure, which is not ideal for surgical applications.

a)   b)
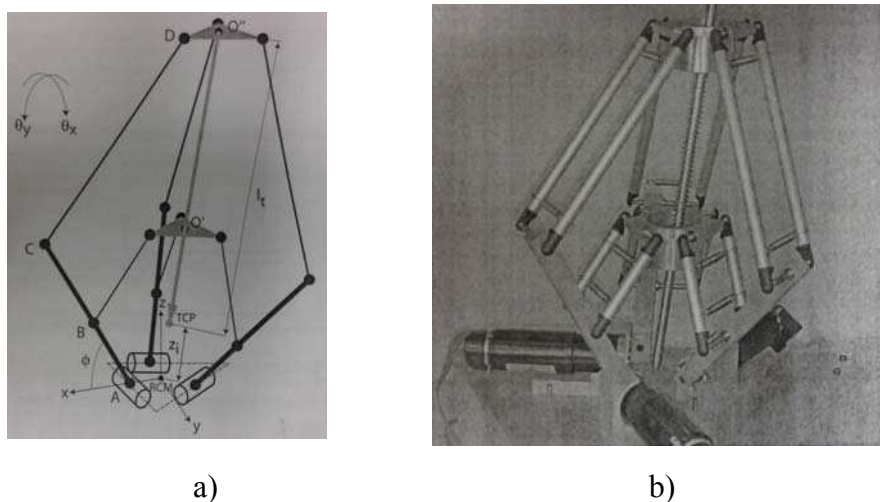
Figure 4-8: The Thales Manipulator: a parallel robot based on the Delta Kinematics (Pham et al., 2006)

The system shown in Figure 4-9b can provide an RCM located outside the workspace volume by combining two parallelograms on the same mechanism, in a parallel configuration, Figure

4-9a. The two kinematic structures comprise only revolute joints and define two planes in the three-dimensional space, which can be rotated about two intersecting axes (Baumann, 1997).

b)

a)
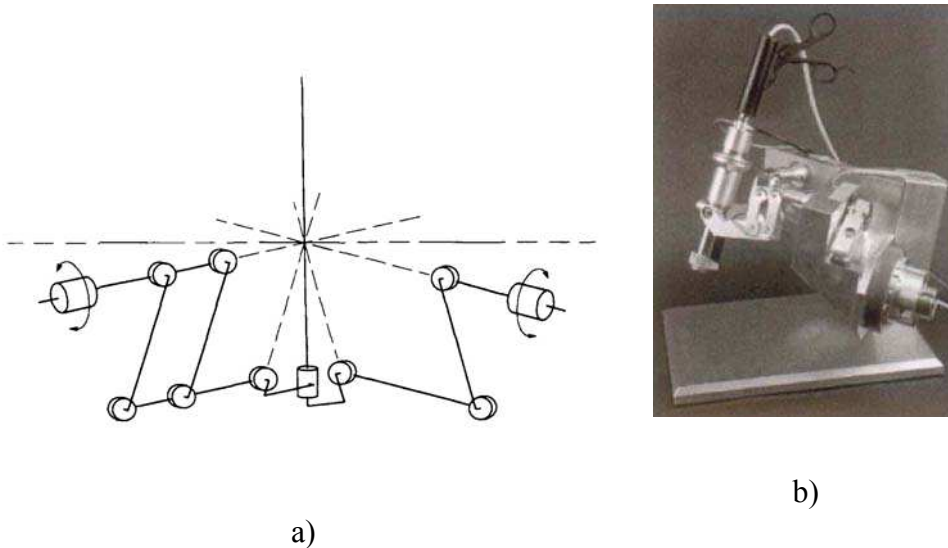
Figure 4-9: The PantoScope: an MIS robot using parallelogram systems in a parallel configuration axes (Baumann, 1997)

In most of the above shown manipulators, the basic kinematics of the RCM mechanism can only generate a 2-DOF orientation, while the rotation around the insertion axis and the translational motion are usually achieved by two additional actuations placed on the output link. The two additional DOFs will then directly and independently control the surgical tool to spin and to move in-and-out through the entry port. This solution provides a relatively simple way to complement the surgical instrument with the required four DOFs. However, additional payload has to be induced by the additional actuation at the output link, which, from the static point of view, can bring undesirable problems such as large inertia, increased extracorporeal volume and reduced stiffness.

As an alternative, generating the RCMs by using parallel robots would be a better solution for compensating the additional payload problem. However, in most of the current parallel robots available for surgical applications, the RCM is achieved by the adequate control of the limb actuators on the manipulator, which is not considered to be the safest solution for MIS applications.

4.2 *"Dionis"* Manipulator

In this section, the mechanical design of a novel RCM mechanical system is presented, together with solutions for its geometrical analysis. It was developed to be used on the SST Platform described in the previous section, while meeting the design requirements discussed on Chapter 3. Due to its unique design and kinematics, the proposed mechanism is stiff and its dexterity fulfils the workspace specifications for MIS procedures. One of the main features of this new parallel kinematic design is its compactness. Several position configurations of this

structure are possible, always leaving enough access to the patient and significantly increasing the safety of robotic surgery.

4.2.1 Concept Generation

Despite showing good operating characteristics (large workspace, high flexibility and dexterity), serial manipulators present disadvantages, such as low precision, low stiffness and low payload. On the other hand, parallel kinematic manipulators offer essential advantages, mainly related to lower moving masses, higher rigidity and payload-to-weight ratio, higher natural frequencies, better accuracy, simpler modular mechanical construction and possibility to locate actuators on the fixed base. These characteristics make parallel manipulators extremely suitable for surgical applications. Taking into account that stiffness and precision are considered to be key features on external positioning mechanisms for MIS, the proposed manipulator is based on a parallel kinematics, to reproduce the needed degrees of freedom.

A schematic of the proposed manipulator is shown in Figure 4-10. The RCM, point O, is placed on the X-axis of the fixed reference frame, $F(x, y, z)$, and is distant by an offset t from the origin, O', which is placed in the intersection of lines t_1, t_2 and t_3, that belong to the stationary platform, P_S, in the XY plane. In addition, lines t_1, t_2 and t_3 are perpendicular to axes a_{11}, a_{12} a_{13}, respectively. Three identical limbs connect the moving platforms, P_M and P_I, to the stationary platform. Each limb consists of an input link, directly connected to the actuator, placed on P_S and two driven links, connected to P_M and P_I. The input links are labelled D_{11}, D_{12}, and D_{13} and have length d_1. The driven links are composed by planar four-bar parallelograms, D_{21}, D_{22}, D_{23}, D_{21}, D'_{22} and D'_{23} and have length d_2 and d'_2 respectively. All of the links and platforms are considered as rigid bodies (Figure 4-10).
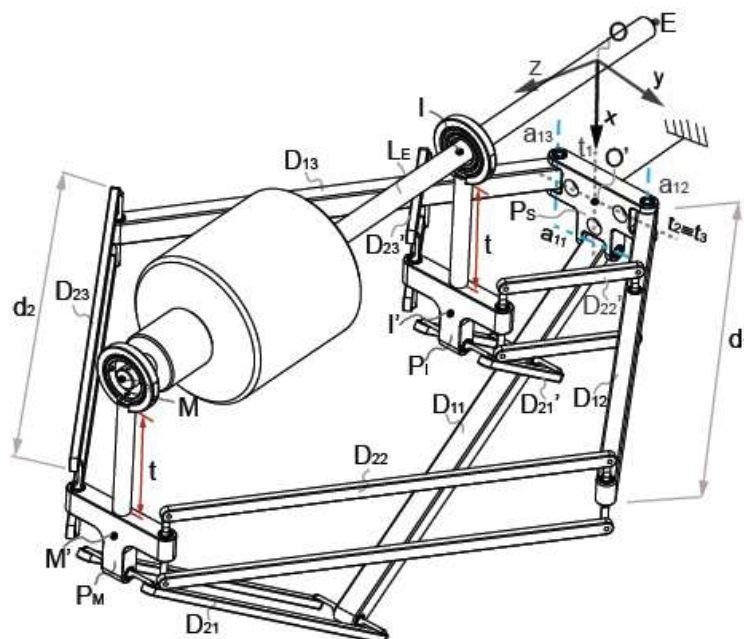
Figure 4-10: Dionis Schematics (Beira et al., 2011a)

The nth limb of the manipulator is shown in Figure 4-11. In each limb, the driven links, the input link, and the three platforms are connected by four parallel revolute joints, at axes a_{1n}, a_{2n}, a_{3n}, a'_{2n} and a'_{3n} that are perpendicular to the axes of the four-bar parallelogram for each limb. A coordinate system, $L_n(u_n,v_n,w_n)$, is attached to the fixed base, P_S, in the actuated joint of each limb, such as the u_n axis is perpendicular to the axis of rotation of the joint, a_{1n}, and at an angle θ_n from the x-axis, while being in the plane of P_S. The v_n-axis is along a_{1n}.
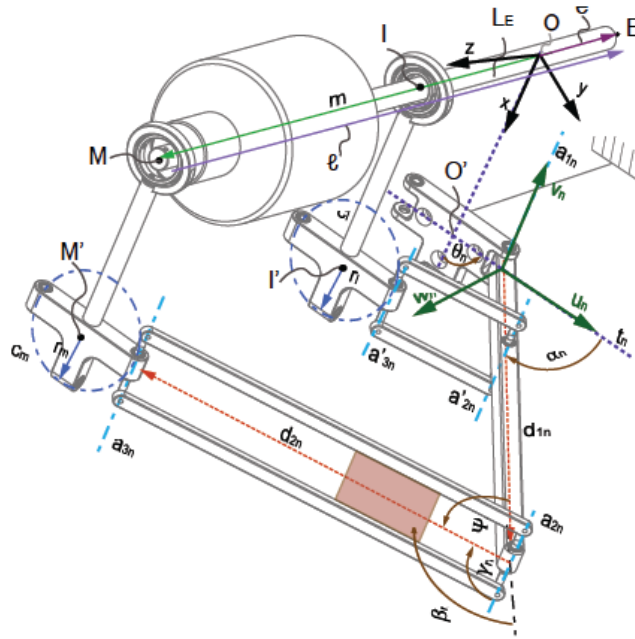
Figure 4-11: Limb Schematics (Beira et al., 2011a)

The actuation angle, α_n, for the nth limb, defines the angular orientation of the input link relative to the *XY* plane, on platform P_S. Vectors **m** and **e** are respectively the position vectors of points *M* and *E*, in the *F* coordinate frame. *M* and *I* are placed at the centre of circles c_M and c_I of radius r_M and r_I, that belong to platforms P_M and P_I. Vector **l** is aligned with the output link, L_E, from point *M* to point *E*. Angles β_n and β'_n are defined from the direction of input links, axis d_{1n}, to the direction of the plane containing the parallelograms of driven links, d_{2n} and d'_{2n}. Angles γ_n and γ'_n are defined by the angles from the directions of the driven links, d_{2n} and d'_{2n}, through axis a_{2n} and a'_{2n}.

The configuration of the limbs is based on the well-known Delta robot (Clavel, 1988a). It is in fact composed by a pair of 3 four-bar-parallelogram-links fixed on the same input links. Therefore, the two platforms (the intermediate, P_I, and the distal one, P_M) move in the same manner except that P_M moves with larger ranges than P_I. Link, L_E, containing the end-effector, *E*, is then connected to points *M* and *I* by an universal joint and a sliding spherical joint respectively. The output of the proposed design results in: two rotations of L_E around the *X* and *Y* axis, and a translation of *E* on the direction *MO*.

To guarantee a perfect RCM, a geometrical ratio is needed. This ratio is based on the *Intercept Theorem*, which states that: if two or more parallel lines are intersected by two self-intersecting lines, then the ratios of the line segments of the first intersecting line is equal to the ratio of the similar line segments of the second intersecting line. In other words, and for the example of Figure 4-12:

$$\frac{\overline{SD}}{\overline{CD}} = \frac{\overline{SB}}{\overline{AB}} \tag{1}$$
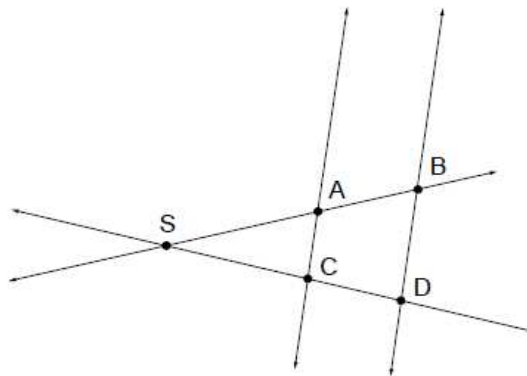
Figure 4-12: Illustration of the Intercept Theorem (Beira et al., 2011a)

On Figure 4-13a, a simplified 2D representation of the Dionis[1] is shown. The upper limb ("dashed") is virtually rotated π rad from the one bellow, around the Z axis. According to the *Delta* principle (Clavel (1988)), the rotations of the moving platforms are blocked and P_M and P_I are always parallel and vertical. Consequently, in order to have the link ME always aiming at the RCM, it is necessary to have points A, C' and C aligned. This is true if segments $B'C'$ and BC are parallel and if $BC/B'C' = AB/AB'$ (*Intercept Theorem*). If these conditions are not fulfilled, the behaviour of the robot will be similar but without a perfect RCM. By contrast, if they are satisfied, point I will always be aligned with O and M, for any position of M, and platform P_I is passively moved to guarantee this configuration. According to the above mentioned constraints, a geometrical simplification can be made, assuming zero-size platforms, which significantly simplifies the kinematic analysis of the mechanical structure, Figure 4-13b. In addition, an equivalent architecture can be introduced, extending the platforms at O, I and M by a distance t, as shown in Figure 4-13c. In this way, the RCM, is translated by a distance t, in the platform's extension direction, resulting in a mechanism with the same kinematics.

---

[1] It is the name of a 17th century mathematician and astronomer, *Achille Pierre Dionis*, who studied, among other topics, the alignment of eclipses. The alignment of points O, I and M is precisely the characterization of the new parallel kinematic structure.
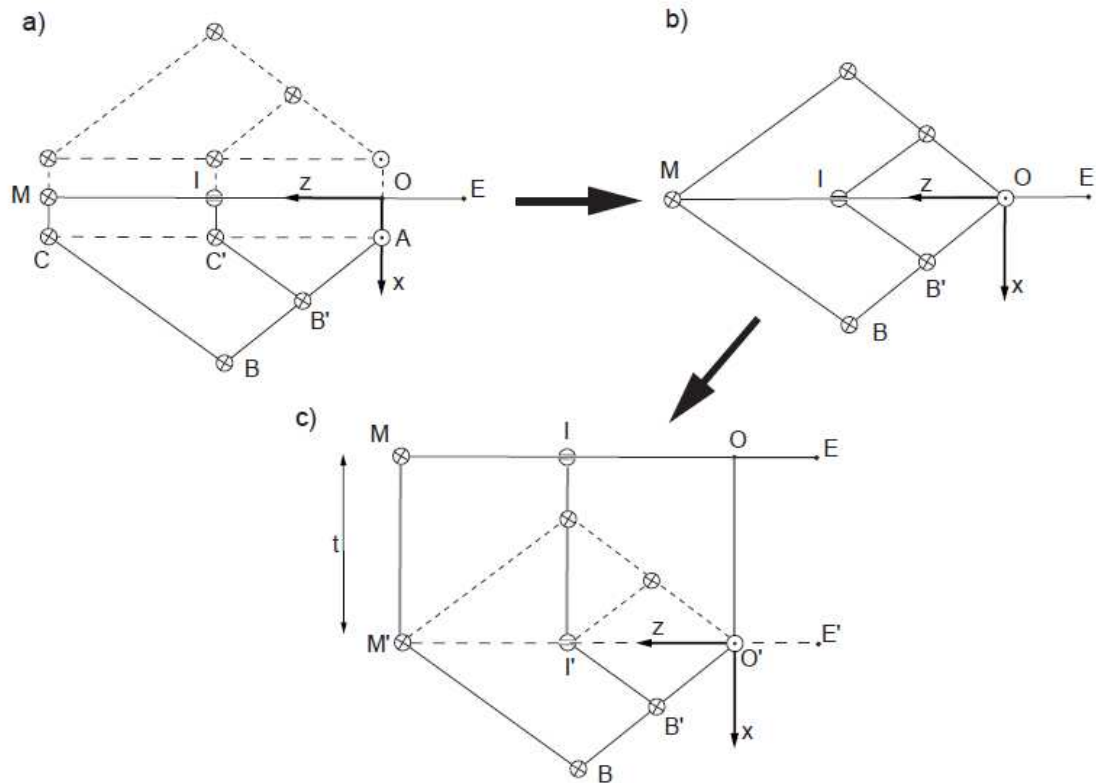
Figure 4-13: 2D representation of Dionis Manipulator (Beira et al., 2011a)

It is also important to point out that this kinematics can also be applied in other configurations specific to different surgical procedures. Figure 4-14 shows two other possible configurations of the proposed kinematics.

a)

b)
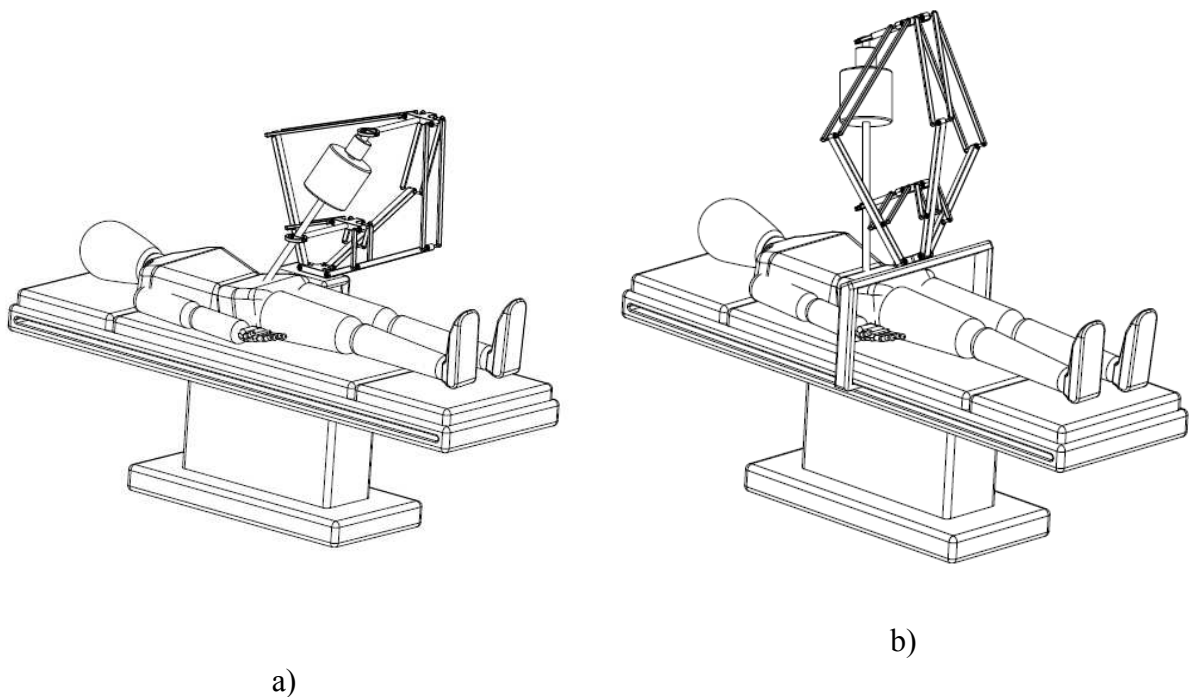
Figure 4-14: Example of potential working configurations for the *Dionis* Manipulator a) Lateral position configuration and b) Superior position configuration (Beira et al., 2011a)

4.2.2 Manipulator Mobility

The proposed parallel platform hereafter is characterized by the kinematic structure shown in Figure 4-15. Considering the manipulator mobility, let F be the degrees of freedom, n the number of parts, k the number of articulations, f_i the degrees of freedom associated with the ith joint, and $\lambda = 6$, the motion parameter. Then, the number of DOFs of a mechanism is determined by the *Grübler-Kutzbach* Criterion:

$$F = \gamma(n - k) + \sum_{i=1}^{j} f_i = 6(13 - 18) + 33 = 3 \qquad (2)$$

For the *Dionis* manipulator, we have: $n = 13$ (3 inputs links, 6 driven links, 2 moving platforms, 1 slider-mount, 1 end-effector link); $k = 18$ (3 actuated revolute joints, 1 spherical joint, 13 universal joints and 1 slider) and $\Sigma f_i = 33$. Applying Eq. 2 to the Dionis manipulator results in: $F = 3$, and consequently a mechanism with 3 DOF. The result would be the same considering all the bars of the parallelograms with a ball and a universal joint at each tip.
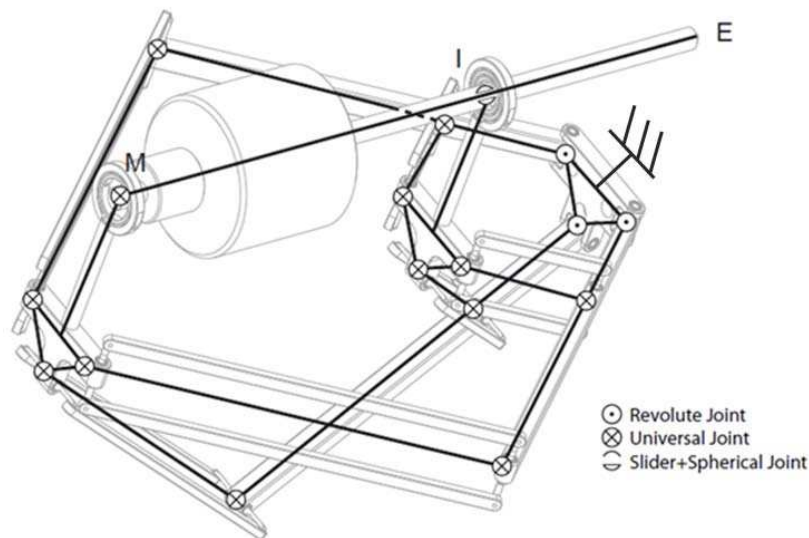
Figure 4-15: Kinematic structure of Dionis Manipulator (Beira et al., 2011a)

4.2.3 Manipulator Kinematics

The kinematics of Delta-like manipulators has been extensively studied by several authors (Clavel, 1988a, Tsai, 1999). Although they look similar in form, *Dionis* kinematics is simpler due to the dimensional constraints imposed by the *Intercept Theorem* as well as by the geometrically equivalent zero-sized platforms simplification (represented in Figure 4.10). Although the RCM might not be completely stationary in a real prototype, due to a deficient

production of the different components, in the following analysis it is assumed so, with the *Intercept Theorem* constraints perfectly fulfilled.

4.2.3.1 Inverse Geometrical Model

For the inverse geometrical model, the objective is to find the set of joint angles, $(\alpha_1, \alpha_2, \alpha_3)$, that achieve a certain position of the end-effector, $E(e_x, e_y, e_z)$ in the $F(x,y,z)$ coordinate system.

Considering the geometry of the manipulator, shown in Figure 4-11, it is possible to write the following relations for each limb:

$$d_{1n} + d_{2n} = m = e - l \tag{3}$$

where l is the vector going from point M to point E and:

$$^F e = \begin{bmatrix} e_x \\ e_y \\ e_z \end{bmatrix}, \quad ^F l = -\frac{e}{\|e\|}\|l\|, \quad ^F d_{1n} + {}^F d_{2n} = {}^F R_L \left({}^{L_n} d_{1n} + {}^{L_n} d_{2n} \right), \tag{4}$$

$$^F R_L = \begin{bmatrix} \cos\theta_n & -\sin\theta_n & 0 \\ \sin\theta_n & \cos\theta_n & 0 \\ 0 & 0 & 1 \end{bmatrix}, \quad {}^{L_n} d_{1n} + {}^{L_n} d_{2n} = \begin{bmatrix} d_1\cos\alpha_n + d_2\sin\gamma_n\cos(\alpha_n + \beta_n) \\ d_2\cos\gamma_n \\ d_1\sin\alpha_n + d_2\sin\gamma_n\sin(\alpha_n + \beta_n) \end{bmatrix}, \tag{5}$$

Expanding those relations in the $L_n(u_n, v_n, w_n)$ coordinate frame, the analytical expressions of α_n, β_n and γ_n, for the three limbs, can be obtained.

4.2.3.2 Direct Geometric Model

The Direct Geometrical Model describes the position of the end-effector, $E(e_x, e_y, e_z)$, given a set of known actuated joint angles, $(\alpha_1, \alpha_2, \alpha_3)$, in the $F(x,y,z)$ coordinate frame.

Given its special kinematics, the first step to solve the direct geometric model of this manipulator consists in finding the solutions for point M. The surface of each sphere represents the range of motion of distal end of the nth limb, when point B_n is located at a known position. The radius of each sphere is equivalent to length d_2 and the intersection points of the three sphere surfaces are the possible positions that point M may occupy. The equation of the sphere generated by the nth limb is given by:

$$(m_x - b_{nx})^2 + \left(m_y - b_{ny}\right)^2 + (m_z - b_{nz})^2 = d_2{}^2 \tag{6}$$

Finally, after calculating the coordinates of point M, the end-effector coordinates are obtained by:

$$e = -\frac{m}{\|m\|}(\|l\| - \|m\|) \tag{7}$$

which solves the direct kinematics problem for this manipulator.

4.2.4 Velocity and Statics Analysis

Due to the relatively high complexity of the inverse kinematics equations for this manipulator, it is not computationally efficient to calculate the Jacobian Matrix, differentiating those relationships with respect to x, y and z. As an alternative, the velocity of the end-effector, v_E is obtained by differentiating the equation of the limb geometrical constraints with respect to time:

$$v_E = v_M - \left(\frac{m}{\|m\|}\|l\|\right)' \tag{8}$$

which, after some expansion, results in three scalar equations that can be arranged as follows:

$$J_x v_M = J_q \dot{q} \tag{9}$$

where the direct and inverse kinematics Jacobian matrices are respectively:

$$J_x = \begin{bmatrix} j_1^T \\ j_2^T \\ j_3^T \end{bmatrix}, \qquad J_q = \begin{bmatrix} b_1 & 0 & 0 \\ 0 & b_2 & 0 \\ 0 & 0 & b_3 \end{bmatrix} \tag{10}$$

with:

$$j_n = \begin{bmatrix} cos(\alpha_n + \beta_n)sin\gamma_n cos\theta_n - cos\gamma_n sin\theta_n \\ cos(\alpha_n + \beta_n)sin\gamma_n sin\theta_n - cos\gamma_n cos\theta_n \\ cos(\alpha_n + \beta_n)sin\gamma_n \end{bmatrix}, \text{for } n = 1,2,3 \tag{11}$$

$$b_n = a \, sin\beta_n sin\gamma_n, \text{ for } n = 1,2,3 \tag{12}$$

and

$$q = \begin{bmatrix} \dot{\alpha}_1 \\ \dot{\alpha}_2 \\ \dot{\alpha}_3 \end{bmatrix} \tag{13}$$

4.2.5 Singular Configurations

The identification of singular configurations is an important issue that must be addressed at the first stages of mechanisms design. This topic has been studied for a long time (Gosselin and Angeles, 1990) and comprehensive classifications have been proposed in past years (Zlatanov et al., 1998). The most remarkable cases are usually called (1) inverse kinematics singularities, when an infinitesimal motion of a limb does not yield a motion of the platform (that "loses" one or more DOF in certain directions) and (2) direct kinematics singularities, when the moving platform can move along certain directions even if all actuators are completely locked (and the mechanism "gains" one or more DOF). From the previous section:

$$v_E = f(m, v_M) \tag{14}$$

Which can be simplified by:

$$v_E = f(m, J_x^{-1} J_q \dot{q}) \tag{15}$$

To summarize, singularities can occur when:

- all the pairs of the bars composing the parallelograms are parallel - the moving platforms have three degrees of freedom and move along a spherical surface rotating about an axis perpendicular to the platforms, Figure 4-16a.
- two pairs of bars composing the parallelograms, for each moving platform, are parallel - the moving platforms have one degree of freedom, moving in only one direction Figure 4-16b.
- two pairs of bars composing the parallelograms are in the same plane or in parallel planes - the moving platforms have only one degree of freedom, rotating about a vertical axis, Figure 4-16c.
- three parallelograms, of each moving platform, are placed at three parallel planes or on the same plane - the platforms keep three DOFs, namely: two

rotations about axes contained in the plane of the platform and one translation perpendicular to the same plane, Figure 4-16d.

a)   b)

c)   d)
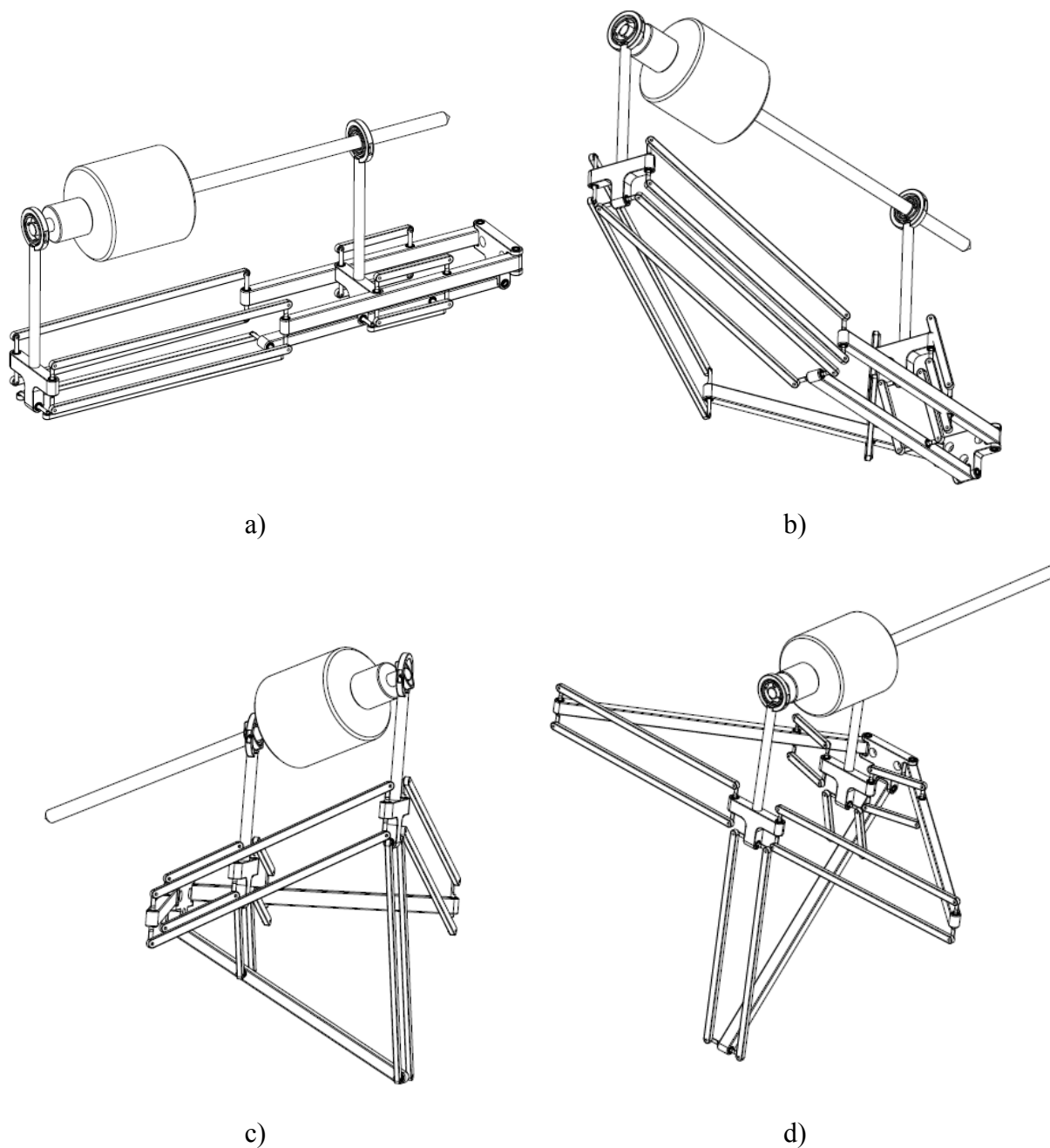
Figure 4-16: Example of singular configurations (Beira et al., 2011a)

4.2.6   Workspace Analysis

Workspace is one of the most important issues when designing a parallel manipulator since it determines the region that can be reached and, therefore, it is a key point in robotic mechanism design (Gosselin and Angeles, 1990). The designs based on a workspace calculation use methods in which the first step is to develop an objective function that might be reached by the result. The result is generally obtained by recursive-numerical-algorithms

(Zlatanov et al., 1998). These methodologies have the disadvantage of being extremely time consuming, due to the highly non-linear objective functions that are manipulated. In this paper, the workspace representation of the *Dionis* manipulator is analyzed geometrically.

Knowing in advance all the singular configurations presented in the previous section, it is possible to introduce some constraints in the manipulator's design in order to avoid those postures and collisions between mechanism components. Therefore, it was decided to analyze the workspace of the *Dionis* manipulator in the boundary of those conditions, where $\alpha_n \in [0, \pi/2]$, $\gamma_n \in [0, \pi]$ and $d_1 = d_2 = d$.

For a given position of the moving point *M*, the position of the end-effector, *E*, can be determined by a translation through vector *l*. In other words, the workspace generated by the nth limb is a translation of the reachable workspace of point *M* by *l*. In addition, the motion of the limb is constrained, not only by the joint limits, but also by the other limbs. Therefore, the workspace of *Dionis* Manipulator is the intersection of the three individual reachable workspaces generated by the three limbs.

According to the specific *Dionis* limb design, the workspace of the limb point *M* is a solid sphere with radius *d*, if there are no joint limitations for the revolute joints. However, point B_n (b_{nx}, b_{ny}, b_{nz}), which is able to move along a circular path in the *ZX* plan, is limited to avoid singular configurations and collisions with other components of the mechanism. The workspace of each limb is the solid envelope shown in Figure 4-17:

Figure 4-17: Profiles generating the nth limb workspace (Beira et al., 2011a)

In order to calculate and visualize the workspace for each limb, the following steps have to be achieved:

1. parallel translation of profile P_1 (generated by the path of point M at full range of γ_n, for $\alpha_n=0$) along the guide-line g, until P_2;
2. rotation of profile P_2 along axis a_1, until P_3;
3. parallel translation of profile P_3 along the guide-line g, up to P_4;
4. rotation of profile P_4 along axis a_2, back to P_1 again.

The corresponding analytical equations of these profiles and guide lines are the following:

- P_1: $u_n = d \wedge v_n^2 + w_n^2 = d^2$
- P_2: $u_n = 0 \wedge v_n^2 + (w_n - d)^2 = d^2$
- P_3: $w_n = d \wedge u_n^2 + v_n^2 = d^2$
- P_4: $w_n = 0 \wedge (u_n - d)^2 + v_n^2 = d^2$ (16)
- g: $v_n = 0 \wedge u_n^2 + z^2 = d^2$
- a_1: $w_n = d \wedge u_n = 0$
- a_2: $w_n = 0 \wedge u_n = d$

It is possible to generate the surfaces shown in Figure 4-18.
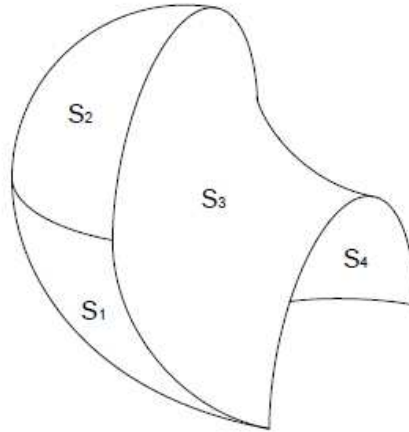
Figure 4-18: Workspace surfaces for each limb (Beira et al., 2011a)

The resulting surfaces, $s_i(i = 1, 4)$ in Figure 4-18 are generated from the following equations:

- s_1: $u_n^2 + (w_n - (d^2 - v_n)^{1/2})^2 = d^2$
- s_2: $u_n^2 + v_n^2 + (w_n - d)^2 = d^2$ (17)
- s_3: $u_n^2 + (v_n - (d^2 - w_n)^{1/2})^2 < d^2$
- s_4: $u_n^2 + (v_n - d)^2 + w_n^2 = d^2$

Once these expressions have been identified, it is possible to represent them in the 3D space, using *Wolfram Mathematica 7*, and visualize the workspace of a single link of the manipulator, as in Figure 4-19.
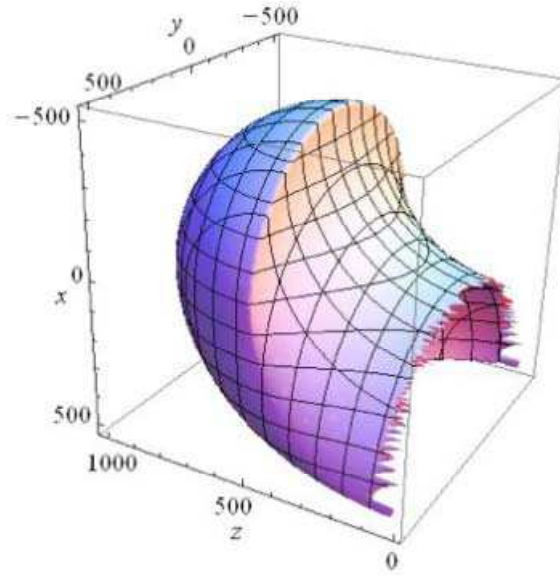
Figure 4-19: 3D representation of the workspace of the distal point, *M*, for a single limb (Beira et al., 2011a)

The workspace of *M,* considering the entire manipulator, is the result of the intersection of the workspaces of the 3 limb workspaces, Figure 4-20.
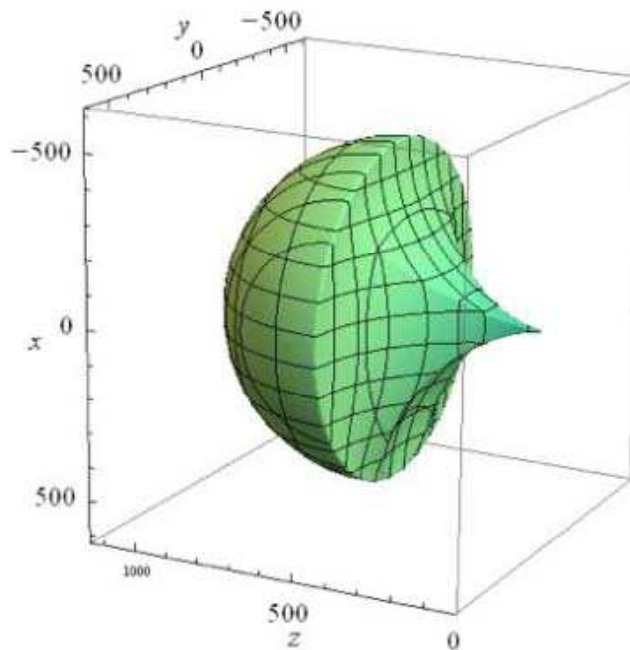
Figure 4-20: 3D representation of the workspace of the distal point, *M*, for a single limb (considering $\alpha_1 = 0$ rad, $\alpha_2 = \pi/2$ and $\alpha_3 = -\pi/2$ rad) (Beira et al., 2011a)

Having the Workspace of point *M*, W_M, defined, the workspace of *E*, W_E, is calculated using Eq. 13, Figure 4-21. On the left part of the plot, for $z > 0$, we may find the workspace of *M*,

while the workspace of *E* is represented for *z* < 0. As can be seen by the workspace distribution around point O (0,0,0), the stationary of the mechanism's RCM is verified.
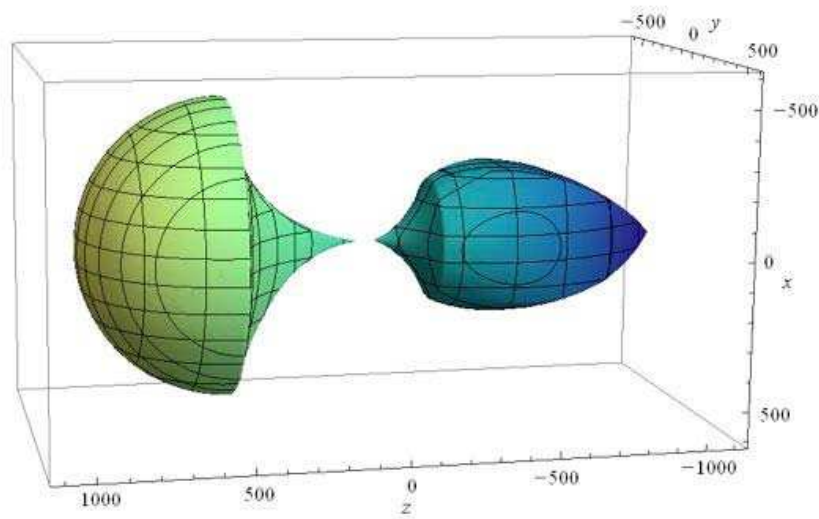
Figure 4-21: 3D representation of the workspace of the distal point for a single limb, *M,* (*z* > 0) and the manipulator end-effector, *E,* (*z* < 0) (Beira et al., 2011a)

4.2.7   Implementation

In this section, the practical implementation of the Dionis manipulator is described. The required internal workspace, entry port DOFs, payload requirements and extracorporeal volume represent severe constraints on it mechanical design. Compactness has therefore been among the most important design issues, besides structural stiffness and precision.

4.2.7.1   Workspace

In order to reach a desired work volume, required for a MIS application, an iterative process was performed and the sizes of the different links composing the manipulator were defined. The final dimensions used in the several components of the mechanism are shown in Figure 4-22.
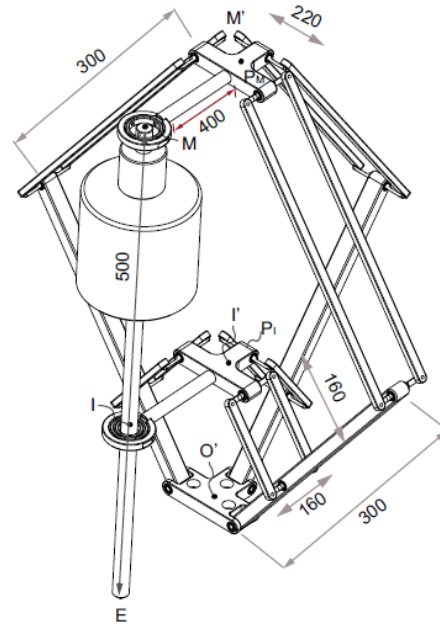
Figure 4-22: Overall dimensions of the Dionis Manipulator (Beira et al., 2011b)

The reachable workspace of the Dionis Manipulator can be represented easily using the commercial CAD software such as *SolidWorks 2009*, having the shape shown on Figure 4-23. It can be seen that it fills the patient's abdominal cavity, meeting the specifications in terms of task workspace, for MIS.
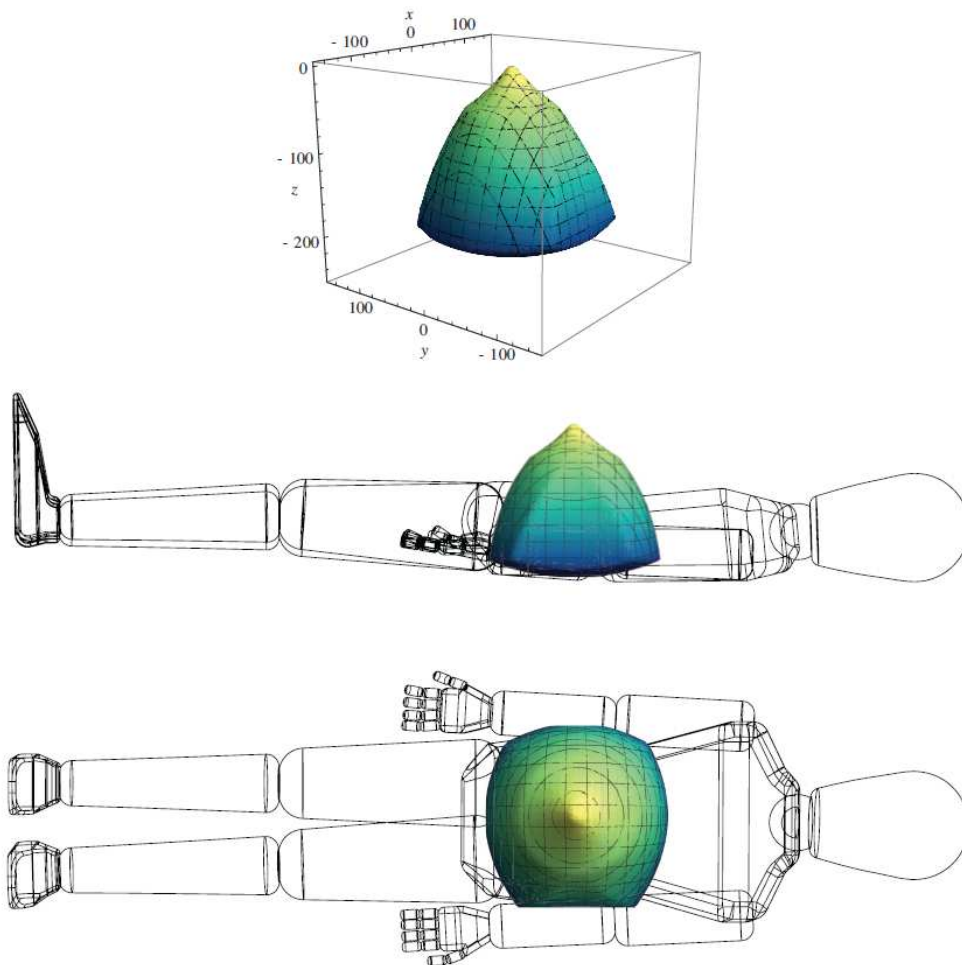
Figure 4-23: Workspace of the Dionis Manipulator with respect to the patient (Beira et al., 2011b)

4.2.7.2   Actuators Selection and Prototype Details

The dynamic simulation of the manipulator enables the appropriate selection of the actuators for this specific surgical application. This choice is done considering the maximum moving speed and the maximum torque required for a set of typical trajectories of the surgical instrument's distal part. A simplified simulation model of the robot was developed in *COSMOSMotion®*, a complete functional virtual prototyping package for *SolidWorks®*, powered by *ADAMS®*, Figure 4-24.
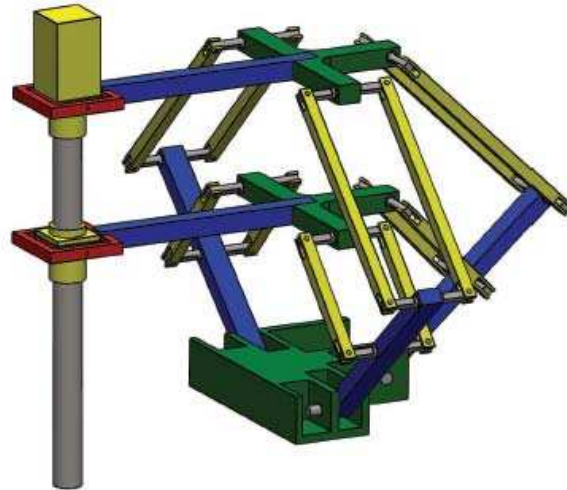
Figure 4-24: Simplified Simulation Model of the Dionis Manipulator (Beira et al., 2011b)

Considering the required joint velocities, the dynamic simulation of the robot in *COSMOSMotion®* enables the calculation of the suitable set of torques for the execution of specific movements. In order to do so, the robot was programmed to move between its critical positions (those where the required torque is maximum) through smooth movement profiles, in certain periods of time. Several trajectories have been considered and analyzed. As an example, Figure 4-25 shows one of the most critical trajectories of the system.
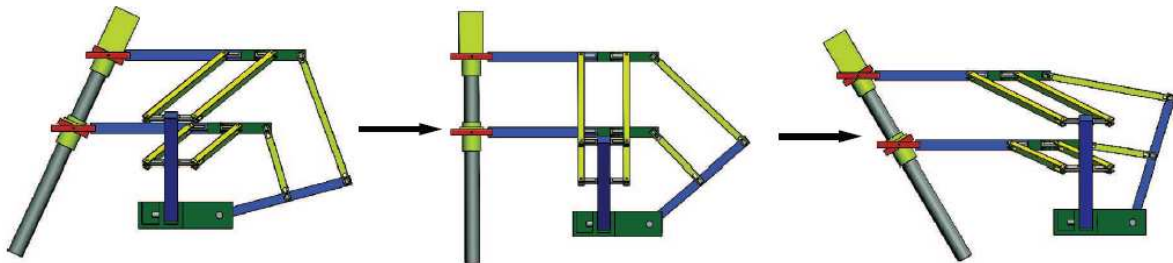
Figure 4-25: Example of a Critical Trajectory

The trajectories were generated in the joint space and the motion profiles were used as input for the motors, with an accelerating/decelerating period of 20% of the overall trajectory time. Figure 4-26 presents the torque evolution for the three base actuators in the most critical movement of the system. At the end position, the maximum torque reaches almost 70 Nm for the most charged actuator.
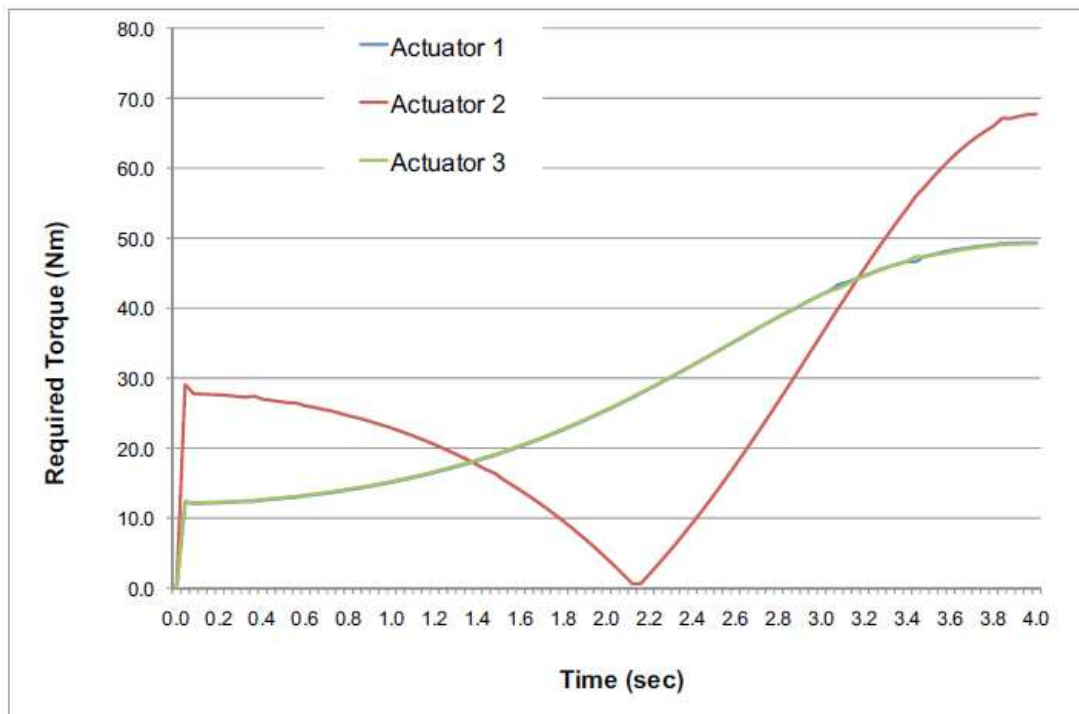
Figure 4-26: Evolution of the Required Torque for each of the Base Actuators (Beira et al., 2011b)

Considering the result of the dynamic simulations, all the system actuators were selected. For the first three degrees of freedom, the chosen actuator is the harmonic drive FHA-25C (Harmonic Drive Systems, Japan). This actuator additionally integrates an absolute encoder with 15 bits of resolution and a safety brake and is controlled by the amplifiers type SC-610. For the fourth degree of freedom of the robot (rotation about the IT axis), the chosen actuator is the RSF-11B (of the same manufacturer) that features an incremental encoder with 1000 counts per turn of resolution. This motor uses the HA-680 amplifier, Table 4.1.

Table 4.1: Actuator and Encoder Characteristics of the Dionis Manipulator

Component	Property	Value
AC Servo Actuator	Max output torque	260 Nm
FHA-25C-160-B	Nominal torque	100 Nm
	Brake holding torque	160 Nm
	Harmonic drive gear ratio	1:160
	Max speed	28 rpm
	Mechanical time constant	11 ms
Absolute Encoder	Resolution	15 bits
AC Servo Actuator	Max output torque	11 Nm

	RSF-11B-100	Nominal torque	6 Nm
Incremental Encoder	Harmonic drive gear ratio		1:100
	Max speed		60 rpm
	Resolution		1000 cpt

The base actuators are fixed at the bottom (robot base platform) while the fourth one actuates directly the proximal extremity of the insertion tube, by a timing belt system. The final CAD model is shown in Figure 4-27.
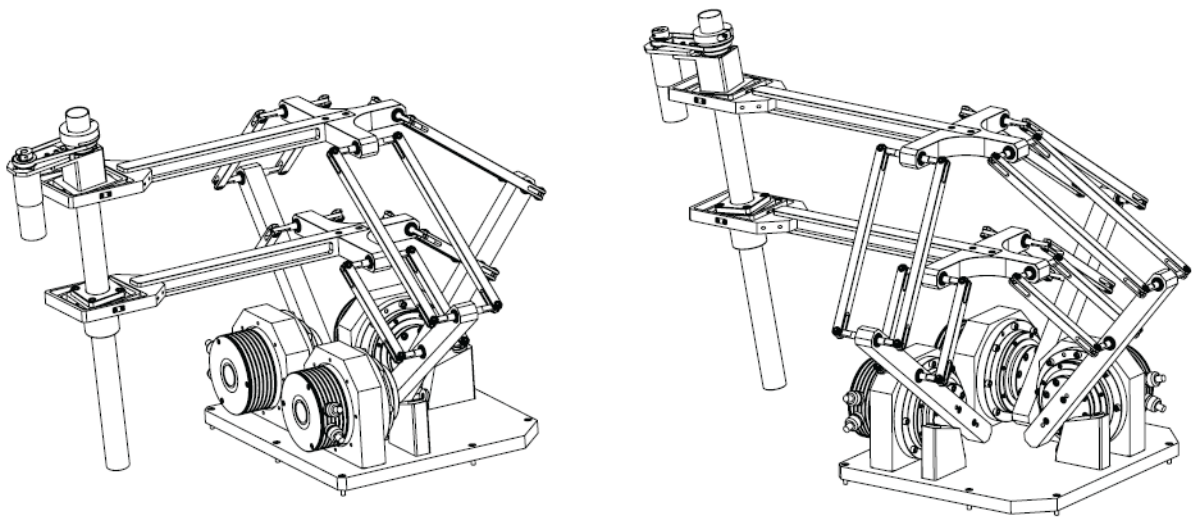
Figure 4-27: CAD Model of the Dionis Manipulator (Beira et al., 2011b)

Safety stops are mounted on the input links to serve as mechanical limits to protect the mechanism from going outside its desired workspace. The different links of the mechanism are connected between each other by revolute and universal joints, composed by sets of ball bearings, whose selection was also based on the reaction forces given by the dynamic analysis. Figure 4-28 shows the final produced prototype of the Dionis Manipulator.

Figure 4-28: Prototype of the Dionis Manipulator

4.2.7.3 Stiffness Analysis

The setup used for the assessment of the structural stiffness of the manipulator is shown in Figure 4-29. The measurements were made at the end-effector, with the three input joint locked. A dial indicator measured the deflection of the overall system at the endpoint, while the applied load was being gradually increased and measured. A *XFTC320* load cell with a range of ±50 N from the company *Measurement Specialties^{TM}* was used.
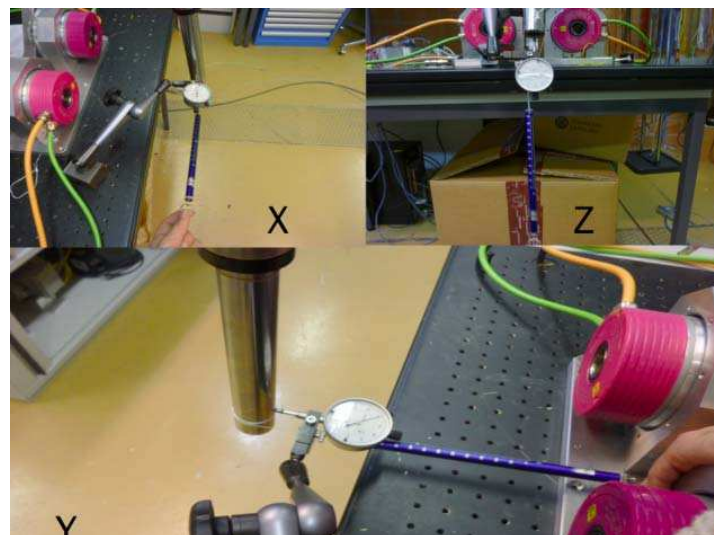
Figure 4-29: Stiffness measurement in x, y and z directions

The corresponding stiffness values can be seen in the table 1, having been measured according to (Madhani et al., 1998). As can be seen, the stiffness value along the *x* direction is relative small compared to the stiffness values in the *y* and *z* direction.

Table 1:

Table 2: Stiffness values along *x*, *y* and *z* direction

Direction	Stiffness
x	2000 N/m
y	30000 N/m
z	40000 N/m

Although these values of structural stiffness are within the reasonable values, when compared to standard laparoscopic instruments, Figure 3-5, they can be considerably increased by performing some optimizations on the structural design of the system. Particularly, by increasing the diameter of the selected shafts of Figure 4-30, the rigidity of the parallelograms composing the Dionis kinematics can be significantly increased, resulting in an overall improvement of the system's stiffness.
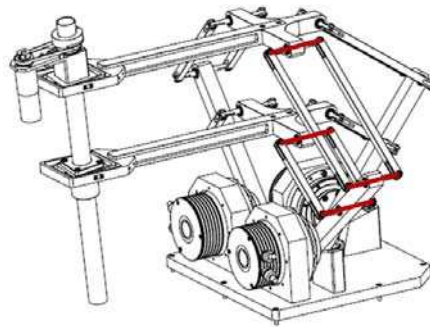
Figure 4-30: Selected shafts to be reinforced for stiffness improvement

4.3   Conclusions

This chapter describes the development of a new mechanical system that can be applied in different external positioning manipulators for minimally invasive surgical procedures. The proposed system provides enough dexterity to position MIS instruments at any location within the abdominal cavity. The implementation of a unique parallel kinematics results in a 4-DOF hybrid mechanism, called *"Dionis"*, which provides three rotations and one translation, with a fixed remote center of motion. A significant advantage of this novel design is its compactness, being able to be placed close to the operation table and allowing direct access to the patient without removing the manipulator. Consequently, safety is improved and considerable space in the operating room is saved. These features are the main merits of *Dionis* as compared to existing solutions. In addition, compactness, simplicity and robustness make the Dionis Manipulator a highly qualified candidate for MIS procedures.

5 Micro Manipulator for MIS

5.1 Introduction

This chapter presents the study and development of a new mechanical system that can be used in compact multi-DOF micro-manipulators for MIS. The concept enables the use of a cable driven transmission for miniature robot manipulators, with different types of revolute joints, making it possible to achieve high levels of dexterity and stiffness compared with existing solutions. Although it can be used in different surgical systems, it was initially developed to be applied on the endoscopic unit of a new SST Surgical Platform, described in Chapter 4.

After a short description of its surgical application, the overall architecture of the SST endoscopic unit is presented, together with its specific dexterity requirements. Then, a review of existing multi-DOF mechanical systems for robotic micro-manipulators is performed and their main limitations are identified. After that, the concept of the new mechanical system is described and its geometrical models are analysed. Finally, a 3-DOF prototype, incorporating the developed mechanical system, is designed and produced to validate the suitability of this concept to be integrated in micro-robotic systems for MIS procedures.

5.2 Concept Overview

The main aim of the SST Surgical Platform consists in bringing bi-manual manipulation and standard surgical procedures inside the abdominal cavity. This should be achieved by an endoscopic micro-system, stabilized with an external positioning manipulator and inserted through a single incision on the abdominal cavity, Figure 5-1.
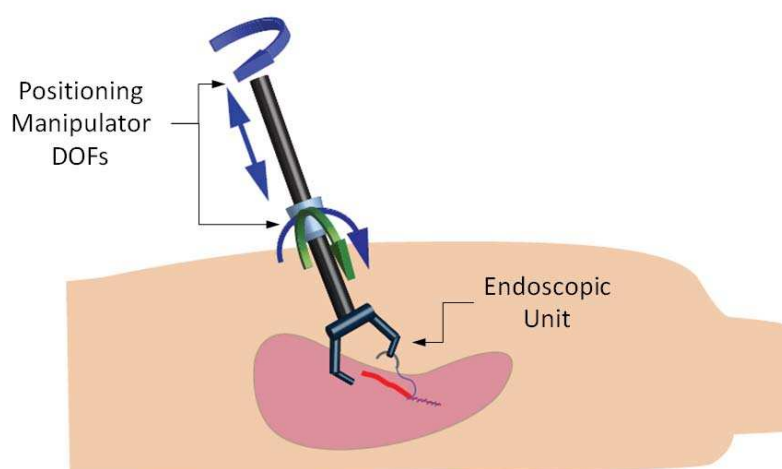
Figure 5-1: Target Concept of the SST Endoscopic Unit

This target concept aims to give the impression to surgeons that they are operating inside the patient's body with their own two hands. The achievement of this goal would not just give back to the surgeon the performance skills, which were lost when procedures were converted from open to minimally invasive surgery, but also the possibility of navigation through all the quadrants of the abdomen, using a single access port.

The Endoscopic Unit should comprise two multi-DOF micro-manipulators and should be equipped with an endoscopic camera system, Figure 5-2. In order to provide the desired articulation needed to perform complicated surgical procedures, like pulling and cutting tissue or suturing, those internal DOFs given by the Endoscopic Unit, should exhibit high dexterity, high payload capacity, stiffness and precision. The stereoscopic camera should be located between the two micro-manipulators, providing eye-manipulator alignment similar to human eye-hand alignment, and thus enhancing the intuitiveness of the system.
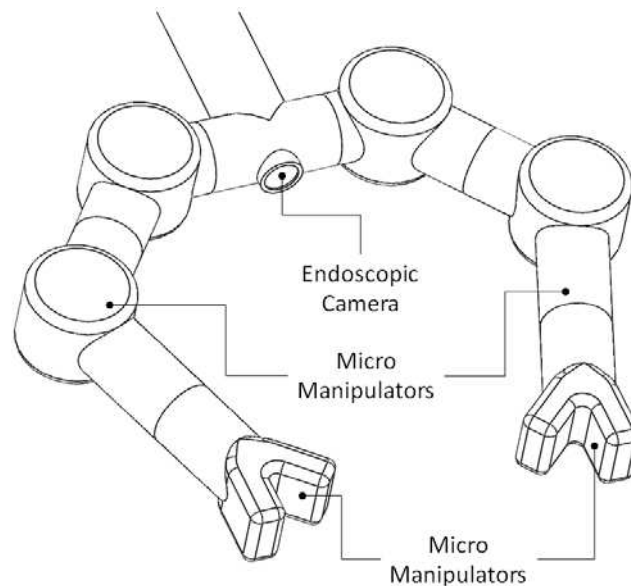
Figure 5-2: Internal Architecture of the SST Endoscopic Unit

The stable fixation and movement of the Endoscopic Unit within the abdominal cavity is provided by an insertion shaft, which corresponds to the output link of the external positioning manipulator described in Chapter 4. The overall view of the complete slave unit of the SST Platform is shown in Figure 5-3.
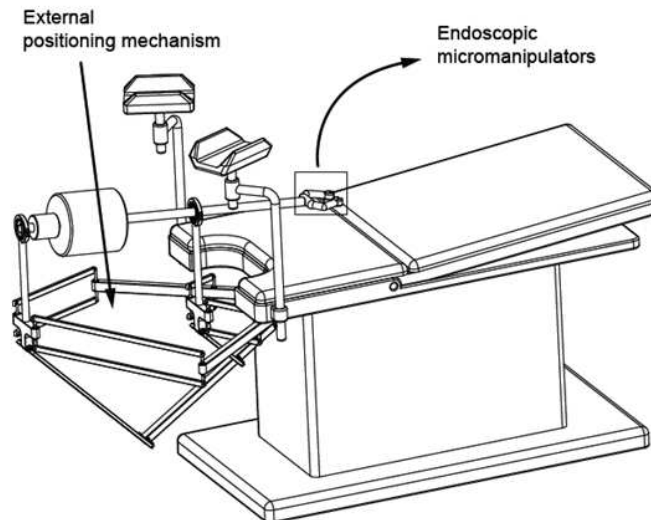
Figure 5-3: Overview of the complete SST Platform (Beira et al., 2011a)

The master interface of the SST Surgical Platform comprises a set of two manipulators, as the one shown in Figure 5-4 (CARRERAS, 2012). Each master manipulator is connected to its respective endoscopic manipulator, in such a way that the surgeon's hand movements are reproduced at the Endoscopic Unit. Thus, the two handles of the master interface assume the same spatial orientation and relative position as the two micro-manipulators of the Endoscopic Unit.

Figure 5-4: Master Interface of the SST Surgical Platform (CARRERAS, 2012)

5.3 Internal Dexterity Requirements

Since the surgeon should have enough mobility to perform complicated surgical procedures, the DOFs provided by the endoscopic unit should have sufficient dexterity inside the patient's body. In order to be as intuitive to control as possible, the degrees of freedom should designed to resemble a simplified human arm.

Anthropomorphic joint approximations can be modelled at varying degrees of accuracy and complexity (Morrey and An, 1998, BRIAN and MARCUS, 1999) and the level of complexity needed for a suitable representation depends highly on the desired tasks to be performed. For this specific system, since the aim is to control the position and orientation of the end-effector in the 3D space, the movement of each anthropomorphic micro-manipulator should be achieved through the articulation of six single-axis revolute joints plus the gripper.

The target kinematic model is represented in Figure 5-5 and the manipulator's DOFs are labelled from 1 to 7, as we move from the proximal to the distal extremity of each micro-manipulator, as shown in Figure 5-5.
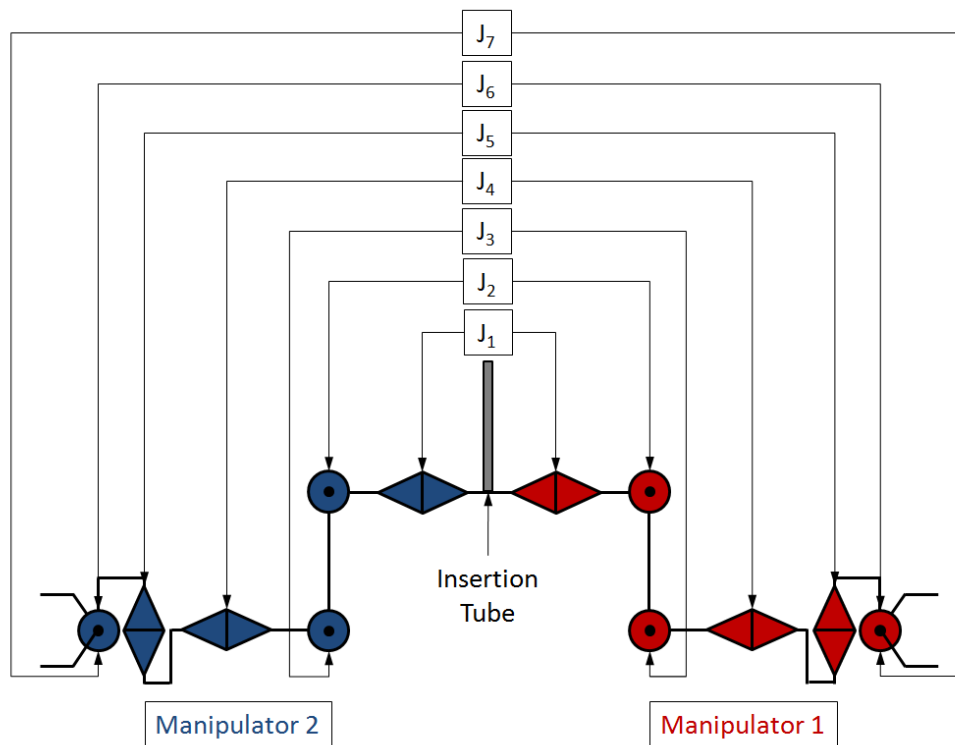
Figure 5-5: Kinematic model of the micro-manipulators

The shoulder abduction– adduction and flexion-extension are then modelled as a composition of two intersecting axes, J_1 and J_2. The elbow flexion-extension is modelled by a single axis parallel to the second shoulder axis, J_3. Forearm prono-supination takes place between the elbow and wrist joints as it does in the physiological mechanism, J_4, while two intersecting orthogonal joints, J_5 and J_6, represent the wrist flexion–extension and radial-ulnar deviation. Finally, the gripper actuation is represented by J_7 and is a result of the actuation of both gripper blades about the same axis.

5.4   Motion Transmission in Micro Manipulators for Surgery

The development of multi-DOF robotic micro manipulators capable of reproducing complex human hand movements in minimally invasive procedures is one of the most important challenges in the field of telemanipulated robotic systems for surgery. On one hand, it is important to increase the dexterity of the end-effectors inside the body, overcoming limited maneuverability in the abdominal cavity. On the other hand, the design should be kept as compact as possible. The final goal is to manage this trade-off, providing the surgeon with user-friendly aids, while keeping the procedure minimally invasive for the patient.

However, although several robotized devices have been proposed to add additional DOFs at the tip of the instruments (Cepolina and Michelini, 2004), surgical manipulations are still restricted due to the limited number of DOFs, which can rarely provide enough dexterity to the surgeon.

Some end-effectors, specially designed for robotic abdominal operations are described along this section, having different concepts of structure, actuation and transmission. In most of the cases, they are mainly distal internal subsystems of wider surgical robotic platforms rather than stand-alone instruments.

5.4.1   Cable Driven Actuation

Cable driven surgical manipulators use thin ropes to transmit movement from the exterior to the distal part of the system. This allows the actuators to be placed outside the patient body, being selected without major weight/volume constraints. As a consequence, this kind of systems can be extremely compact while being able to produce significant forces.

Regarding their mechanical architecture, cable-driven manipulators can be divided in flexible or rigid systems, according to the stiffness of their structural components.

5.4.1.1   Flexible Structure

Cable driven systems with flexible structure directly moved from the catheter concept or classic endoscopes (flexible oblong structures, driven by the surgeon from outside the body), and lead to a new class of surgical devices, where two or more micro-manipulators are placed on the distal extremity of either a flexible oblong element or a sequence of small segments articulated to each other by pivot joints. In most cases, a Bowden cable is used, decreasing dramatically their force-reflecting properties. In addition, and due to their mechanical architecture, this family of systems cannot provide enough stiffness, payload, dexterity and precision to perform complex surgical tasks.

One of the best known flexible surgical systems, the *Remote Microsurgery System*, is a micro-manipulator developed at Nagoya University, Department of Micro System Engineering (Ikuta et al., 2002). The target of this work consists in performing microsurgery in deep, narrow sites of the human body. It is similar to a classical endoscopic instrument, which limits

the implementation of an effective force feedback. The system uses a flexible guide tube (Figure 5-6), through which it can be inserted into the desired operation area, having a cable driven micro-manipulator with 7 DOF in the distal extremity, actuated by a decoupled wire driven mechanism. Since the wires for driving the distal joints always pass through the axis of the proximal joints, the path length of the driving wire remains constant regardless of the angle at which the base joint is bent. Therefore, there is theoretically no interference of the proximal joints on the distal joints. However, due to its flexible nature, the system cannot be inserted easily in narrow space between the tissues or organs, and cannot be stabilized completely when approaching target (Yagi et al., 2006). The fact that the cables are sliding directly on structural components, instead of passing by idler pulleys, also bring additional friction to the system.
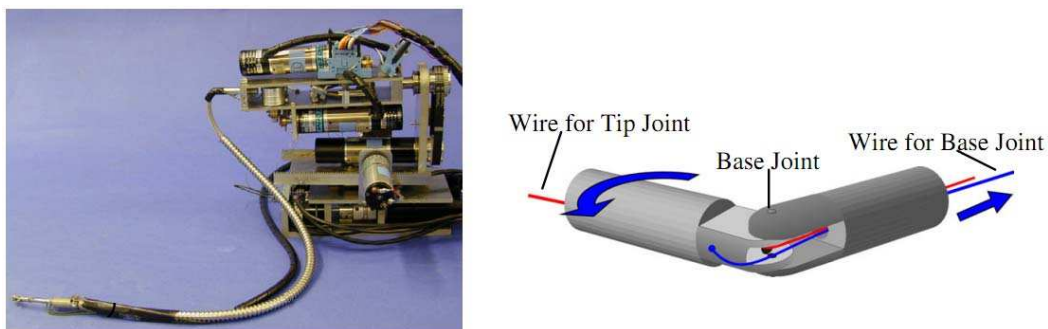
Figure 5-6: The Remote Microsurgery System (Ikuta et al., 2002)

Another flexible device, the *ViaCath System*, developed by *EndoVia Medical*, is one of the first generation of teleoperated robots for endoluminal surgery (Abbott et al., 2007). The system uses long-shafted flexible instruments that run in conjunction with a standard endoscope. The two articulated robotic micro-manipulators on the tip are placed in front of the endoscope, allowing the performance of bimanual manipulations under visual control, Figure 5-7. The joints are arranged to reproduce the kinematics of the human arm, with 6 DOF plus the gripper. Cable guides were designed to ensure that the actuation cables travel through the micro-manipulators in a predetermined way, forcing the cables to remain near the pivot axis for any given proximal joint.

The main disadvantages of this system are related with the difficulty to be introduced into the body and insufficient manipulation forces that it can generate (around 0.5N).
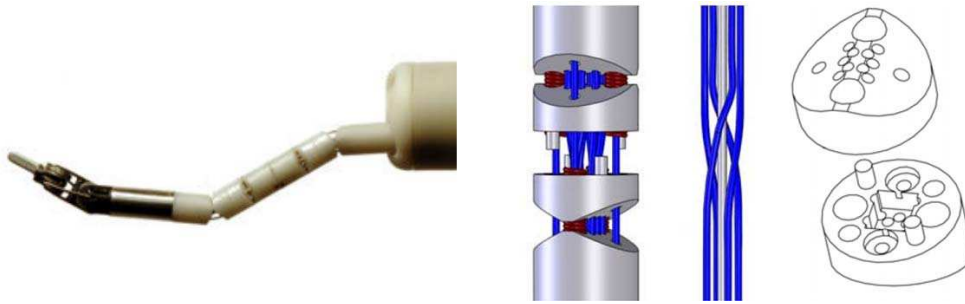
Figure 5-7: *Viacath* – robotic endoluminal surgical system (Abbott et al., 2007)

In 2006, a research group from Nanyang Technological University reported the master–slave surgical robotic system for therapeutic gastrointestinal endoscopic procedures that could also be used for NOTES-related applications (Phee et al., 2008). The developed system includes a long and flexible body that enables advancement of the endoscope through a small incision, Figure 5-8. To make the slave manipulator as intuitive to control as possible, the DOFs for the slave manipulator were designed to resemble a simplified human arm, with 7 DOF each. A Bowden-cable actuation mechanism was used. The actuators were located outside the human body and transmitted power to the mechanism by pulling and releasing flexible tendons in the flexible sheath to control the actuation of the joints. However, using this mode of actuation a considerable amount of friction is generated between the long tendon and the sheath, which subsequently reduce the amount of possible output force at the end manipulator and diminish its force-reflective features. In addition, due to the backlash on the Bowden cables, the control of the joint is imprecise, which makes the system difficult to use for fine procedures.

Figure 5-8: Master–slave surgical robotic system (Phee et al., 2008)

At Columbia University, a flexible robotic platform, the IREP, was developed for single port surgical procedures, using two 5 DOF snake-like continuum robots as slave surgical assistants for tissue manipulation (Xu et al., 2009). The system can be deployed into body cavity through a 15mm skin incision and each snake-like unit has a diameter of 4.2 mm, which can bend at angles between −90∘ to +90∘ in any direction by push and pull modes of three superelastic tubes, Figure 5-9. The force sensing capabilities of the micro-manipulators are investigated in (Xu and Simaan, 2008). However, rigidity and large bending force are not achieved.
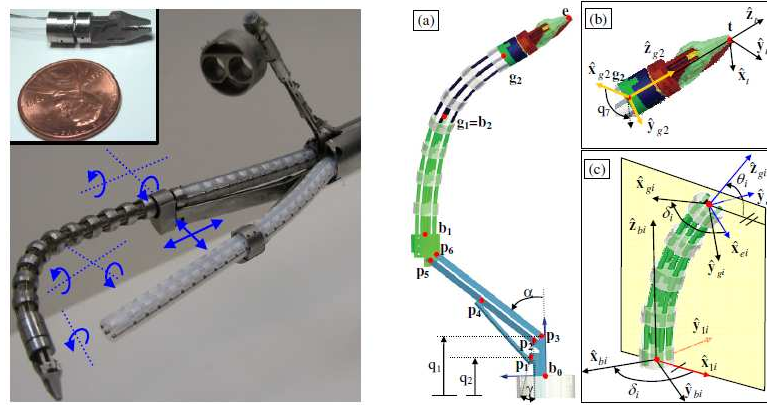
Figure 5-9: System Overview of the IREP Robot (Xu et al., 2009)

An outer sheath for flexible endoscopic manipulators was developed at the University of Tokyo (Yagi et al., 2006). This sheath can switch from flexible to rigid, providing a working path for inserting surgical instruments, Figure 5-10. The flexible mode can be curved into a required shape. The rigid mode can hold the shape of the sheath, and then keep the path for instruments. A serial multi joint model was proposed to realize the flexible mechanism, being composed by a set of frame units which are connected serially. Each unit can passively be rotated to a given angle around the center of the joint. A slider-link mechanism was developed and a gear stopper controlled by air pressure for rigid mode. However, the dexterity this system can provide is extremely far from the minimum requirements to perform precise manipulations.
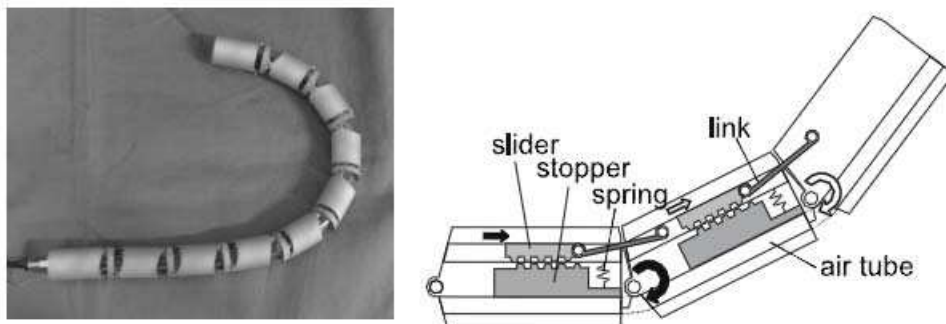
Figure 5-10: Flexible Sheath Prototype (Yagi et al., 2006)

ARTEMIS (Rininsland, 1999) was developed by Karlsruhe Research Centre in Germany for minimally invasive surgery, particularly in the abdominal region. Two cable-driven slave units are guiding the surgical instruments, each consisting of an articulated robotic micro-manipulator. The distal end of the instrument is designed as a multi-link structure (Figure 5-11) which bends by more than 90° and allows to bring the surgical effector precisely into the desired position and to circumvent organs, vessels or nerves. In addition to bending, rotation of the surgical tool at the instrument tip is also possible, providing two additional degrees of freedom do the system. Thus in total six degrees of freedom are

available guaranteeing a reasonable access to any spatial point and motion of the surgical effector (Schurr et al., 1996).
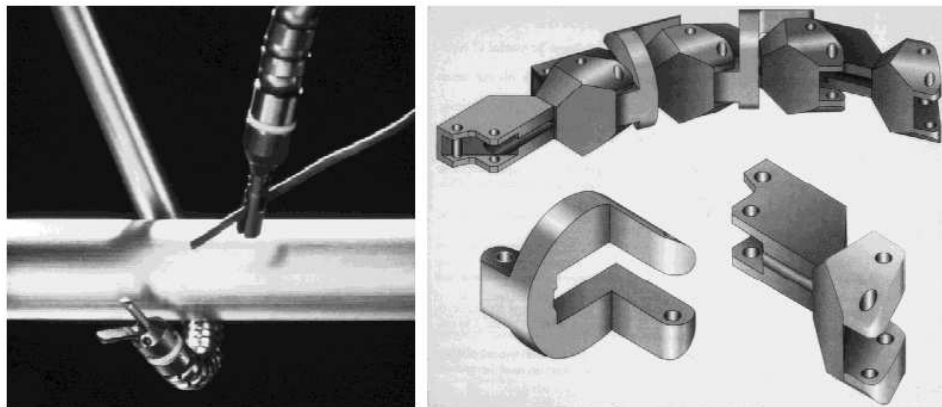
Figure 5-11: ARTEMIS' Slave manipulators (Schurr et al., 1996)

5.4.1.2 Articulated Rigid Structure

As opposed to flexible manipulators, the structural components of articulated rigid systems are unbendable. They have well defined moving joints, corresponding to the actuated degrees of freedom and, although some transmission elements might be flexible, the components through which they are passing are rigid.

The most known articulated rigid system is the *EndoWrist*, a 3 DOF end-effector used in the da Vinci Robot, which is intended to mimic the motion freedoms of the human wrist (Figure 5-12). This system is remotely driven by actuators at the proximal end of the tool module through cable drives inside an 8 mm tool shaft. The wrist orients a grasper, also driven through the internal cables. The roll axis is driven by the external actuator module rotating the entire tool body.
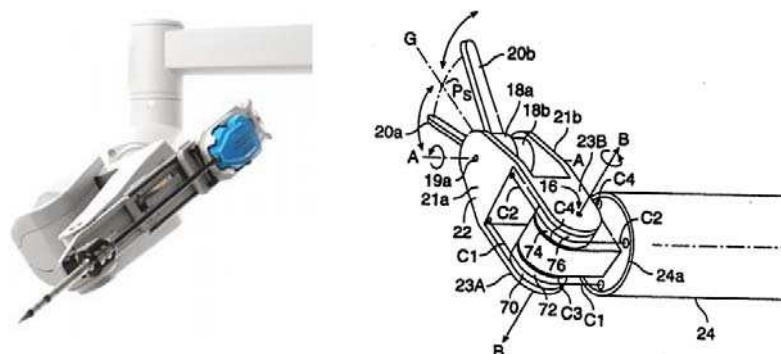
Figure 5-12: The Da Vinci system, the EndoWrists and their cabling topology (Madhani et al., 1998)

At *Korea Advanced Institute of Science and Technology*, KAIST, a group of researchers has developed a new laparoscopic robotic manipulator with increased dexterity (Song et al.,

2009). The main idea of the suggested design was to resemble the human arm, by using a kinematic architecture with 5 internal DOF, behaving like a human elbow and a wrist, Figure 5-13. A differential mechanism is used in the elbow joint, enabling the actuation of the 2 proximal DOFs. Although the dimensions and force performances of the system are not specified, it is claimed in (Song et al., 2009) that, thanks to the steel cable driven actuation, the payload and stiffness of the system are suitable for the performance of standard surgical tasks.
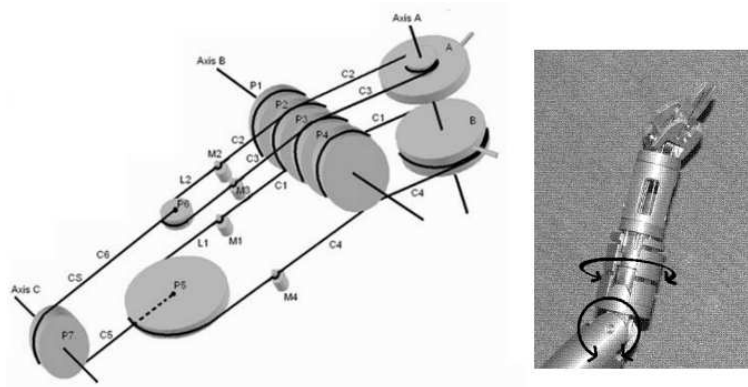
Figure 5-13: Laparoscopic robotic manipulator form Korea Advanced Institute of Science and Technology (Song et al., 2009)

5.4.2   Gear Transmission

The Michigan State University College of Engineering proposes the Dexterous Articulated Linkage for Surgical Applications (DALSA), designed for minimally invasive procedures (Minor and Mukherjee, 1999). Gears and gear links compose this 3 DOF tool, Figure 5-14. The device rotates the surgical tip by gears and actuates the gripper by a cable. Three segments form the spine, each allowing a 60° rotation for an overall 180° articulation (Minor and Mukherjee, 1999). DALSA is about 36 mm long, can pass through a 10 mm port, and is capable of applying forces in the range of 4.4 N. The tool is compact, while assuring high load capacity, and fine motion capability.
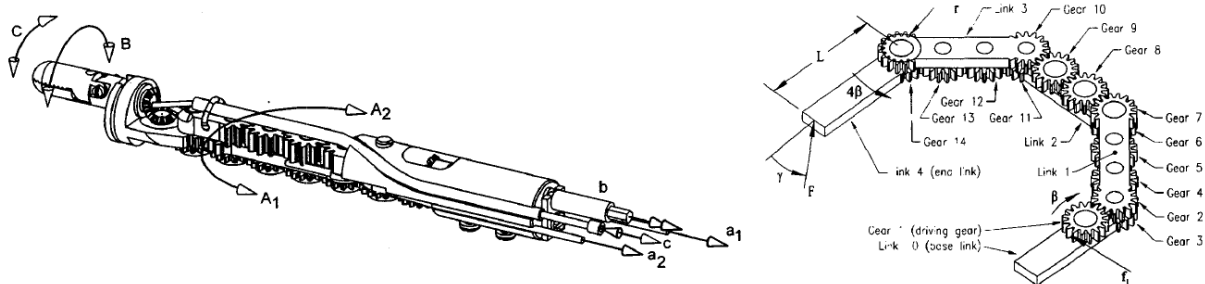
Figure 5-14: Dexterous Articulated Linkage for Surgical Applications (DALSA) (Minor and Mukherjee, 1999)

5.4.3 Rigid Links

In order to improve the rigidity and the sterilization capability of the manipulator, multi-DOF robotic forceps manipulators, which use methods different from cable actuation, have been developed.

A linkage-driven micro-manipulator that does not use cables for bending or gripping motions was developed by the *University of Tokyo*, designed as a part of the minimally-invasive surgical system in order to realize complex tasks in an abdominal cavity (Arata et al., 2005, Takahashi et al., 2006). The system has 3 DOF, consisting of a β_1-axis and a β_2-axis, which realize independent blade motions (grasping motions), and an α-axis, which realizes a bending motion perpendicular to the blade motions β_1 and β_2, Figure 5-15. All joints of this mechanism consist of two-dimensional joins, such as pins and holes. The three linear actuation motions of the axes of Link$_1$, Link$_2$ and Link$_3$ are driven by DC servomotors and ball screws. However, even for a relatively simple kinematic model, this kind of mechanism is not able to provide high range of motions to the different joints (bending motions of ± 70 degrees in the α -axis, and ± 50 degrees in the β –axis).
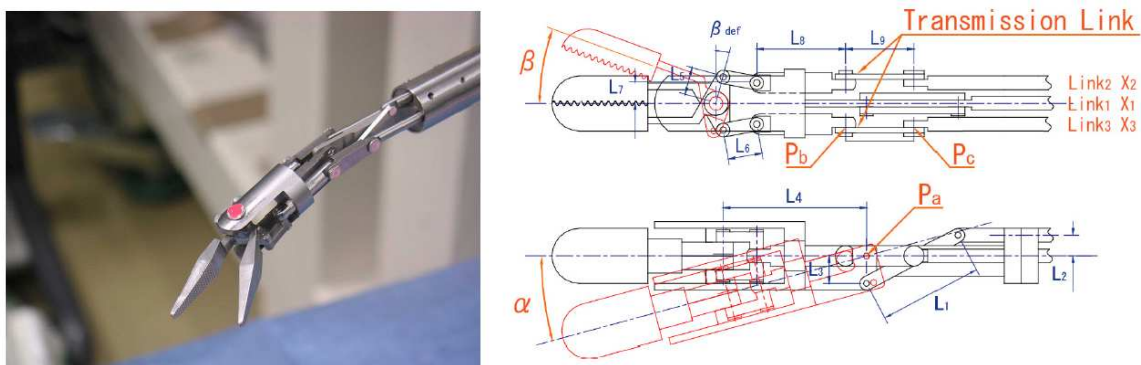
Figure 5-15: Linkage-driven micro-manipulator from *University of Tokyo* (Takahashi et al., 2006)

5.4.4 Direct Actuation

Internal actuation simplifies the mechanical configuration of the joint, reducing the complexity of the transmission chain. In particular, it has the great advantage that the motion of the joint is kinematically independent with respect to other joints. However, the size of the manipulator links is imposed by the dimension of the actuators, which can be an important drawback due to technological power-to-volume limitations of available robotic actuation. With an appropriate reduction gear box, high torques can be achieved, however, this solution often implies further addition of friction losses.

A manipulator for coronary artery bypass grafting surgery is proposed by the Institut des Systèmes Intelligents et de Robotique, ISIR, (Salle et al., 2004), in which a brushless micromotor with a diameter of 3 mm is embedded inside a joint unit, and bending motion is attained by using a worm gear transmission, Figure 5-16. However, this module generates a

torque of only 6 mNm due to the use of low-torque micromotors. Therefore, this equipment is not suitable for surgical tasks that require greater forces, such as lifting internal organs.
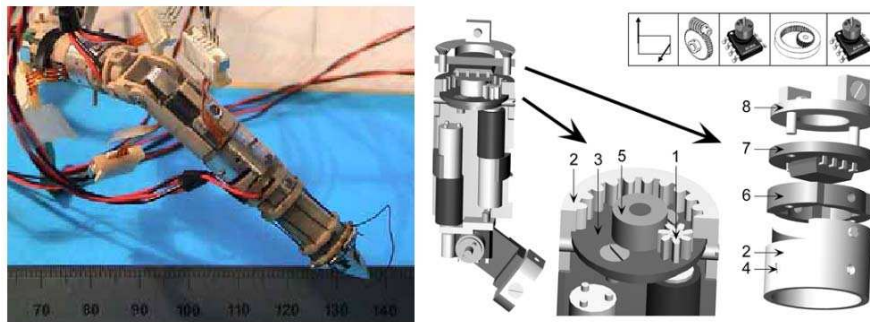
Figure 5-16: Mechanical modular manipulator (Salle et al., 2004)

Another micro-manipulator, specifically designed for single-port laparoscopy, was developed at *Scuola Superiore Sant'Anna* (Piccigallo et al., 2010). It is a high-dexterity miniature robot, able to reproduce the movement of the hands of the surgeon, who controls the system through a master interface. It comprises two arms with six degrees of freedom, where the distal degrees of freedom are actuated by three motors hosted in the forearm, with a miniature differential mechanism that allows the intersection of roll– pitch–roll axes, Figure 5-17. However, due the use of geared components in high-payload miniature systems, the backlash of the manipulator is considerable (8mm at the end-effector).
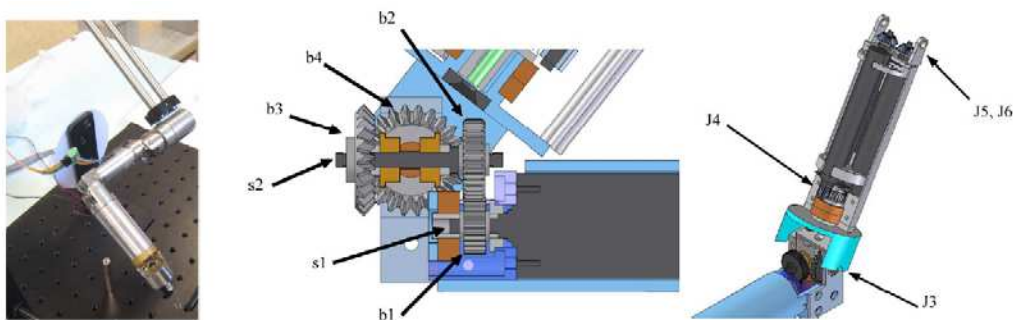
Figure 5-17: SSSA Manipulator (Piccigallo et al., 2010)

5.4.5   Conclusion

The development of multi-DOF robotic micro-manipulators, capable of reproducing complex human arm movements in MIS has been an extremely active research field in surgical robotics. A large number of design solutions have been developed, using different concepts in terms of actuation, transmission and structure. However, there is not, in the current state-of-the art, a concept that can successfully manage the delicate trade-off between internal dexterity, compactness, stiffness and manipulation force.

5.5 Concept Development

The mechanical design of micro-mechanical systems can be performed according to many possible concepts and options, even if the kinematical architecture has already been defined and size and shape specifications have been imposed. One of the main issues is related with the design of a proper actuation and transmission system. In case of micro-mechanical systems for MIS, and especially for high-dexterity endoscopic units, this aspect is crucial because the working space and incision dimensions are extremely limited and the high dexterity kinematics and demanding performance constraints are tough design goals to be pursued. Micro mechanisms for MIS should meet highly demanding requirements of stability, precision, force and compactness to effectively perform a minimally invasive surgical task. Therefore, a special effort was placed in the study and development of a novel mechanical system, able to meet all those specified requirements.

5.5.1 Actuator Selection and Placement

In order to actuate the joints of a micro-manipulator for MIS, two basic approaches are possible: (1) placing the actuators within the moving links of the manipulator, or integrating them in the joints directly, without transmission elements; or (2) placing the actuators on an external location, outside of the patient's body, having the motion transmitted to each joint by means of a mechanical transmission.

Internal actuation simplifies the mechanical configuration of the joint, reducing the complexity of the transmission chain. In particular, it has the great advantage that the motion of the joint is kinematically independent with respect to other joints. However, the size of the manipulator links is imposed by the dimension of the actuators and, due to technological power-to-volume limitations of available robotic actuation, it is quite difficult to obtain an anthropomorphic kinematics and the required working performances and dimensions required for an endoscopic system. Furthermore, the motors occupy a rather large space inside the robotic structure, making it difficult to host other elements, like different kind of sensors or internal structural components.

A further negative aspect is related with the routing of both power and signal cables of the actuators. This issue is more serious for the actuation of distal joints than for the proximal ones, since the cables in distal joints produce a relatively large resistant torque and volume disturbance on the proximal joints. As a consequence of all those disadvantages, internal actuation was discarded in favour of a remotely actuated solution.

Due to their very good performances in terms of position and velocity control and reasonable mass/power ratio electrical actuators have been selected as external actuators. Being the most common choice for actuating robotic systems, electric motors are a quite well established driving technology that does not require external devices (such as for hydraulic or pneumatic actuators).

5.5.2 Motion Transmission

5.5.2.1 Transmission Elements

In remote actuation systems the joints are driven by actuators placed outside the moving links. This requires a motion transmission system, which must pass through the intermediate joints, between the motor and the actuated joint, without bringing problems of kinematic coupling. In addition, in order to achieve good force reflection properties, the mechanical transmission is composed by flexible elements (cables) that are routed about ball-bearing-mounted pulleys, which are placed between the actuator and the actuated joint.

5.5.2.2 Remote Cable actuated Architectures

Remote cable driven actuation can be applied according to different types of organization, depending on the number of actuators used per DOF. In particular, it is possible to recognize two main actuation architectures for cable drives: (1) two actuators per DOF, Figure 5-18a, - each one can generate a controlled motion in one direction only and the return motion in the opposite direction must be obtained by an external action, which can be a passive (e.g., a spring) or an active system (e.g., an antagonistic actuator); this is the case of tendon-based transmission systems; (2) a closed-loop cable with one actuator per DOF, Figure 5-18b, - each one can generate a controlled motion in both directions and can be used alone to drive the joint.
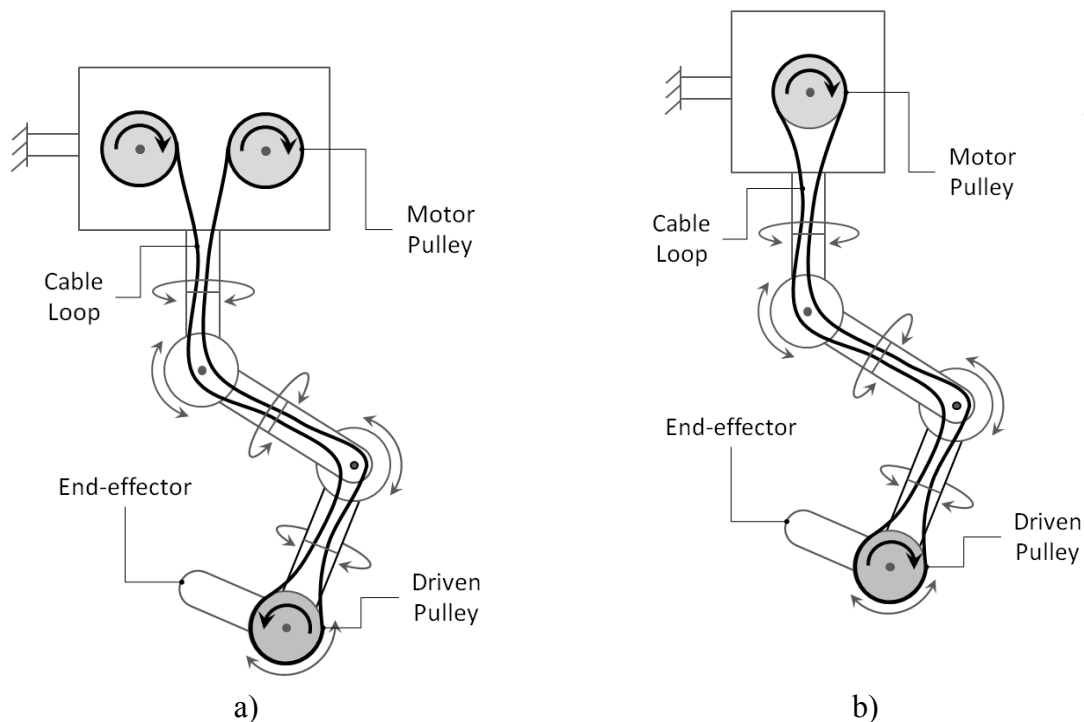
Figure 5-18: Two different architectures for remote actuated cable driven systems
a) Two actuated pulleys per DOF b) One actuated pulley per DOF

Since the first solution requires a higher number of components and brings additional complexity and cost to the mechanical system, the chosen architecture was the one that uses a single actuated pulley per DOF. In this case, the achievable performances are similar in both directions, but particular attention must be paid to backlash. Usually, it is necessary to preload the transmission system. Furthermore, the adoption of a closed loop tendon transmission requires that the overall length of the cable route must be kept constant, for all possible configurations of the manipulator.

In spite of this additional complexity, this actuation scheme has been used (Madhani et al., 1998), for simple applications, with only a few DOF. However, in a multi-DOF configuration, with high dexterity, reduced dimensions and high payload requirements, several open problems will have to be addressed.

5.5.2.3 Joint Cable Routing

In the required kinematic model shown in Figure 5-5, two joint configurations may be identified, which can be classified as (1) pivot joints or (2) co-axial joints. The distinction is related to the relative alignment of adjoining links. While in the first kind, the angle, between the proximal, P, and distal link, D, changes with the movement of the joint, θ_{pd}, Figure 5-19a, in the co-axial configuration the axes of the proximal and distal links are always collinear and coincident with the axis of the joint, Figure 5-19b.

a)
b)
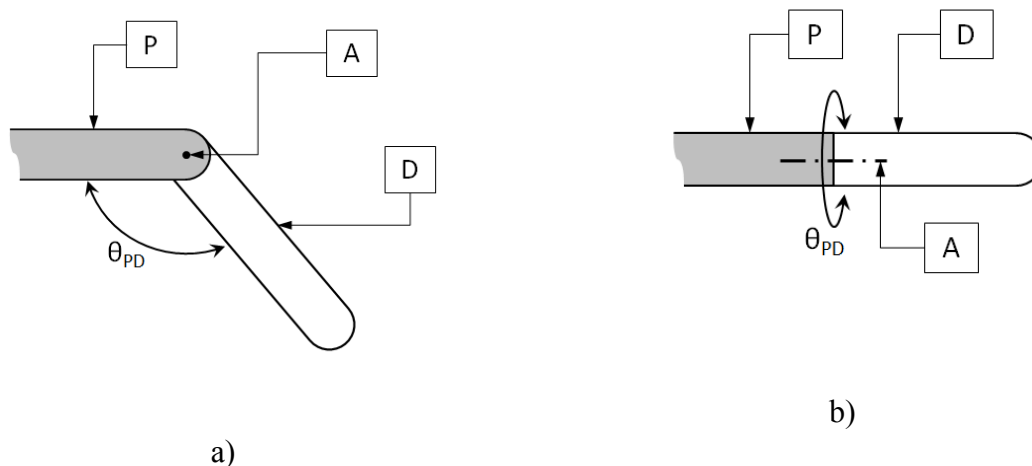
Figure 5-19: Joint configurations of the micro-manipulator's kinematic model
a) Pivot Joint b) Co-axial Joint

The cable routing method used for pivot joints is relatively standard and can be seen in a few already developed solutions (Madhani et al., 1998, Lum et al., 2009). As illustrated in Figure 5-20, for this kind of configurations, the cable is wrapped around a set of pulleys, called the "joint idle pulleys", I, whose axis is concentric with the joint's axis.
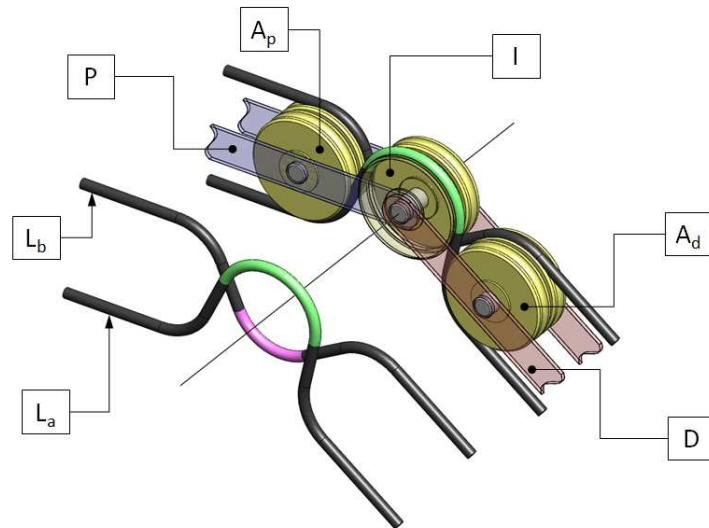
Figure 5-20: Single-DOF cable set, passing through a pivot joint

To maintain a constant the length of the closed cable loop, which goes from the driving pulley of the motor to the driven pulley of the joint, the cable must always remain in contact with the joint idler pulleys, Figure 5-21. In this way, if the joint angle θ_j is increased by a value $\Delta\theta_j$, the length of the closed loop segment L_a, in contact with the idle pulleys, I, on θ_a, will increase and the segment on θ_b will decrease, by the same value, $R\Delta\theta_j$, guaranteeing the overall constant length of the cable closed loop. In order to keep the segments L_a and L_b constantly in contact with the joint idler pulleys, I, two sets of auxiliary pulleys, A_p and A_d, are often used on the proximal and distal links.
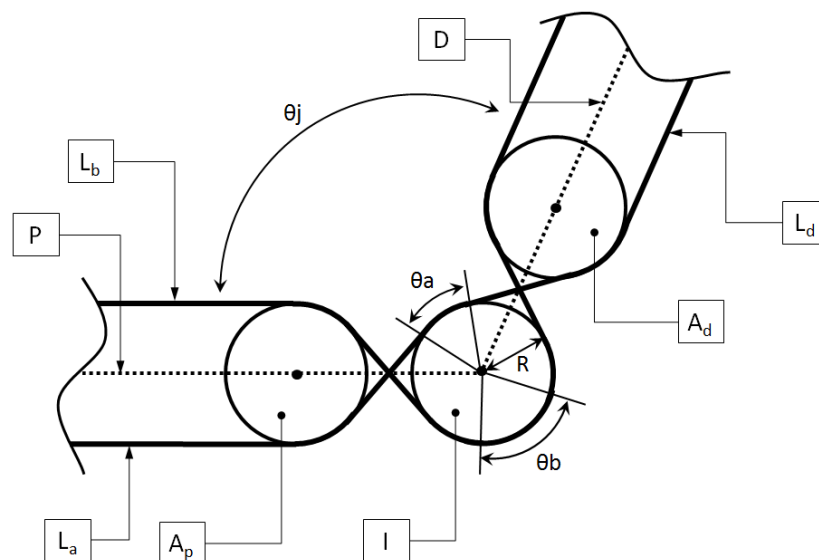
Figure 5-21: Single-DOF cable rooting along a pivot joint

However, for the co-axial joints, the cable routing is much more complex. Some solutions to avoid this problem have already been proposed (Madhani et al., 1998) but, to the best of the

author's knowledge, not for such a small dimension multi-DOF system with such a high dexterity requirements. The problem consists in having an array of cables being twisted about a co-axial axis, as shown in Figure 5-22, with the two cable segments, L_a and L_b, being stretched in the same way, increasing the total length of the closed loop.
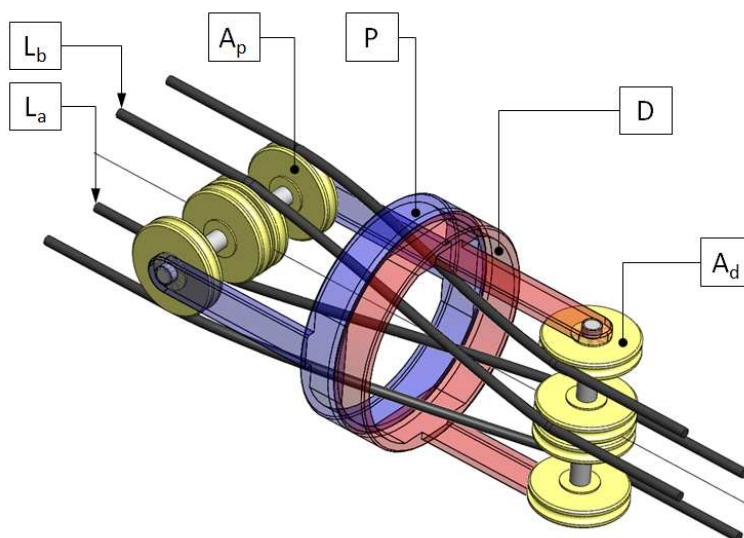
Figure 5-22: Cable set, passing through a co-axial joint

This stretch of the different closed loops generates a resistant rotation moment that might be critical for multi-DOF systems. Another source of problems caused by this twist, as seen in Figure 5-23, is the misalignment of the cables in relation to the auxiliary pulleys, α, which may cause the disengagement of the cables from the auxiliary pulleys.
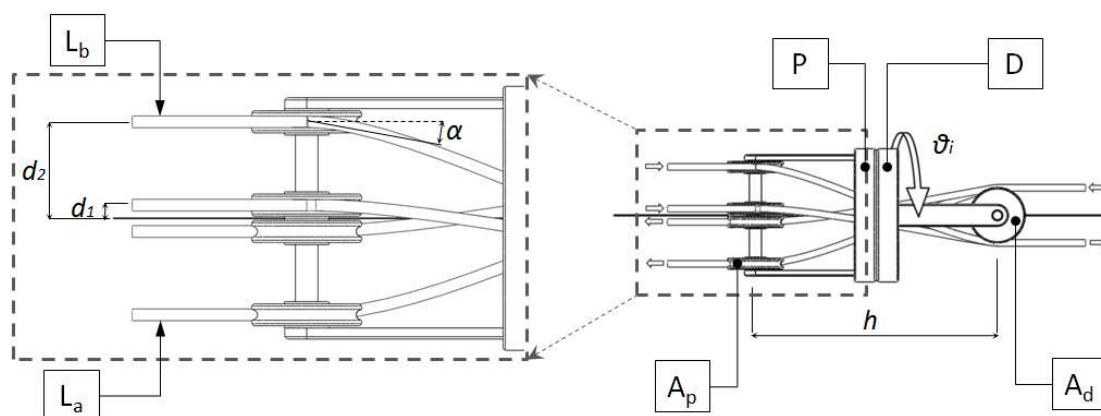
Figure 5-23: Disengagement of a cable routed along a co-axial joint

In addition, the twist of the set of cables passing through a co-axial joint may also cause the different cables to rub on each other, generating a significant amount of friction and wear,

Figure 5-24. These problems are especially severe on the proximal joints of the manipulators, due to the high density of cables and short moving links.
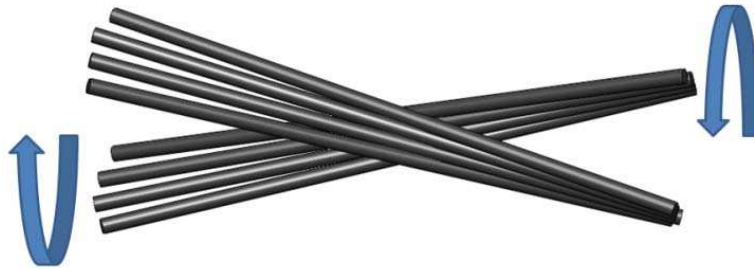
Figure 5-24: Contact of cables when passing through a co-axial joint

In some applications of micro cable driven manipulators for MIS (Madhani et al., 1998, Song et al., 2009), this difficulty is minimised due to the low complexity (low number of internal DOF) of the system and the large ratio between the length of the instrument shaft, h, and the distance between the joint axis and the cables, d (Figure 5-23). In this way, the misalignment of the cables in relation to the idle pulleys is almost negligible and the change in length of the cables is small, generating a very small resistant moment. In this case, however, due to the high number of internal DOF and the anthropomorphic kinematic configuration, this solution could not be applied.

One possible solution to this problem consists in trying to adapt the routing configuration of the pivot joint, Figure 5-25a, to the co-axial joint. So, the joint axis is turned 90° in relation to the axes of the auxiliary pulleys. This new co-axial configuration can be seen in Figure 5-25b.

a)   b)
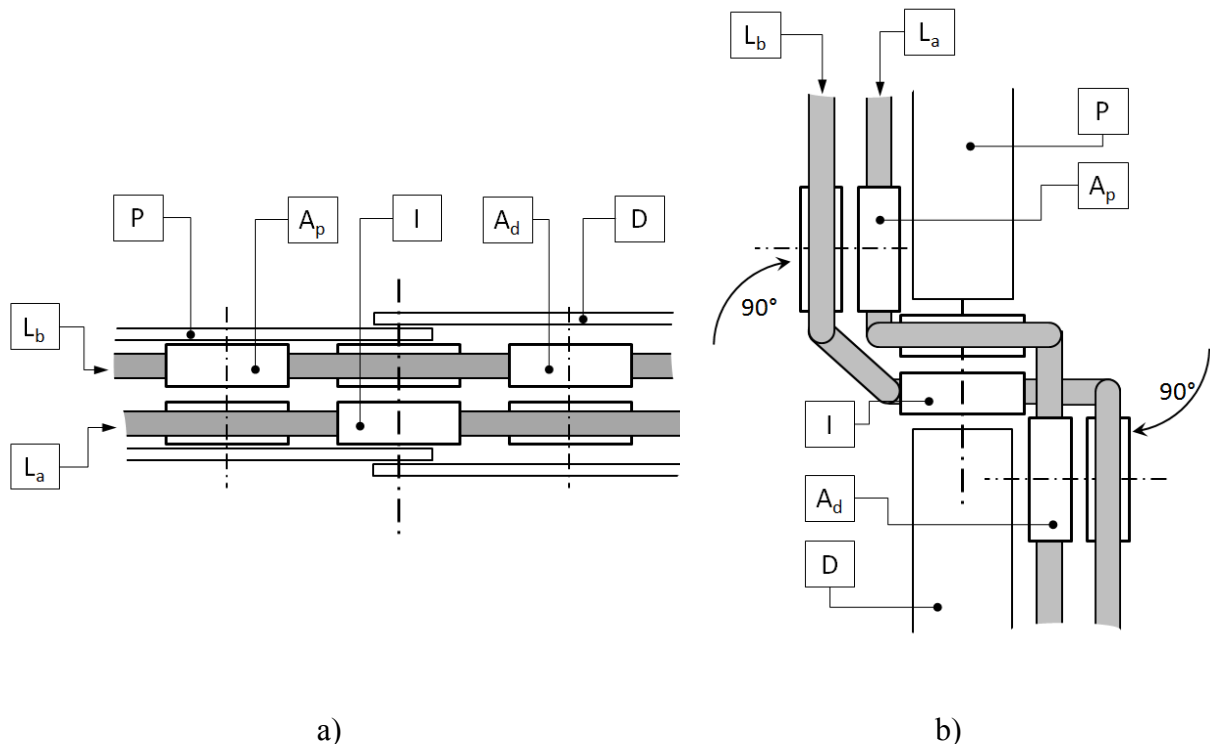
Figure 5-25: Adaptation of the routing configuration from a) a pivot joint to b) a co-axial joint

In this way, the conservation of the closed loop length is guaranteed. However, the two cables would rub on the transition from the auxiliary pulleys to the idler pulleys. Additionally, the routing of the segment L_b would cause the cable to be misaligned on the same transitions, as shown in Figure 5-26. These physical limitations disable its application.
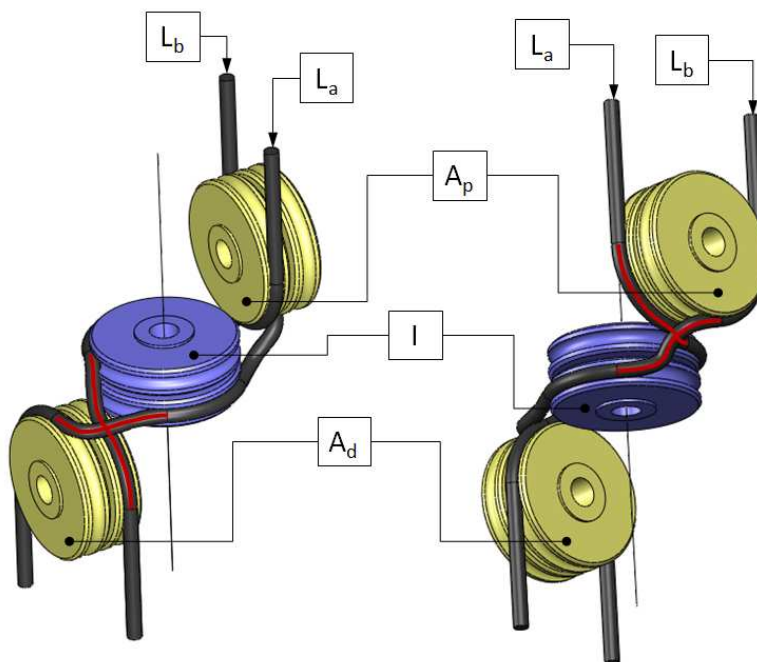
Figure 5-26: Misalignment and intersecting issues of a co-axial joint

To overcome these limitations, the two sets of proximal and distal auxiliary pulleys, A_p and A_d, can be separated while remaining tangent to the axial pulley, Figure 5-27a. This could avoid the cables to touch each other and would still guarantee a constant length of the closed loop.
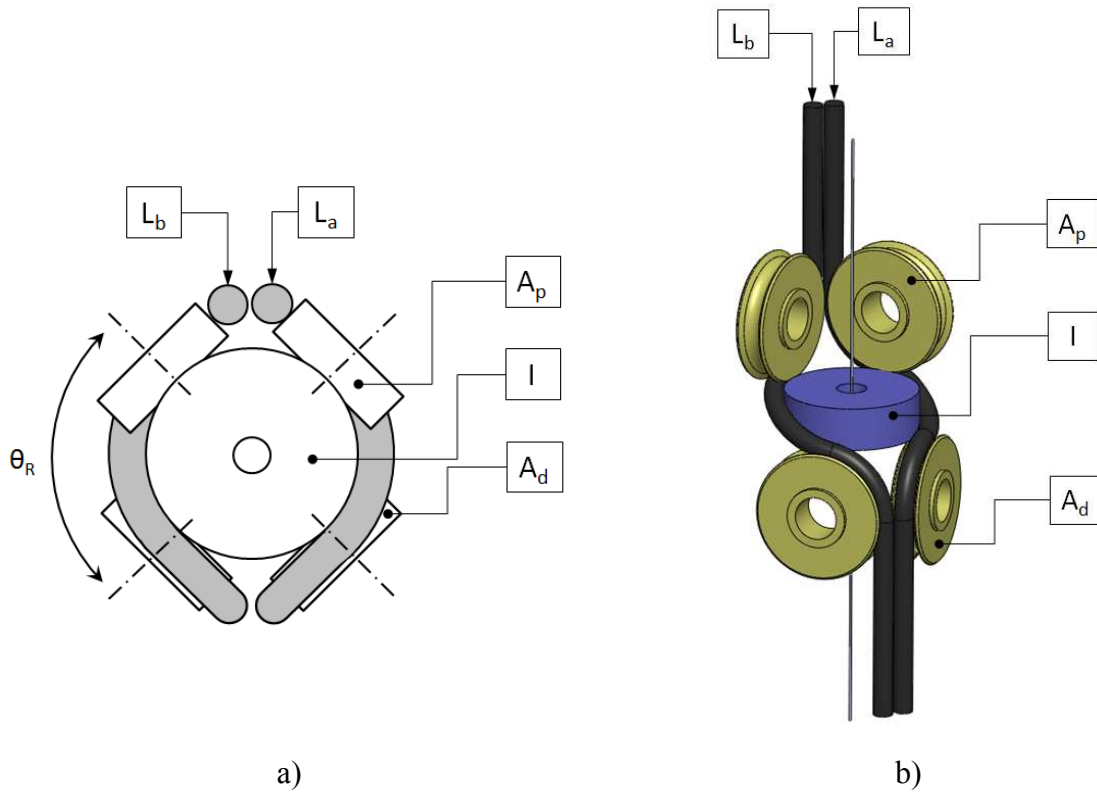
Figure 5-27: Single-DOF cable set, passing through a co-axial joint, with separated auxiliary pulleys a) 2D schematics b) 3D model

However, this solution would hardly be applicable to a multi-DOF system of micro dimensions since hosting all the sets of proximal and distal auxiliary pulleys would oblige the use of a θ_R configuration, Figure 5-27a, reducing drastically the range of movement of the joint to $\pm$ θ_R. The perfect co-linearity and rotation of the axial idler pulleys (that for this specific configuration would have the form of very thin rings) would also be extremely problematic, Figure 5-28.
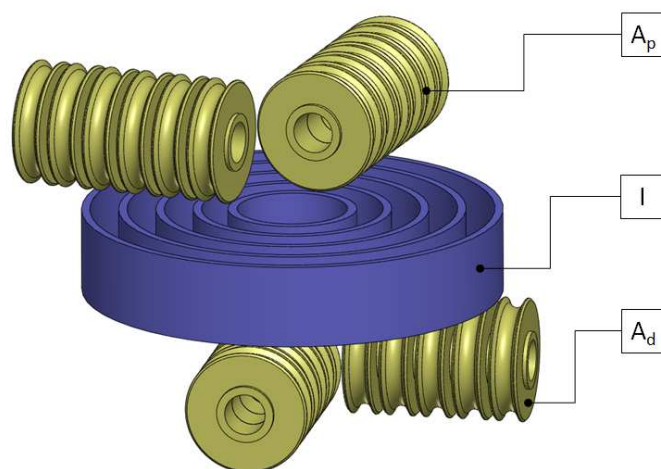
Figure 5-28: Multi-DOF pulley set, with separated auxiliary pulleys, for a co-axial joint

The developed solution for this system is based on the concept shown in Figure 5-27. The configuration is similar but the two set of proximal and distal auxiliary pulleys are separated to allow the cables, belonging to the same closed loop, to be wrapped around a single joint idler pulley, which is in a perpendicular configuration, aligned with the axis of the joint, Figure 5-29.

a)   b)
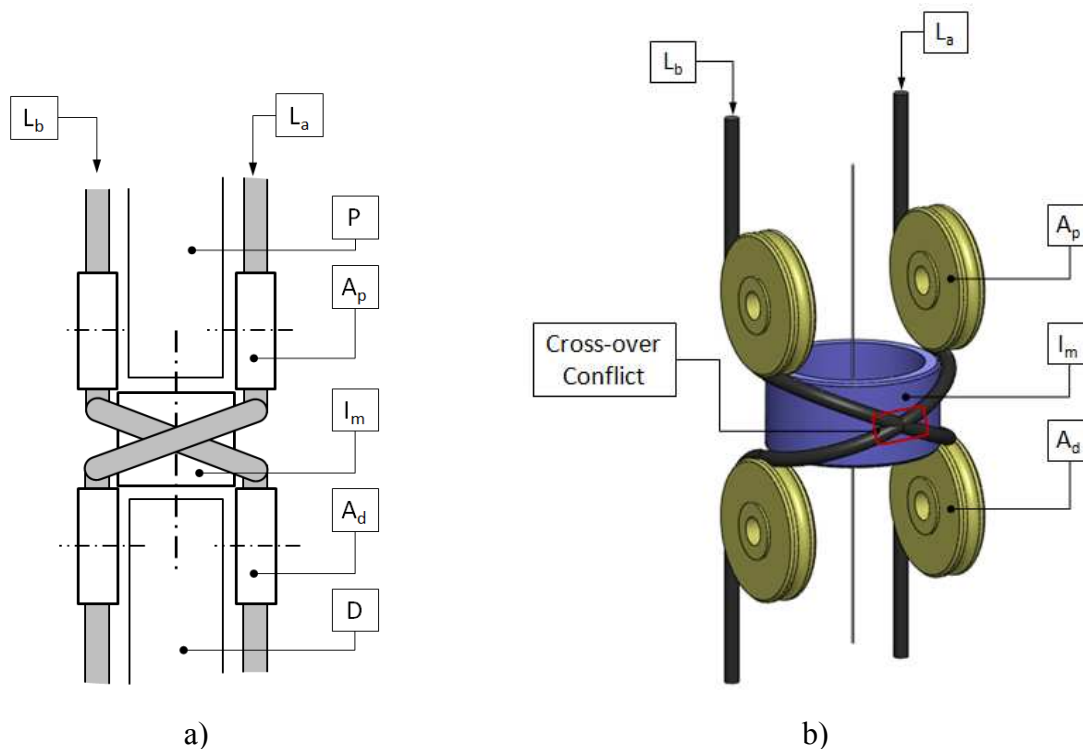
Figure 5-29: Preliminary co-axial concept with a cross-over conflict a) 2D schematics b) 3D model

In this configuration, although the problem of the pulleys' hosting is solved, the rub cross-over between the two segments, L_a and L_b, of the closed loop is evident and the only way to avoid it consists in trimming the closed loop in two. By doing this, the single closed loop is divided in two closed loops, whose motion in transmitted through an axial idle pulley, Figure 5-30.
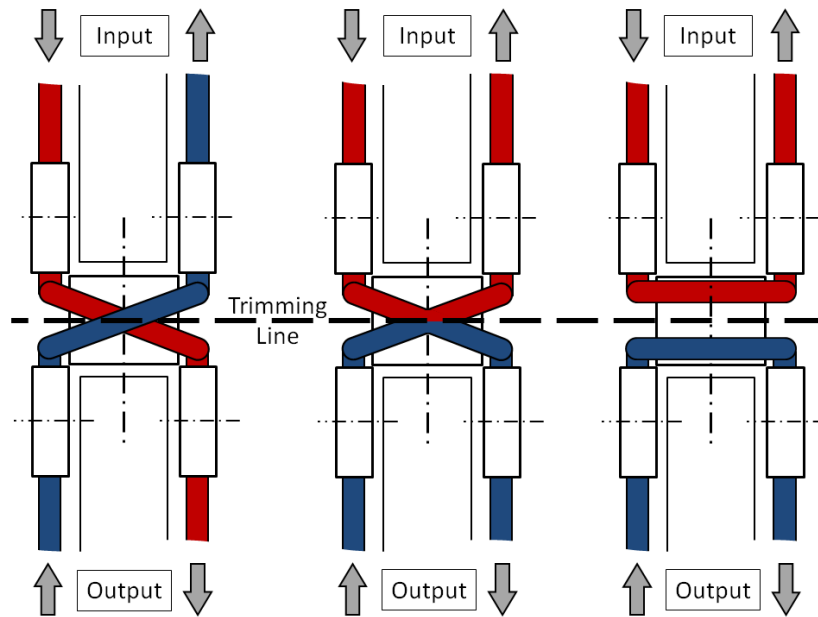
Figure 5-30: Co-axial joint concept development, by the resolution of the cross-over conflict

In a multi-DOF system, the co-axial joint is composed of several co-axial idler pulleys, having a form of co-axial tubes with different lengths. In addition, it also comprises two different sets of proximal and distal auxiliary pulleys, A_{pi} and A_{di}, for the different closed loops, $^{j}L_{ai}$, passing through the joint, Figure 5-31.

a)

b)
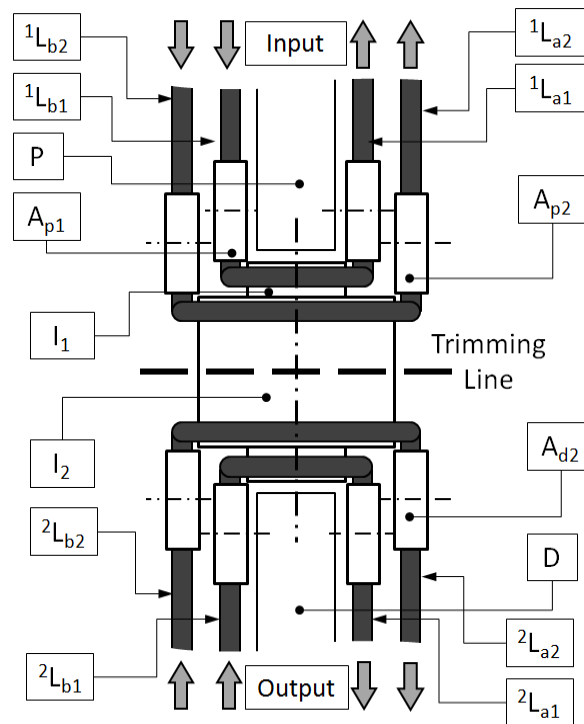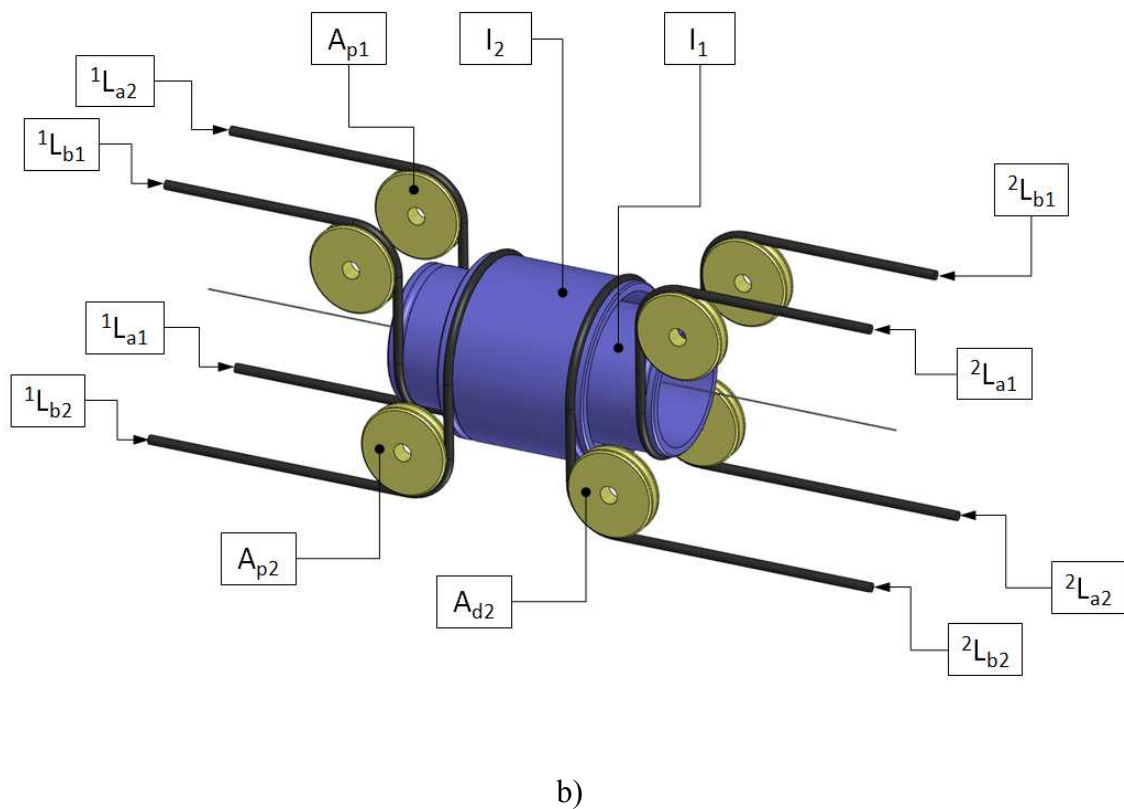
Figure 5-31: Co-axial joint concept for a 2-DOF example a) 2D schematics b) 3D model

5.5.2.4 *Motion transmission on the Co-axial Joint*

Systems with several stages of endless cables have been used in different mechanical systems where, in order to ensure enough static friction to transmit the motion between consecutive closed loops, timing belts have been frequently used. However, for this specific solution, they are not a suitable choice. The main problem is related to the fact that, although timing belts might be used in out-of-plane configurations, in this reduced dimensions application, since the out-of-plane idler pulleys are too close to each other, this kind of configuration is not feasible.

A standard cable could be a solution. However, the friction generated by the cable in contact with the idle pulley, for any pair of materials, wouldn't be sufficient, and the wear would be excessive. The cable could also be wrapped several times around it, with an exponentially increased friction, but it would lead to an unacceptable axial movement of the idler pulley, Figure 5-32.
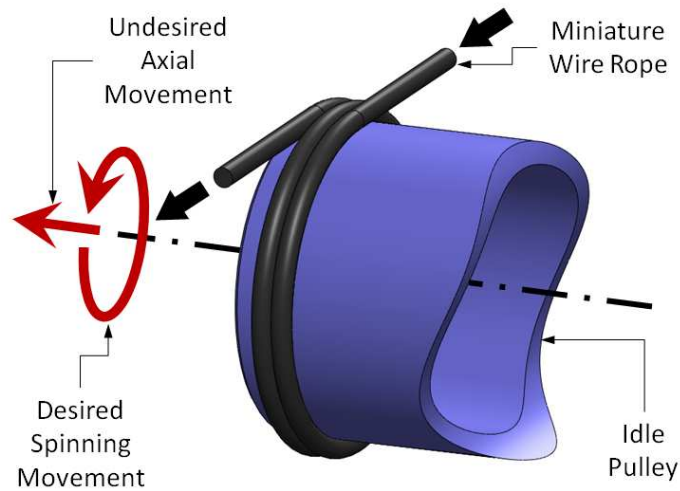
Figure 5-32: Multi-turn wrapped cable on an idle pulley

Since in this configuration the motion transmission can only be made through half a turn of contact of cable around the idle pulley, the friction in the contact is maximized by a specially developed bead chain, as shown in Figure 5-33. Being a key element for the viability of this concept, it is composed by a continuous wire rope with several spherical beads, placed at a constant pitch, in the segment of the cable that can be in contact with the idle pulley. The bending flexibility, axial symmetry, strength and compactness of this bead chain make it suitable for this application, where high load resistance, no slipping, low volume and right-angle driving are major requirements.

Wire ropes are available in a variety of strengths, constructions, and coatings. While their strength generally increases with diameter, the acceptable minimum bending radius is decreased.

During operation, the cable runs in a grooved surface on the idler tubes and the beads seat in sprocket indentations, where the shear force is generated.
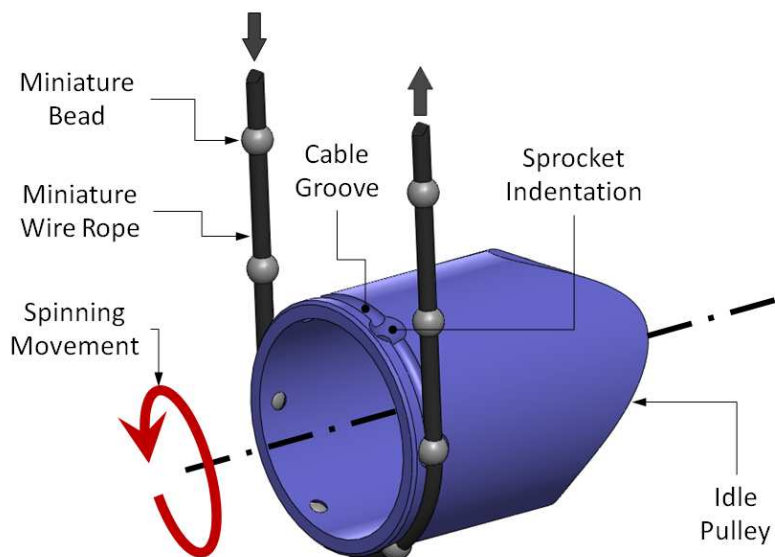
Figure 5-33: Bead chain turning the idler cylinder

5.5.2.5   Structure of the Co-axial multi-DOF Cable Driven Joint

As explained in the previous section, in a multi-DOF configuration, the primitive closed loop is trimmed in two new closed loops, whose motion in transmitted through the single axial idle pulley, which should be able to rotate independently from the others, while keeping its fixed axial position. This could be ideally achieved by the use of two internal radial ball bearings, in a standard configuration, as shown in Figure 5-34.
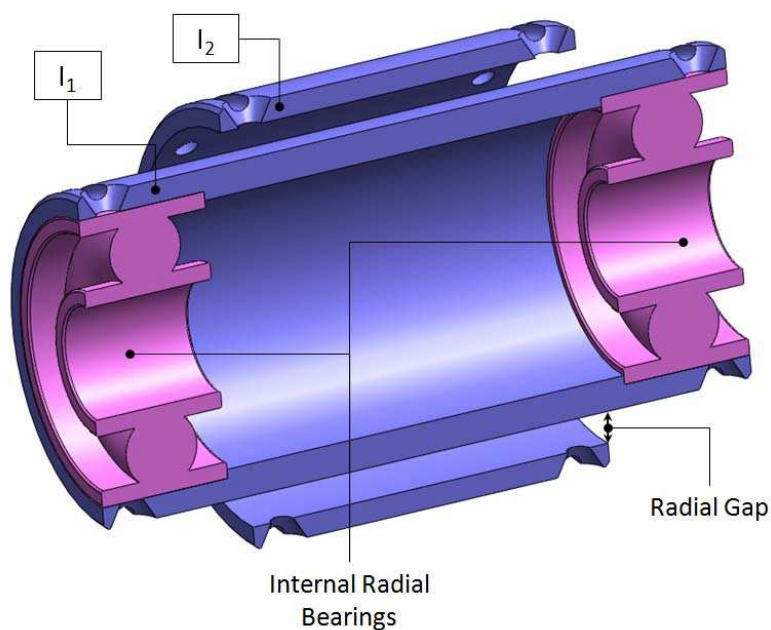
Figure 5-34: Use of two ball bearings to mount an idler tube

However, for a multi-DOF system, the space gap between the concentric tubes is not enough to place the two ball bearings for each idle pulley. To overcome this problem, six miniature ball bearings are used to guarantee the concentricity of each idle pulley. On each extremity of the pulley, I, three miniature bearings, A, B and C, guarantee the position of point P, which is coincident with the axis of the pulley, a. On the other extremity, the miniature bearings, A', B' and C', guarantee the position of point P'. By the fixation of this two points, the axis, a, of the idle pulley is also fixed and the free DOF of the pulley, I, are limited to the translation, d_a, along the axis a and a rotation, θ_a, around the same axis, Figure 5-35.
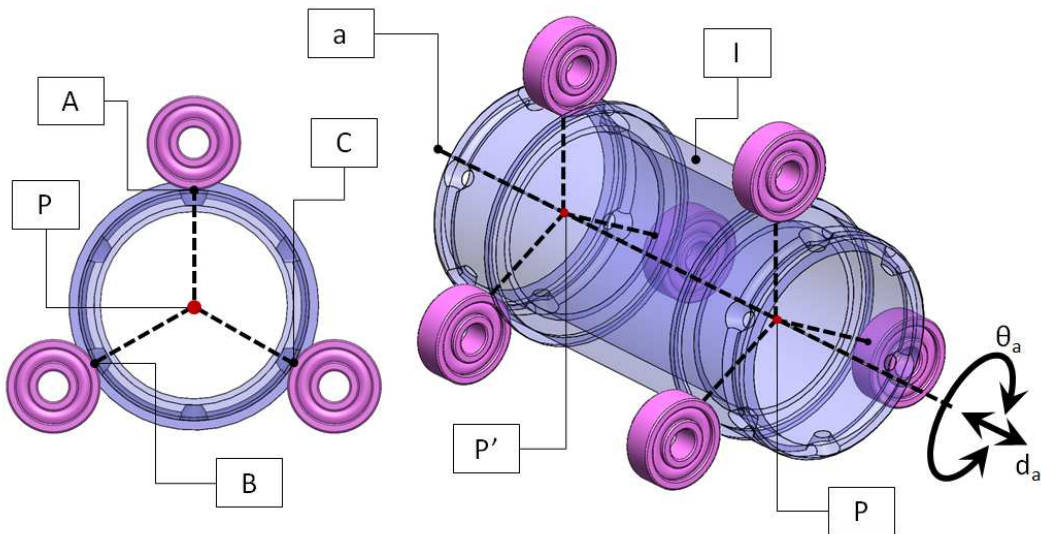
Figure 5-35: Radial and axial restriction of the joint idler tubes

The axial movement, d_a, is constrained by the contact of two radial flanges with the six miniature bearings, which allows these tubular idle pulleys to be used in a multi-DOF configuration, Figure 5-36.
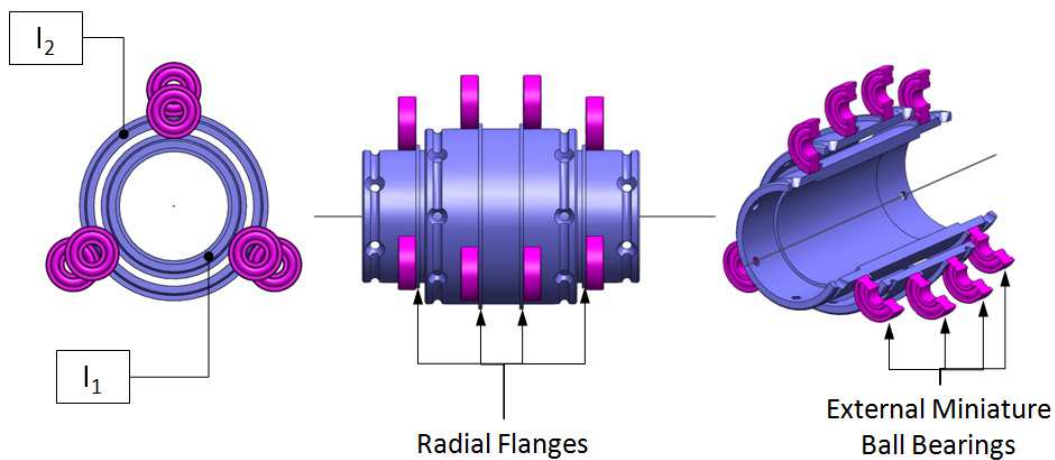
Figure 5-36: Radial and axial restriction of the joint idler tubes

For an application example with two transmitted DOF, the final layout of the joint will look like the one shown in Figure 5-37.
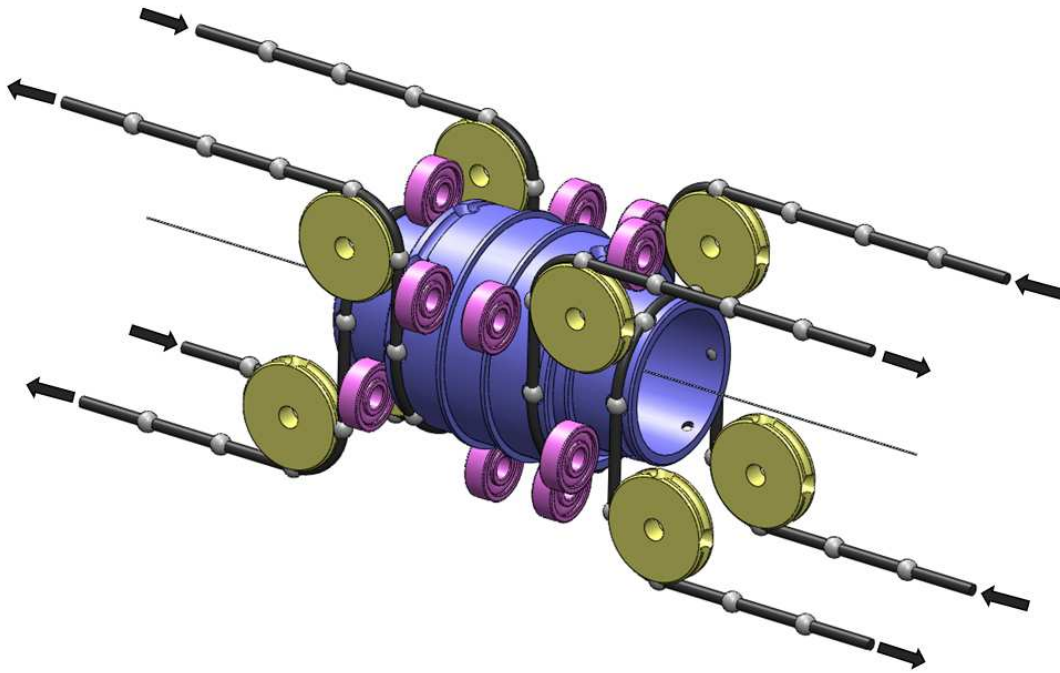
Figure 5-37: Bead chain turning the idler cylinder

This transmission concept enables the design of several novel mechanical surgical instruments can be implemented. The main goals are: (1) to provide high dexterity within the abdominal cavity, (2) to provide enough precision and stiffness, enabling the performance of accurate surgical procedures, (3) to have reduced dimensions and (4) to have low friction, allowing good force reflecting properties, increasing the mechanical transparency of the teleoperated system.

5.6 Geometrical Modeling

The geometric modelling of this micro cable driven system should be performed in two sequential steps. The first step consists of the standard derivation of the kinematic relationship between the location of the end-effector and the joint angles of the serial chain. The second step implies the derivation of the kinematic relationship between the joint angles and the cable displacements at the actuators.

A simplified scheme of the system's kinematic structure is represented in Figure 5-38, in which the links are labelled sequentially from 0 to n and the joints are labelled sequentially from 1 to n. Each cable transmission T_i, which is composed by a set of m closed cable loops, T_{ij}, links the driving pulley P_{i0}, on motor M_i, to the correspondent pulley P_{ii}, on joint J_i of the ith DOF. In this way, T_i crosses $i - 1$ intermediate proximal joints, which can be of either

pivot or co-axial type. Due to the high stiffness of the wire ropes, the cable loops, T_{ij}, are considered to be inelastic.
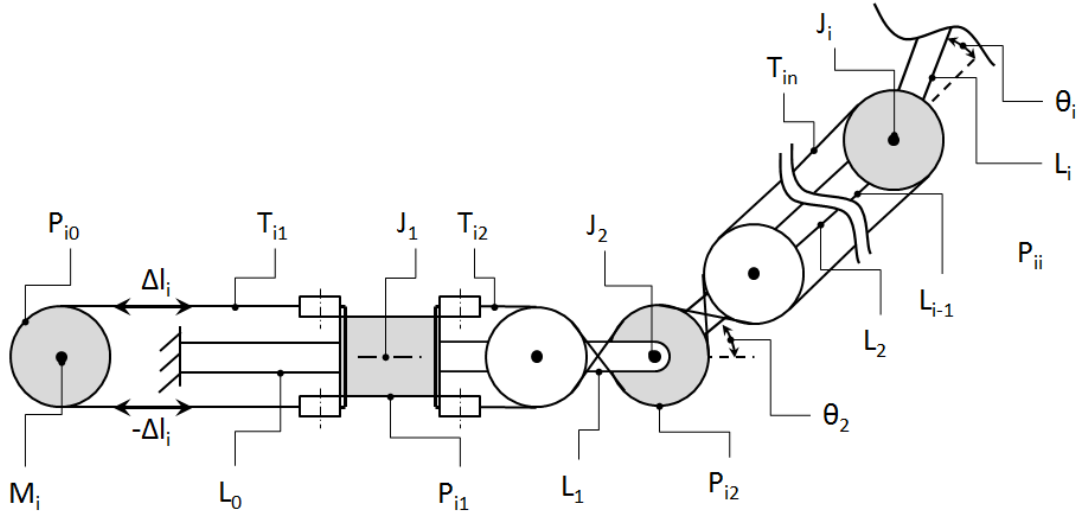
Figure 5-38: Simplified scheme of the system's kinematic structure

The model of the cable routing for each cable transmission, T_i, is obtained by calculating its proximal displacement, Δl_i, as a function of the different joints angles of the manipulator, θ_j. Assuming that each cable loop is always in contact with the idler pulleys of the intermediate joints through which it is passing, Δl_i can be obtained by:

$$\Delta l_i = \pm r_{i1}\theta_1 \pm \dots \pm r_{in}\theta_n , \tag{18}$$

where r_{ij} is the radius of the idle pulley at the jth joint and belonging to the cable transmission T_i. Pulleys with parameters characterized by $i \neq j$ represent idle pulleys (which allow the cable to cross the joint), while the ones characterized by and $i = j$ represent driven pulley (which are fixed to the actuated link i and can produce its movement with respect to link $i-1$). θ_i denotes the angular displacement of link i with respect to link $i-1$. The sign $\pm$ depends on whether the tendon path gets longer or shorter when the angle θ_i is changed in a positive sense. Therefore, the equation can readily be obtained by an inspection of the tendon routing topology.

Considering that the transmission displacement can be related to the angular displacement of the motor pulley M_i the motor pulley radius, r_{i0}, the following equation can be obtained in matrix form:

$$\Delta l = C\theta \tag{19}$$

where $\Delta l = [\Delta l_1, \Delta l_2, \dots, \Delta l_n]^T$ denotes an n-dimentional vector of proximal displacements, $\theta = [\theta_1, \theta_2, \dots, \theta_n]^T$ denotes an n-dimensional vector of joint angles and C is an *nxn* square

coupling matrix. The elements of C are functions of the pulley sizes and the cable routing topology, being independent of the posture of the manipulator.

5.7   Force Analysis

Once the tendon extension functions have been computed, we can determine the relationships between the tendon forces and the joint torques by applying conservation of energy.

Given the low-friction mechanical transmission, the work done by the cables can be considered equal that done by the manipulator. Consequently, it can be concluded that

$$\tau = C^T f, \tag{20}$$

where f is the vector of forces applied to the proximal extremities of the tendons, τ is the vector of output joint torques and C^T is called structure matrix, whose columns represent each cable transmission.

5.8   Application on a 7-DOF Micro-Manipulator for SST

Figure 5-39 shows the overall design of a high dexterity micro-manipulator, to be used in the SST Surgical Platform. By using the kinematic model shown in Figure 5-5 and the micro-mechanical system developed in the previous sections, this manipulator is able to deliver high dexterity, stiffness and precision to the performance of complex surgical tasks inside the abdominal cavity.
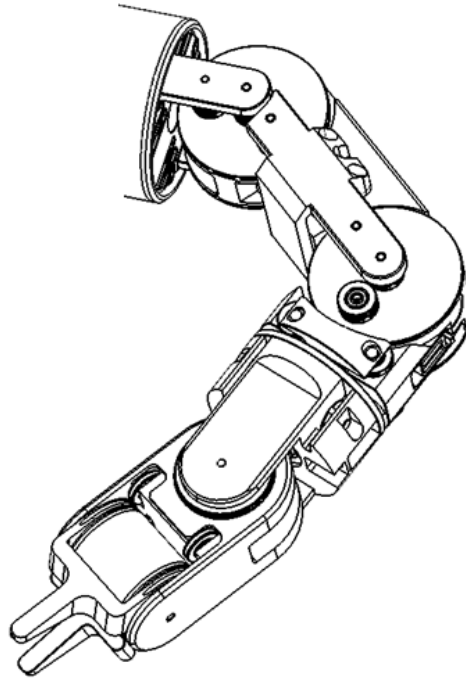
Figure 5-39: 3D Model of the SST Micro-Manipulator

The cabling topology of the entire manipulator is schematically shown in Figure 5-40. The design of the mechanism is such that the diferent closed cable loops that control each degree of freedom are moved by the same actuated driven pulley placed in the external part of the body.
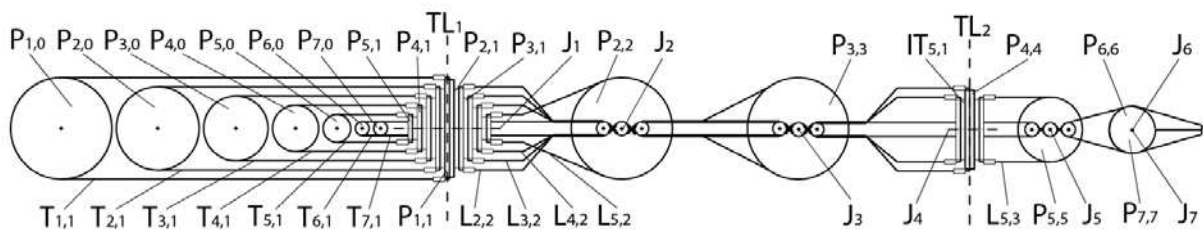
Figure 5-40: Cabling schematics of the 7-DOF micro manipulator

Figure 5-41 shows a 3D layout of the cabling for each 7-DOF endoscopic micro-manipulator, related to the cabling schematics described before.
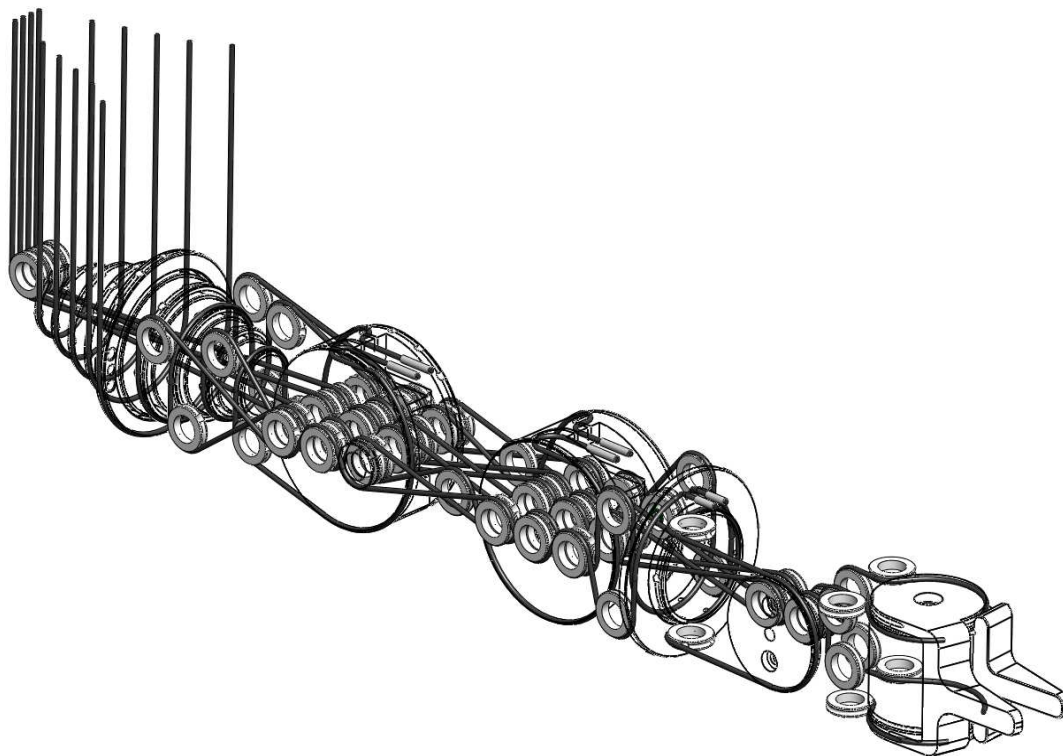
Figure 5-41: 3D cable layout of the 7-DOF micro-manipulator

To hold in the 3D space all the components of the cabling scheme, like idle pulleys, ball bearings, and positioning pins and screws, special parts were developed, guaranteeing the perfect positioning and support of all the joint components and allowing the route of the different cables, Figure 5-42. A final overall diameter of 24mm can be achieved.
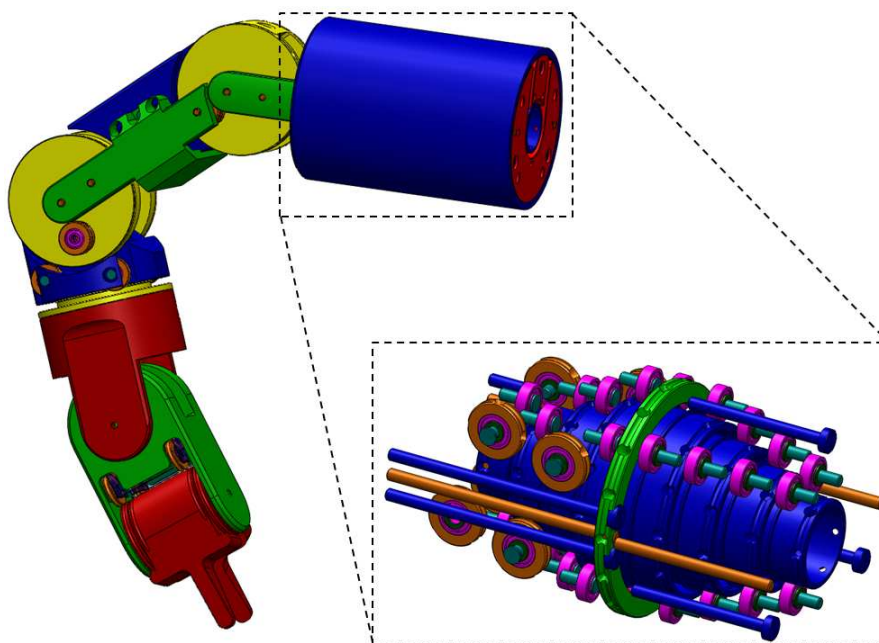
Figure 5-42: 3D cable layout of the 7-DOF micro-manipulator

Special attention was paid to the assembly precision of the mechanism. Since each idle pulley is radial and axially positioned by six external miniature bearings (three on each extremity), their precise positioning is guaranteed by mounting them on a unique base part, Figure 5-43, whose production process, by CNC milling machining, ensures extremely fine tolerances. Their alignment is then guaranteed by means of positioning pins, which cross all the mounting parts.
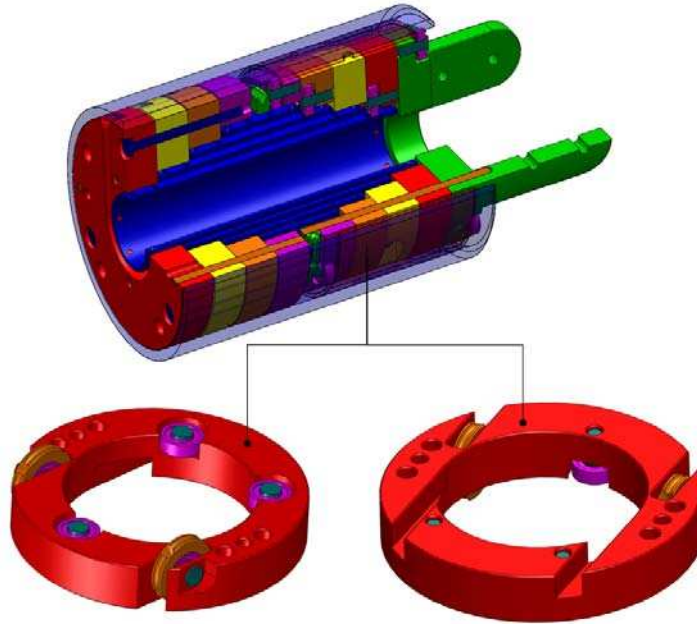
Figure 5-43: Component mounting parts

In a co-axial joint, the distal link has an axial rotation movement in relation to the proximal one. Due to the lack of space, this axial rotation and the linear axial movement constraints are guaranteed by six miniature ball bearings, in a configuration similar to the one used for the idler tubes, Figure 5-44.
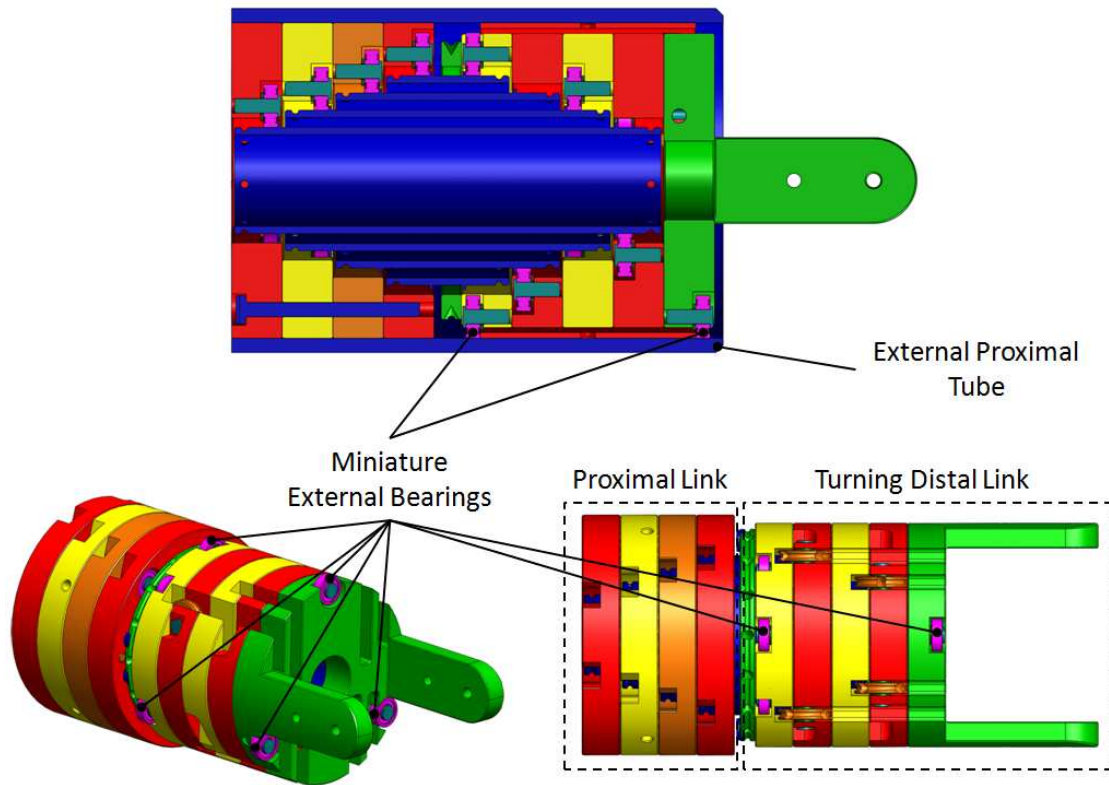
Figure 5-44: Radial and axial restriction of the joint turning distal link

5.9   Validation on a 3-DOF Prototype

In order to validate the concept and access its real performances, the proposed co-axial joint mechanism was applied in a multi-DOF micro-manipulator. Figure 5-45 shows the kinematic structure of the 3-DOF micro-manipulator, which can be seen as a simplified version of the 7-DOF Anthropomorphic micro-manipulator, but without wrist. In this way, the concept of the mechanical system can be tested without the extremely high complexity of a 7-DOF manipulator.
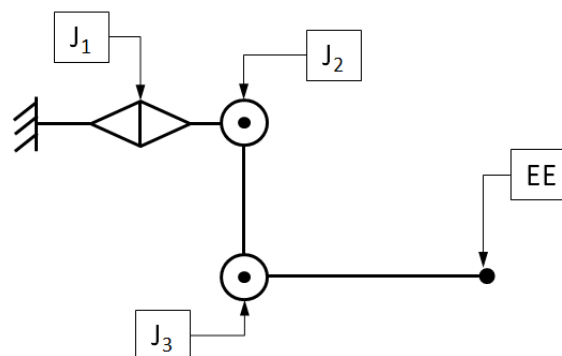
Figure 5-45: Kinematic Model of the 3-DOF Arm

The 3D model of the system can be seen in Figure 5-46. As can be seen, the mechanical solutions are the same as the one used on the 7-DOF prototype.
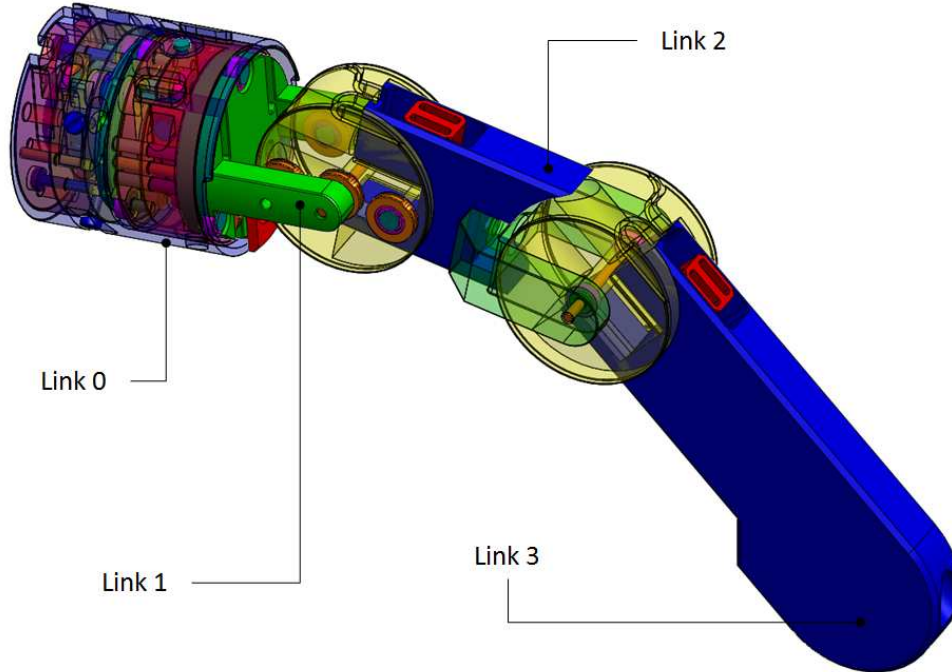
Figure 5-46: 3D Model of the 3-DOF Arm

The 3-DOF prototype of the 3-DOF Manipulator can be seen in Figure 5-47, being mounted on a stable reference base part, in order to be easily actuated and fixed to the laboratory experimental bench. The employed mechanical system, developed on this chapter, allows for smooth, backlash-free, high force and precise actuation, which can be done manually or via computer-controlled actuators.
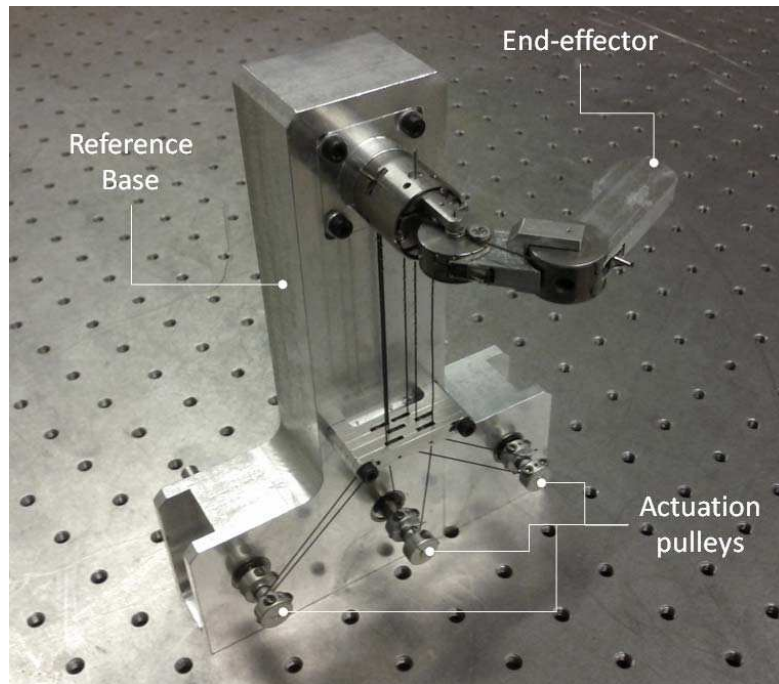
Figure 5-47: Prototype of the 3-DOF Arm

Apart from the reference base and other few components with reasonable size, most the parts composing this mechanical system are made from stainless steel (303ss), which guaranteed a very high stiffness of the mechanical system. The reason behind this choice is related with the considerable forces that have to be supported by extremely small components. The biocompatibility and capacity of being sterilized are also assured by using this material.

In order to minimize frictional effects and avoid backlash, all joints are implemented with miniature ball bearings and most of the components are produced by precise CNC machining. Figure 5-48, shows some of the system's components before being assembled.

Figure 5-48: Different mechanical components of the 3-DOF Arm

5.10 Technical Evaluation

The evaluation of the micro-manipulator is made through the following measurements: mechanical transparency and stiffness. These measurements assess the quality of the force interaction between the end-effector of the manipulator and the tissue inside the patient's body. The force sensors used are two *A XFTC320* load cells, one with a range of ±50 N and the other with ±10 N, both from the company *Measurement Specialties^{TM}*. The deformations are measured by using a standard dial gauge.

5.10.1 Stiffness

In order to measure the stiffness of the system, the position of the three input pulleys was locked, while the applied force on the manipulator's end-effector was increased gradually and registered by the force sensor. This operation was repeated for the *x* and *y* directions, Figure 5-49. The *z* direction was not considered, since it corresponds to a singularity, where the stiffness of the manipulator reaches the stiffness of the material composing the rigid links.
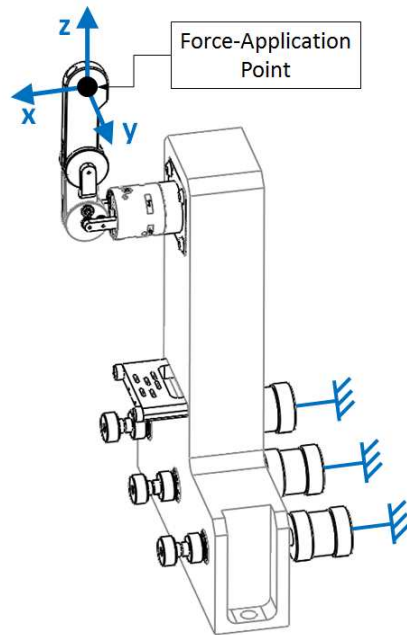
Figure 5-49: Test set-up for stiffness measurement on the manipulator end-effector

As shown in Figure 5-50, the relationship between the applied force and the displacements on the end-effector, along x and y directions, can be linearized within the measured range.
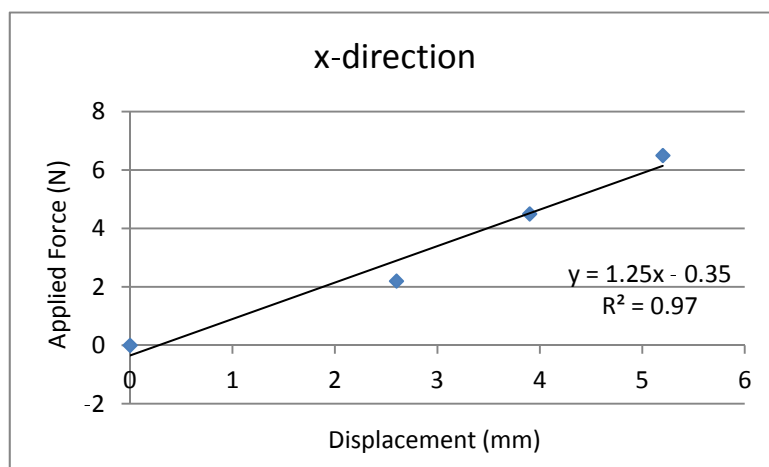
a)
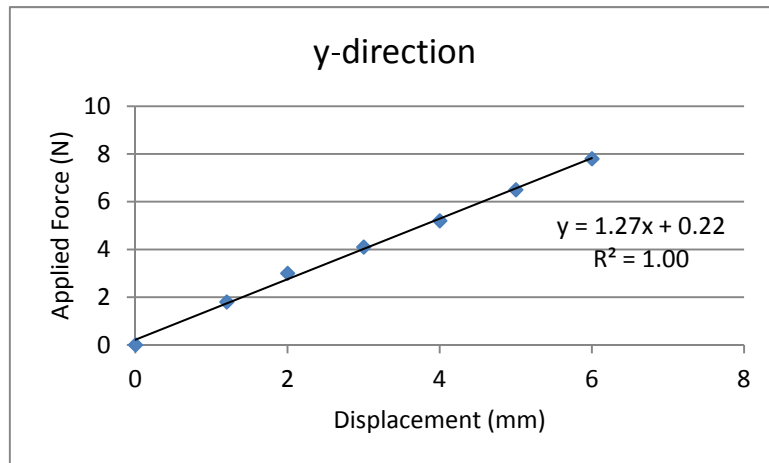
b)

Figure 5-50: Stiffness measurements on the manipulator end-effector, along *x* and *y*

Note that these values of stiffness are considerably higher than the ones in standard laparoscopic and robotic tools, Figure 3-5.

5.10.2 Mechanical Transparency

The mechanical transparency is related with the capacity of a system to appear mechanically invisible to the operator, not exerting any external forces on the user when used on the free space. Therefore, in order to access the transparent behavior of the system, a pair of forces was applied on the manipulator's end-effector and input shaft, Figure 5-51. Both values were measured by the two force sensors (sensor 1 and sensor 2).
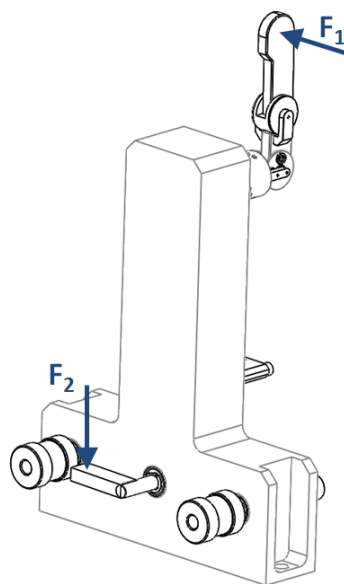
Figure 5-51: Test set-up for mechanical transparency assessment

The relationship between the two forces is shown in Figure 5-52, where the geometrical considerations are already considered. As can be seen, there is a significant matching between the two forces.
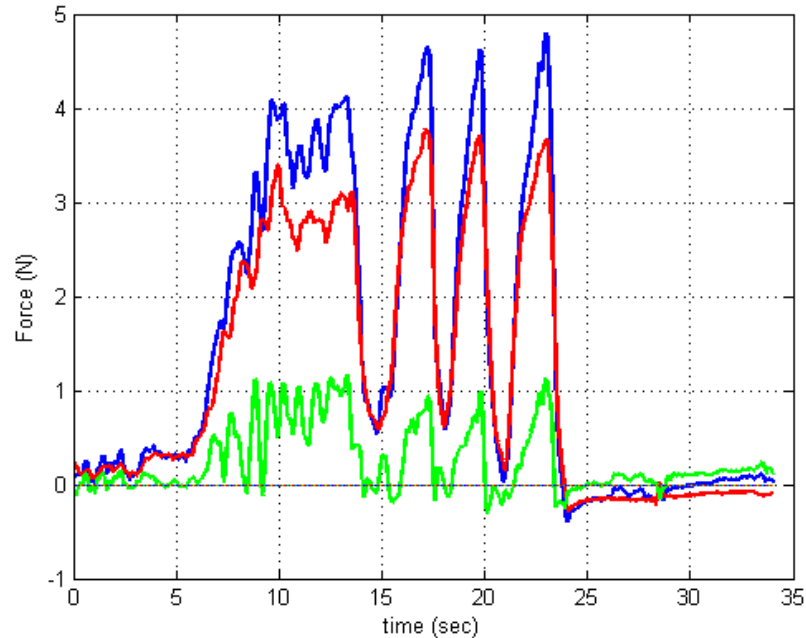
Figure 5-52: Measurements of system's mechanical transparency

5.11 Conclusions

In this chapter, a study of mechanical systems for MIS micro-manipulators has been performed. From this work, a new mechanical system was developed, being able to deliver multi-DOF complex kinematics to remote and narrow places, like the human abdominal cavity. The concept consists of a cable driven transmission for miniature robot manipulators, with different types of revolute joints, making it possible to achieve high levels of dexterity and stiffness compared with existing solutions. After, a review of existing multi-DOF mechanical systems for robotic micro-manipulators, the main limitations of current systems were identified. After that, the concept of the new mechanical system was comprehensively described and its geometrical models analysed. Finally, a 3-DOF prototype, incorporating the developed mechanical system, was designed and produced to validate the suitability of this concept to be integrated in micro-robotic systems for MIS procedures.

6 Dexterous Mechanical Telemanipulation for MIS

6.1 Introduction

The non-intuitive handling of laparoscopic instrumentation limits the use of Standard Laparoscopy to a small range of simple surgical procedures, like the removal of the appendix or gallbladder. With only less than 1% of the urologists using Standard Laparoscopy for complex surgeries, the only techniques that are widely used for complex surgeries are Open and robotic surgery (Camberlin et al., 2009). Being the only technique that enables the performance of complex procedures in a minimally invasive way, robotic surgery has been attracting patients, surgeons, hospitals and health insurers (Camberlin et al., 2009).

The market of robotic systems is dominated by the da Vinci Robot, developed and marketed since 1999 by Intuitive Surgical, Inc. (Sunnyvale, CA, USA) (Camberlin et al., 2009). This system is extremely expensive in acquisition (close to CHF 2 million (Camberlin et al., 2009)), maintenance (about CHF 200'000 per year (Camberlin et al., 2009)), disposable tools (about CHF 3'500 per procedure (Camberlin et al., 2009)) and training, representing much greater direct costs compared with open surgery instrumentation (Camberlin et al., 2009). For this reason, access to Robotic Surgery is limited to a minority of hospitals that (a) can afford to purchase it and (b) have enough patient volume to justify its acquisition.

Given the fact that the additional cost for robot-assisted surgery is not specifically considered by diagnosis-based reimbursements (in the United States and most European countries), most hospitals receive little or no additional payment to offset these added costs (Camberlin et al., 2009). In fact, on a pure profit basis, the purchase of a robotic system is only considered to be worthwhile for high-volume hospitals (with more than 500 procedures per year (Camberlin et al., 2009)). Knowing that the average worldwide number of procedures performed by each robot is about 120 cases (Camberlin et al., 2009), there is an evidence that these systems are being purchased for other than direct economic reasons and that the robot-equipped hospitals will try to attract more patients to their centres. This tendency towards centralisation of complex minimally invasive surgeries removes patients from hospitals without surgical robots and places an additional burden on the health care system.

The research work presented in this chapter addresses this problem, caused by the scarce cost-effectiveness of existing manual and robotic surgical instrumentation. A new mechanical system was thus developed, providing a new generation of cost-effective minimally invasive surgery telemanipulators. It is especially suitable for complex surgeries that require precise manipulation, with difficult access and limited space available inside the body.

Although this work has been applied to a telemanipulator for minimally invasive surgical procedures, it can also be adapted for any suitable remote actuated application requiring a dexterous manipulation with high stiffness, precision and quality force feedback such as assembly manipulation, manipulation in narrow places, in dangerous or difficult environments, and in contaminated or clean work spaces.

6.2 Platform Concept

Today's available surgical techniques for complex minimally invasive procedures are either too difficult for surgeons (Laparoscopy), too invasive for patients (Open Surgery) or too expensive for hospitals (Robotic Surgery). This absence of an optimal solution opens up a considerable research opportunity for improved surgical systems.

When performed by skilled and experienced surgeons, laparoscopy represents the most cost-effective solution, since its equipment is relatively affordable and the minimal invasiveness enables short hospitalization periods. However, its key drawback is related to its non-intuitiveness, which makes it a solution only for a limited number of surgeons (Camberlin et al., 2009).

In spite of its simplicity, a laparoscopic tool can be considered a mechanical telemanipulator, enabling the movements of the surgeon hand to be, to some extent, reproduced inside the body. The laparoscopic instrument embodies: (1) the master, held end of the proximal extremity of the instrument; (2) the slave, the distal extremity of the instrument; and (3) the motion transmission, middle of the tool and actuation rod, which communicates trajectories and forces/torques between the master and the instrument's tip.

By selecting a laparoscopic instrument that is lighter than the surgeon's hand and stiffer than the surgeon's wrist and arm joints, the dynamics of the instrument become extremely transparent.

Furthermore, the laparoscopic instrument is also able to provide communication of forces and positions in either direction. That is, if the instrument touches an object, the force and position effects are communicated instantly to the surgeon's hands. Even the texture of an object might be sensed by sliding the extremity of the instrument across a surface. The texture itself guides the tool across the tissue and the generated forces and motions are communicated back to the master handle.

Of course, while the symmetry of the laparoscopic instrument dynamics may be excellent, its dexterity is not, especially for wrist rotations at the distal extremity of the instrument. The intuitiveness is extremely poor due to the mobility constraints imposed by the entry port and the fulcrum effect. In order to address these limitations, while keeping production costs at affordable levels, the solution pursued in this research work consists in developing a fully mechanical telemanipulator combining dexterity and intuitiveness.

The new surgical system should have a teleoperated architecture, enabling a natural replication of the surgeons' hand movements inside the patient's body. The surgeon should be

able to perform the procedure directly manipulating two intuitive handles, viewing the operation through an endoscopic vision system. The surgeon's movements should be replicated to two intracorporeal multi-articulated distal instruments that reach the abdominal cavity of the patient through small incisions. The multiple degrees of freedom of these distal units should allow the system to overcome the manipulation problems described above, enhancing surgical dexterity and reaching places that are otherwise difficult to access. The technology should also enable tremor-free movements and at the same time provide force-feedback to the surgeon. The ergonomy and comfort of the surgeon will be improved by this system.

To sum up, this system should be equivalent to a robotic telemanipulator in providing control of the surgical instruments by a "master-slave" relationship, whereby the surgeon controls the actions of the "slave" arms by moving the "master" manipulators. However, it should use a fully mechanical technology for the motion transmission instead of a computer-controlled system thus providing better force-feedback. Since most surgeons are not satisfied with the force-feedback provided by current haptic devices, which is poor and too much delayed, a mechanical solution can overcome these limitations. In addition, without electronics, sensors, actuators and software, it has also the potential to be more reliable, affordable to produce and easier to sterilize.

6.2.1   Advantages over Existing Surgical Equipment

Extending surgeons' skills, this mechanical telemanipulator will provide a combination of functional and financial benefits that is unique in the state-of-the-art.

Functional Benefits

- Intuitive instrument movements: The system's kinematic model should be developed to allow a direct replication of surgeons' natural hand movements outside the body into corresponding micro-movements at the operating site. This will enable surgeons to perform delicate tissue handling and dissection with added dexterity even in confined spaces, while reducing their learning time.
- Minimally invasive for patients: Being intuitive to use, the distal units of the system should be extremely compact, enabling the performance of minimally invasive techniques even for complex surgical procedures. As a consequence, patients will benefit from having less painful recoveries, better aesthetical outcomes, less need for drugs and blood transfusions, shorter hospital stays and faster returns to their normal activities.
- More precise, tremor-free movements: Surgeons should be able to use "motion scaling," a feature that translates, for example, a two-millimetre hand movement outside the patient's body into a one-millimetre instrument movement in the surgical field inside the patient's body. Motion scaling is intended to allow greater

precision than is normally achievable in either Open Surgery or Laparoscopy. In addition, the device will provide filtering of tremor inherent in surgeon's hands.

- Superior surgeon ergonomics: The system should allow surgeons to operate while seated, which is not only more comfortable, but also may be clinically advantageous due to reduced surgeon fatigue. Natural hand-eye alignment at the surgeon interface should also be enabled, providing improved ergonomics over traditional laparoscopic and open surgery.

- Simple to use: Although the robotic systems are able to provide a very intuitive manipulation, their general use by the hospital staff is fairly complex. This new mechanical telemanipulator should be as simple as possible to use. Tissue manipulations should be as natural as with a robotic system but the time required to set-up the device should be significantly smaller.

- Force-feedback: The motion transmission should be performed with low levels friction. In this way, as opposed to the da Vinci Robot, the mechanical telemanipulator should offer a natural force-feedback to the surgeon during the surgical tasks.

- Easy sterilization: Being essentially composed by bio-compatible mechanical elements, with no electronics, the entire system is reusable after sterilization.

Financial Benefits

- Less hospitalisation costs: Besides better care for the patient, hospitals strive to reduce the length of the hospital stay and the post-operative care by decreasing the invasiveness of surgical procedures. In this way, they may benefit from a prospective reimbursement system in which longer lengths of stay have been previously established for the Open Surgery (about 8-9 days). In order to reach the same number of recovery days (4-5 days), and a reduction of post-operative costs, this system should enable surgical procedures to be as minimal invasive as Robotic Surgery.

- Affordable upfront investment: Given the fact that a fully mechanical technology does not require the use of a computer-controlled actuated system, the production costs of this system will be significantly lower compared to existing surgical robots.

- Warranty: Due to its huge technologic complexity, when acquiring a surgical robot, the hospital has to sign a compulsory and extremely expensive maintenance contract, whose annual cost is about 10% of the initial acquisition cost, i.e. approx. CHF 200'000 per year. Given its mechanical nature, this system will be more reliable.

- Infrastructure and logistics: As opposed to existing surgical robots, which weigh more than 600kg and are difficult to fit into small operating rooms (Camberlin et al., 2009), the system should be compact and light weight. It will be thus easy to transport and will not need a dedicated operating room.

- Fast set-up: Due to the presence of costly personnel and equipment, it is important to reduce preparation, operating and change-over time per procedure. Without any software to start up and sensors to calibrate, the estimated set-up time for this system will be significantly shorter than for a surgical robot.
- Faster training: Thanks to its intuitive nature, the system should require less training for surgeons and hospital staff compared to other techniques.

6.3 System Overview

6.3.1 General Concept

This combination of advantages can be achieved by a surgical platform comprising two mechanical teleoperated systems for remote manipulation, designed to naturally replicate the movements of both operator hands. These systems are designed by using a cable-driven mechanical transmission similar to the one developed on Chapter 5.

Given that the two teleoperated systems are structurally and functionally identical, the following sections refer to one mechanical teleoperated device only.

6.3.1.1 Kinematics

When a minimally invasive surgical tool is inserted into the patient, its degrees of freedom are reduced from 6 (Figure 6-1a) to 4 (Figure 6-1b), due to the 2-DOF-constraint imposed by the entry port. The remaining degrees of freedom are composed by pan–tilt–spin rotations centered at the entry point and an axial translation passing through the entry port, Figure 10b.
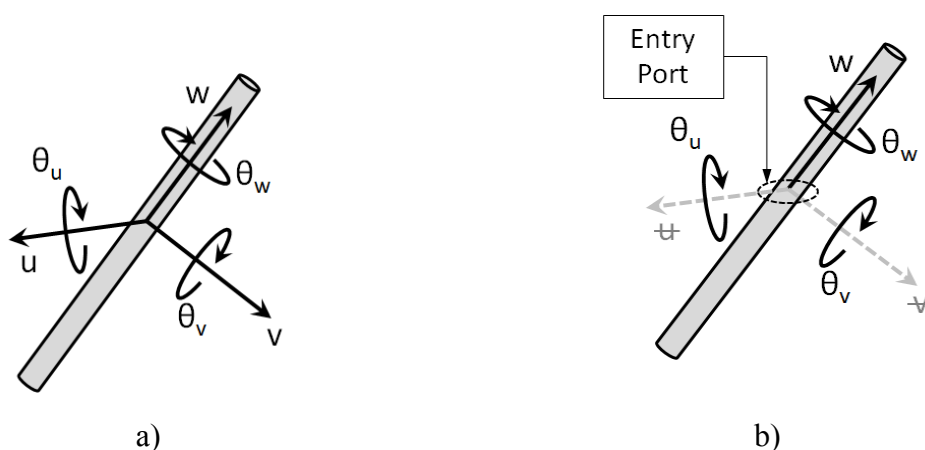
Figure 6-1: Degrees of Freedom of a laparoscopic instrument a) on the 3D space and b) when passing through an entry port

In order to overcome these mobility constraints and deliver 6 DOF to the end-effector, (which has a further actuation DOF), the kinematic model of the surgical manipulator should be

provided with a total of 9 DOF - 6 for the positioning and orientation of the end-effector within the working area, 2 to recover the 2 DOF lost to the entry port constraints and 1 for the actuated end-effector, Figure 6-2a. However, this number can be decreased if the axis of the proximal joint is coincident with the entry port, Figure 6-2b. In this case, the resultant kinematics is still redundant, but only by a single DOF.

a)   b)
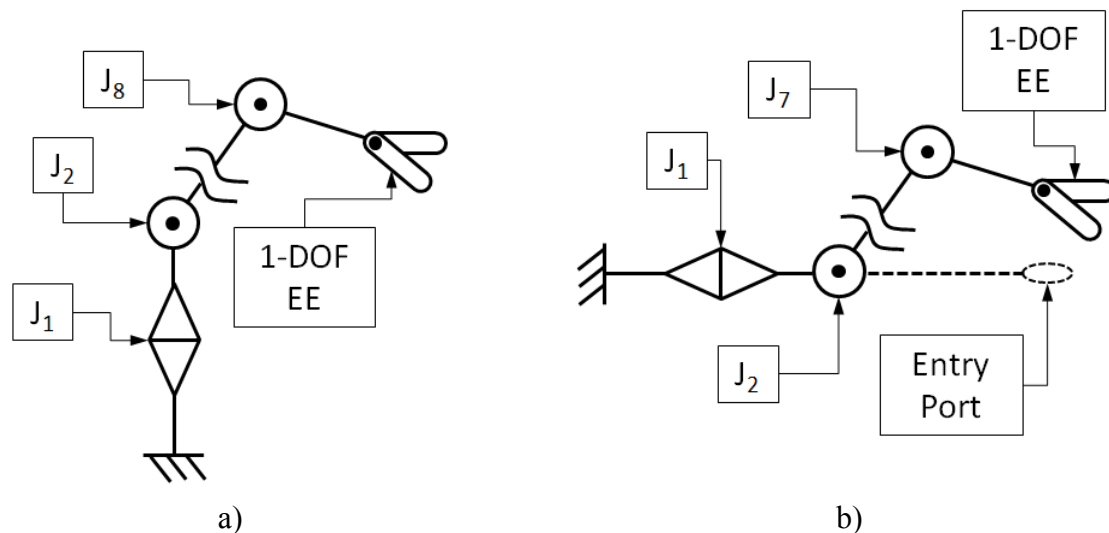
Figure 6-2: Kinematic Structure of the Surgical Manipulator with a) non-aligned proximal joint and b) aligned proximal joint

6.3.1.2 Master-Slave Architecture

One of the key features of this system is the master-slave architecture, where a slave unit and a master unit are configured to be kinematically equivalent, thus working together and achieving a force reflecting teleoperation.

According to Figure 6-3, the mechanical telemanipulator comprises: i) a slave manipulator, having a number of slave links interconnected by a plurality of slave joints; ii) an end-effector (instrument/tool or a gripper/holder) connected to the distal end of the slave manipulator; iii) a master manipulator, having a corresponding number of master links interconnected by a plurality of master joints; and iv) a handle for operating the mechanical telemanipulator. This system can also be described by considering the end-effector to be part of the slave manipulator and the handle to be part of the master manipulator. In a broader sense, the links and joints composing the end-effector can be considered distal slave links and joints of the slave manipulator, while the links and joints composing the handle can be considered distal master links and joints of the master manipulator.

The slave manipulator and the master manipulator are connected to each other by a connecting link, $^{MS}L_0$, which is directly connected to the ground. This connecting link is connected at its proximal and distal extremity to the master and slave joints $^{M}J_0$ and $^{S}J_0$, which can respectively be considered as the first proximal joints of the master manipulator and the slave manipulator.
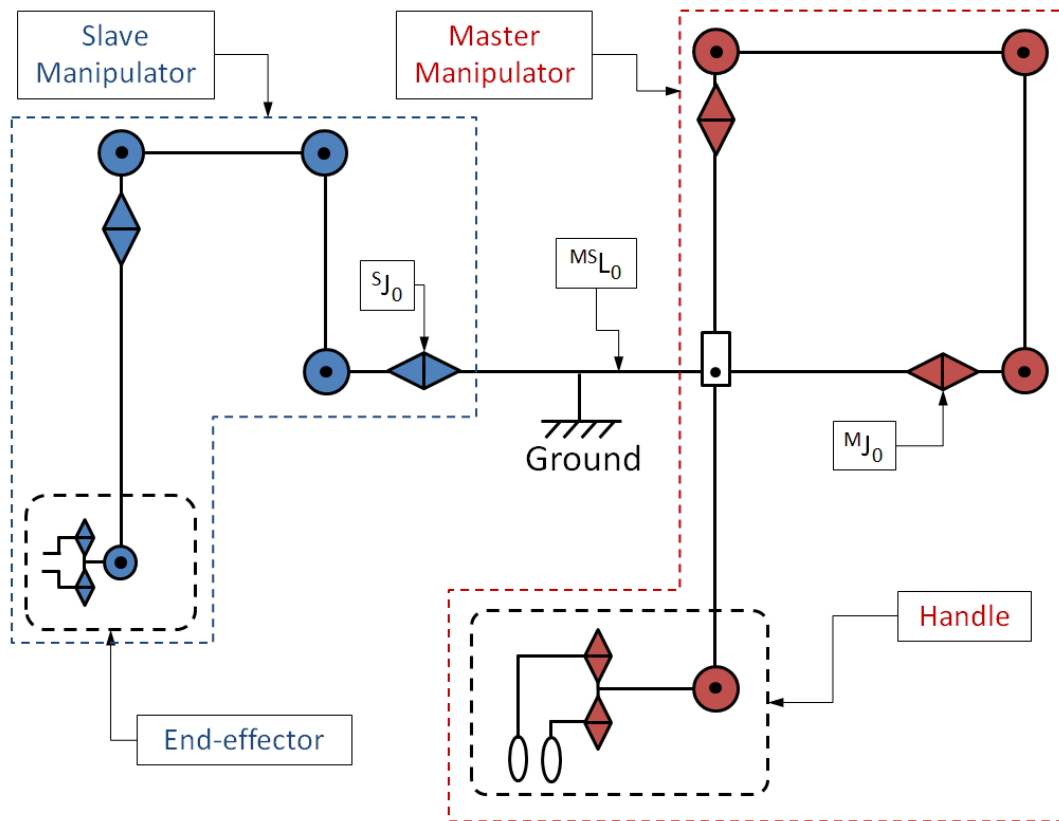
Figure 6-3: Schematic view of the structural parts of the mechanical telemanipulator, in a master-slave relationship configuration

As shown in Figure 6.4, since the first proximal joints of the master manipulator, $^{M}J_0$, and the slave manipulator, $^{S}J_0$, have a co-axial configuration with collinear axes, they can be considered kinematically redundant, Figure 6-4a. In this way, they can be merged in a single joint, $^{MS}J_0$, which connects the connecting link, $^{MS}J_0$, of the telemanipulator to the ground, Figure 6-4b.
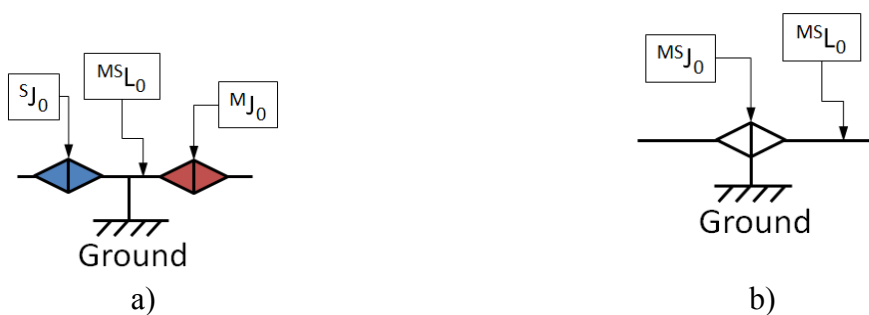
Figure 6-4: Kinematic equivalence between joints a) $^{S}J_0$ and $^{M}J_0$ and b) $^{MS}J_0$

If joints $^{M}J_0$ and $^{S}J_0$ are merged into joint $^{MS}J_0$, the segment that goes from the slave joint $^{S}J_1$ to the master joint $^{S}M_1$ is considered to be the connecting link $^{MS}L_0$. In this case, the proximal slave link, $^{S}L_1$, connects slave joints $^{S}J_1$ and $^{S}J_2$ while the proximal master link, $^{M}L_1$, connects master joints $^{M}J_1$ and $^{M}J_2$. Overall, the slave manipulator comprises a number of slave links $^{S}L_1$, $^{S}L_2$, $^{S}L_3$, $^{S}L_4$ interconnected by a plurality of slave joints $^{S}J_1$, $^{S}J_2$, $^{S}J_3$, $^{S}J_4$ whereas the

master manipulator comprises a corresponding number of master links $^ML_1$, $^ML_2$, $^ML_3$, $^ML_4$ interconnected by a plurality of master joints $^MJ_1$, $^MJ_2$, $^MJ_3$, $^MJ_4$, Figure 6-5.
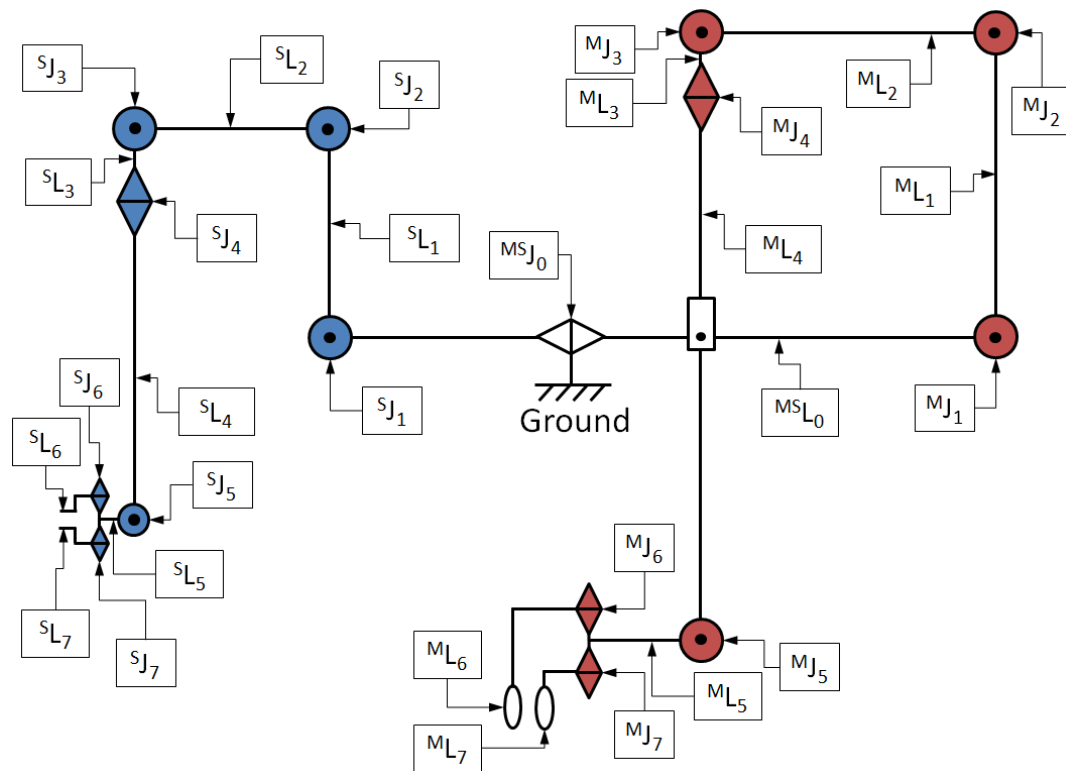
Figure 6-5: Kinematic Scheme of the mechanical telemanipulator

With reference to Figure 6-5, the handle of the mechanical telemanipulator comprises a first handle link, $^ML_5$, which is connected to one extremity of the fourth master link, $^ML_4$, through a first handle joint, $^MJ_5$. The handle further comprises a second and a third L-shaped links, $^ML_6$ and $^ML_7$, articulated at one extremity to the first handle link, $^ML_5$, through respectively a second and a third handle joint, $^MJ_6$ and $^MJ_7$, whose axes are collinear and substantially perpendicular to the axis of the first handle joint, $^MJ_5$.

The end-effector is a surgical tool and comprises, in view of Figure 6-5, a first tool link, $^SL_5$, which is connected to one extremity of the fourth slave link, $^SL_4$, through a first tool joint, $^SJ_5$. This surgical tool further comprises two working blades, $^SL_6$ and $^SL_7$, connected to the first tool link, $^SL_5$, through respectively a second and a coaxially third tool joints, $^SJ_6$ and $^SJ_7$, mounted to each other.

The surgical tool is interchangeable and can be of several types, such as scissors, scalpels, cutters, needle holders and other accessories to be connected to the distal extremity of the salve manipulator. The surgical tool which enters the patient's body is reusable after sterilization.

The system thus essentially consists of two identical kinematic chains. A motion (or force) on one extremity is faithfully reproduced on the other extremity, up to a scaling factor.

6.3.1.3   Motion Transmission

In order to achieve a direct replication of movements between the master an slave manipulators, mechanical transmission means T_1, T_2, T_3 and T_4, as schematically shown in Figure 6-6, are arranged to kinematically connect the slave manipulator with the master manipulator such that the movement applied on the master and handle joints, $^SJ_1$, $^SJ_2$, $^SJ_3$, $^SJ_4$, $^SJ_5$, $^SJ_6$, $^SJ_7$, are respectively reproduced by the corresponding slave and tool joints, $^MJ_1$, $^MJ_2$, $^MJ_3$, $^MJ_4$, $^MJ_5$, $^MJ_6$, $^MJ_7$.
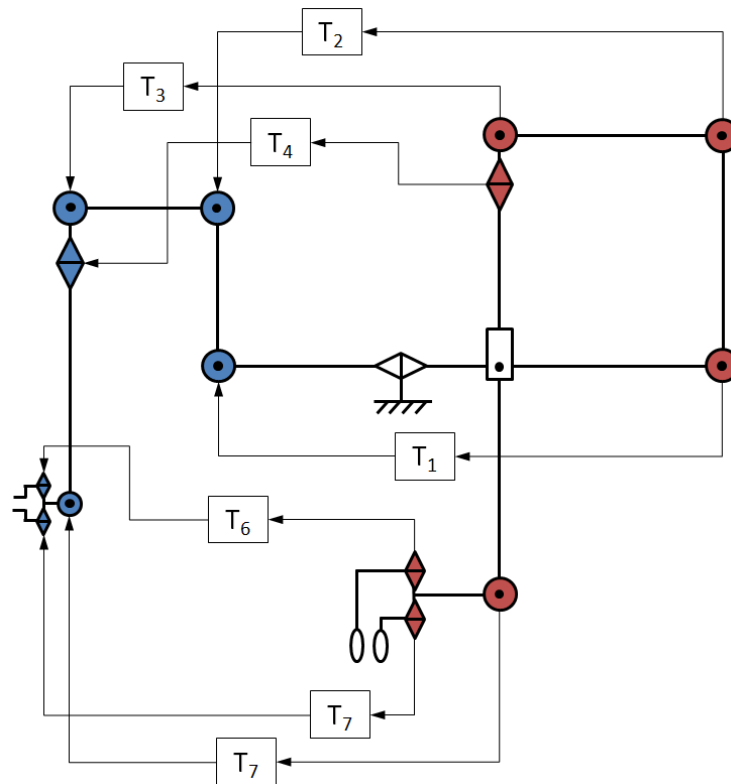
Figure 6-6: Kinematic connections between the corresponding joints of the master and slave manipulators

Therefore, the movements applied on the handle are directly replicated as movements of the slave joints. As a result, the multi-articulated end-effector, connected to the slave manipulator, is moved in an equivalent movement of the handle of the master manipulator. As a consequence, the master links, $^ML_1$, $^ML_2$, $^ML_3$, $^ML_4$, $^ML_5$, $^ML_6$, $^ML_7$, of the master manipulator are always parallel to the corresponding slave link, $^SL_1$, $^SL_2$, $^SL_3$, $^SL_4$, $^SL_5$, $^SL_6$, $^SL_7$, of the slave manipulator, for any position of the device (Figure 6-7).
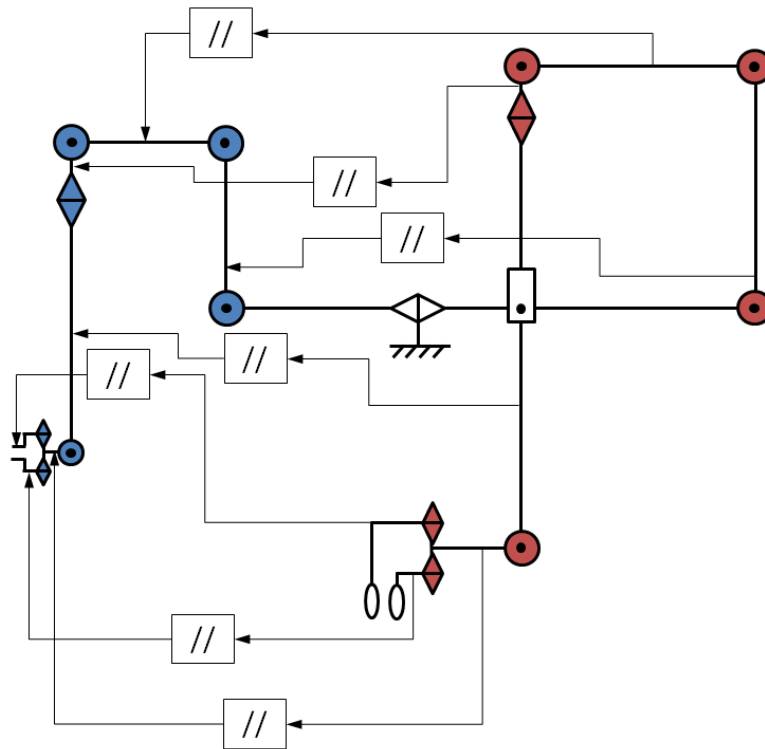
Figure 6-7: Parallelism between equivalent master and slave links

In order to increase the precision of the manipulation, as well as, reduce the tremors of the user's hand, a scale-down of the movements, from the master manipulator to the slave manipulator, is desired. By guaranteeing a perfect match between the movement of each master and slave joint angles, a predefined scale ratio between the length of each master link and the length of the corresponding slave link, will cause the amplitude of the movements on the handle, to be reproduced by the end-effector in the same scale ratio.

For each degree of freedom of the mechanical telemanipulator, different types of mechanical transmissions can be used. In order to minimize the system's overall friction and inertia, while increasing backdrivability and stiffness, the mechanical transmission between most of the master and slave joints is essentially in the form of pulley-routed flexible elements, where each driven pulley of the slave joint is connected to the respective driving pulley of the master joint, by a single-stage closed cable loop transmission. Figure 6-8 shows the working principle of this actuation for the general case of transmitting the motion from a driving pulley, C_m, of the master manipulator to a driven pulley, C_s, of the slave manipulator. This closed cable loop transmission can be composed by a pair of cables, L_a and L_b, whose both extremities are anchored respectively to the driving and the driven pulleys, C_m, C_s to ensure that no relative movement between the cable L_a, L_b and the pulleys C_m, C_s occurs. Both cables L_a, L_b form together a single closed loop L from one pulley to the other.
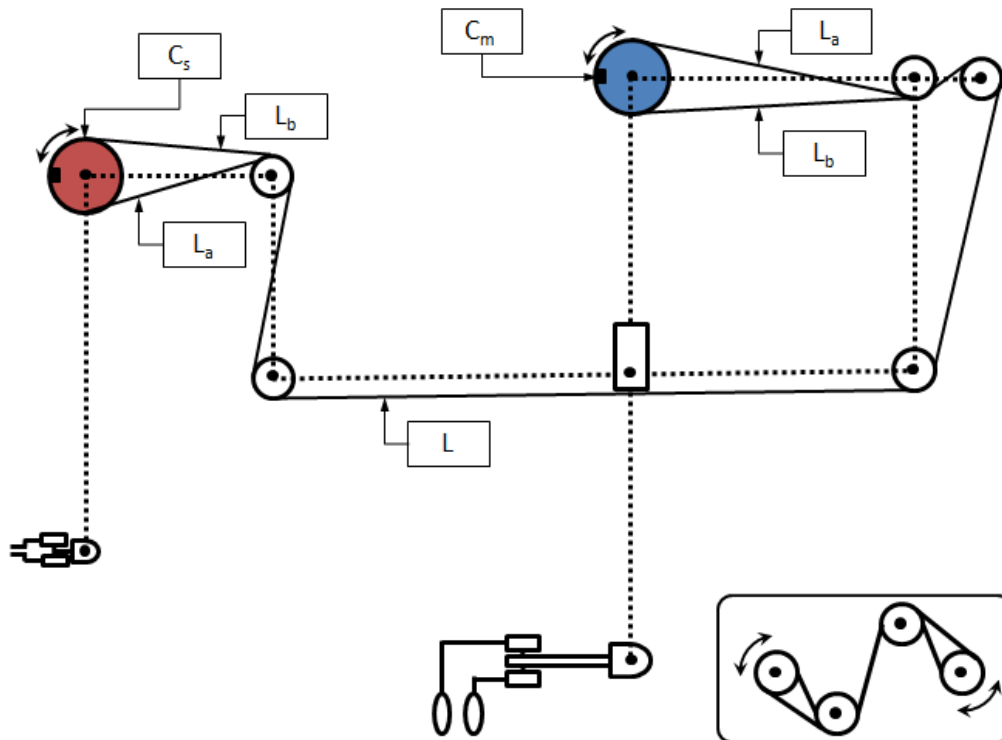
Figure 6-8: Schematic view of a single closed loop (cable) transmission between a general driven pulley of the slave manipulator and the corresponding driving pulley of the master manipulator

The transmission of the movement between each master pulley and the equivalent slave pulley, by using this kind of mechanical transmission, may bring problems of kinematic and dynamic coupling between the driven and the driving pulleys. Furthermore, the adoption of a closed loop cable transmission requires that the overall length of the cable route must be kept constant, for all possible master-slave configurations, independently of the motion performed by the driving pulleys of the master manipulator. Therefore, cables must be routed through joint idler pulleys while maintaining constant cable length. The basics of the cable routing method used is illustrated in Figure 6-9 for the general case of having both cables L_a and L_b, composing the closed loop L, being routed through a general joint. The cables L_a and L_b are wrapped around a set of pulleys, I_m, called the joint idle pulleys, which are concentric with the joint's axis of revolution. To maintain constant cable length of the closed loop, cables La, L_b must remain in contact with the joint idle pulleys at all times. In this way, if the joint angle θ_j is reduced, the length of the superior segment of La, in contact with the idler pulley I_m will decrease and the inferior segment of L_b will increase, by the same value, guaranteeing the constant length of the cable closed loop. In order to keep a permanent contact between the cables L_a and L_b with the idle pulleys I_m, auxiliary pulleys A_p and A_d are added to the proximal and distal side of the joint.
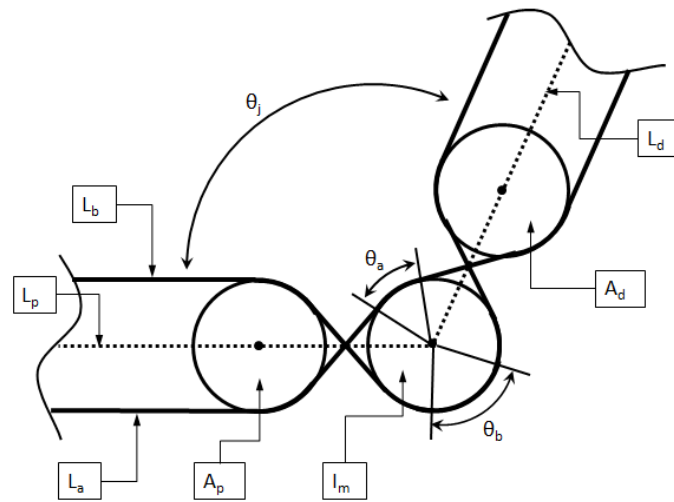
Figure 6-9: Schematic view of a cable rooting method to keep the closed loop with a constant length, at the joint level

Another solution to keep a constant cable length of the closed loop consists in compensating the length change not at the joint level, in the same master or slave manipulator but between the equivalent idle pulleys, I_m and I_s, of respective master and slave joints, as schematically shown in Figure 6-10. In this case, both cables L_a and L_b are passing under I_m and I_s and, when the joint angle θ_j is changed, the constant length of the closed loop is guaranteed because the variation of θ_s is precisely compensated by the opposite variation of θ_m.
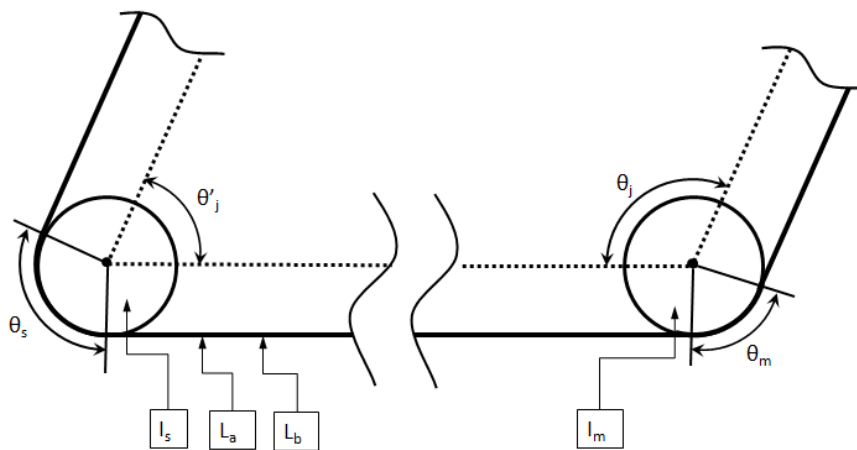
Figure 6-10: Schematic view of another cable routing method to keep the closed loop with a constant length, at equivalent master-slave joints level

The mechanical transmission for each of the eight degrees of freedom are schematically shown from Figure 6-11a to Figure 6-11h.

a)

b)

c)

d)

e)

f)

g)   h)
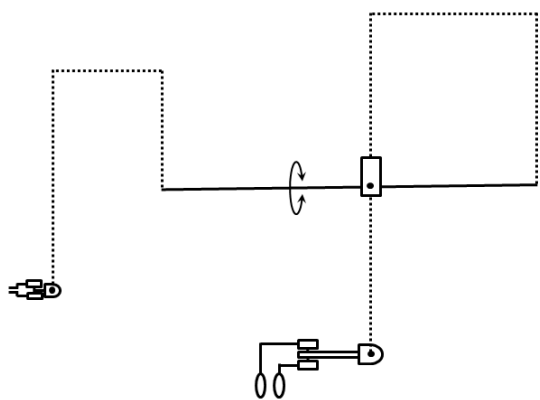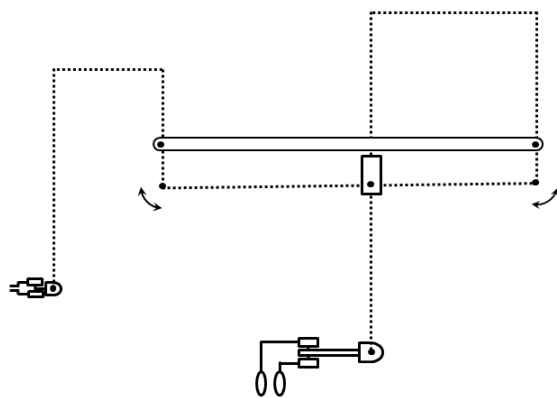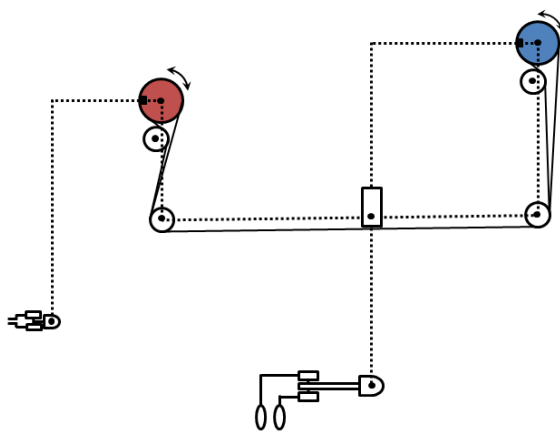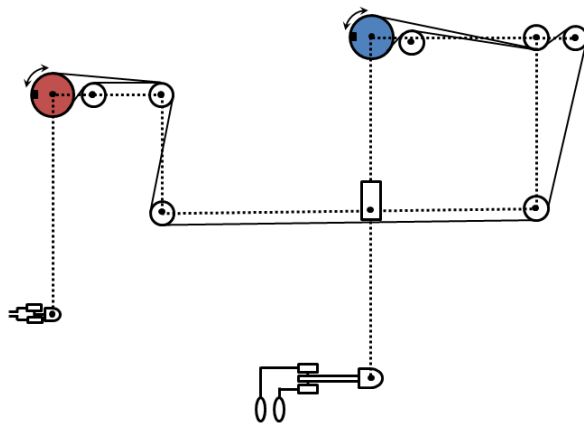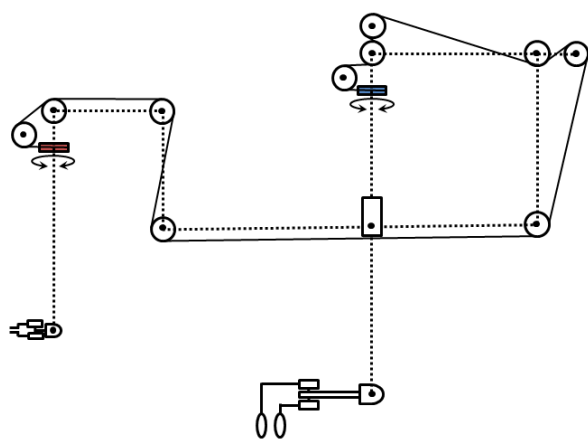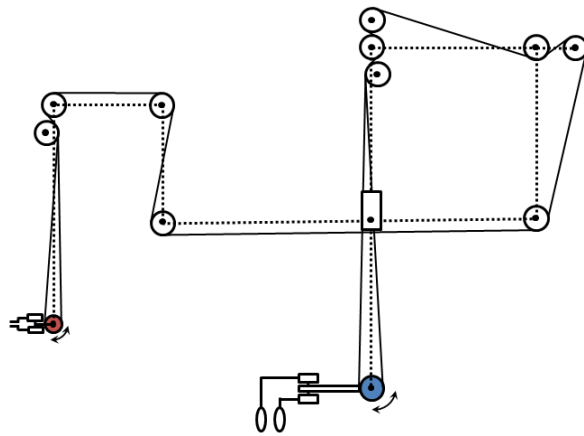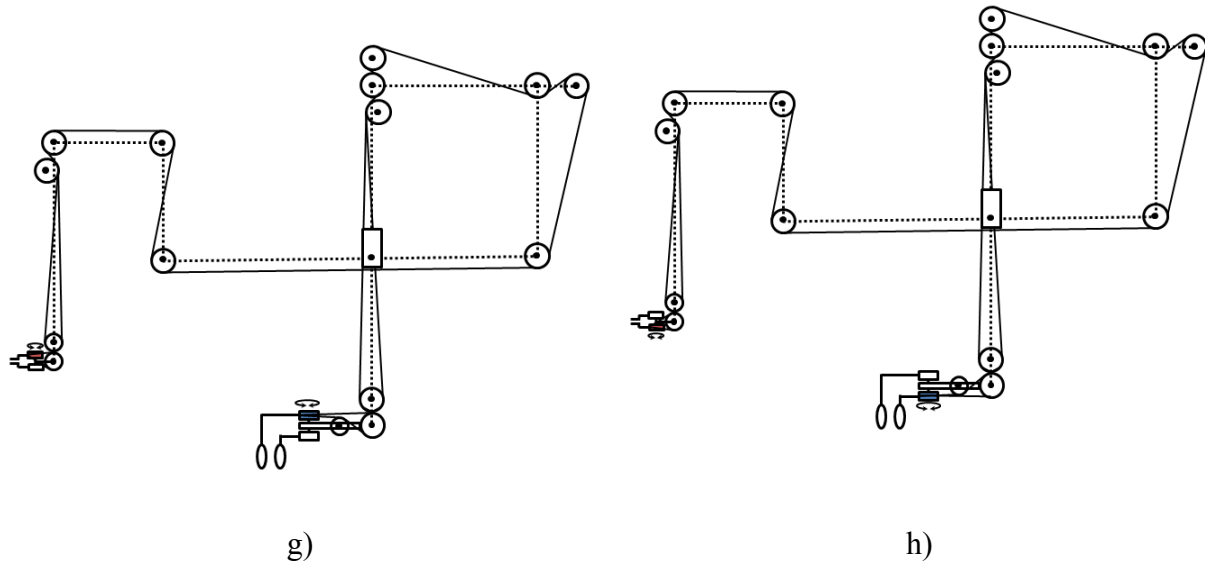
Figure 6-11: Schematic views of the cabling topology for each of the eight degrees of freedom

6.3.1.4 Remote Center of Motion

The main kinematic constraint of the complete system is the requirement of transmitting all motions through the fixed point incision, which is achieved by a mechanical constraint applied on the master manipulator. This kinematic feature is called Remote Center of Motion, RCM. As can be seen in Figure 6-12, the mechanical constraints are configured to ensure that, the fourth master link, $^{M}L_4$, of the master manipulator, always translates along its longitudinal axis a_1 so that the corresponding link, $^{S}L_4$, of the slave manipulator, always translates along a virtual axis a_4, parallel to the longitudinal axis, a_1, of the master link, $^{M}L_4$. These mechanical constraints are further configured to enable the fourth master link, $^{M}L_4$, to rotate about its longitudinal axis a_1, and about a second and a third axis, a_2 and a_3, which are perpendicular to each other. The longitudinal axis, a_1, and the second and third axes, a_2 and a_3, always intersect at a stationary single point, MCM, independently of the orientation of the fourth master link, $^{M}L_4$.
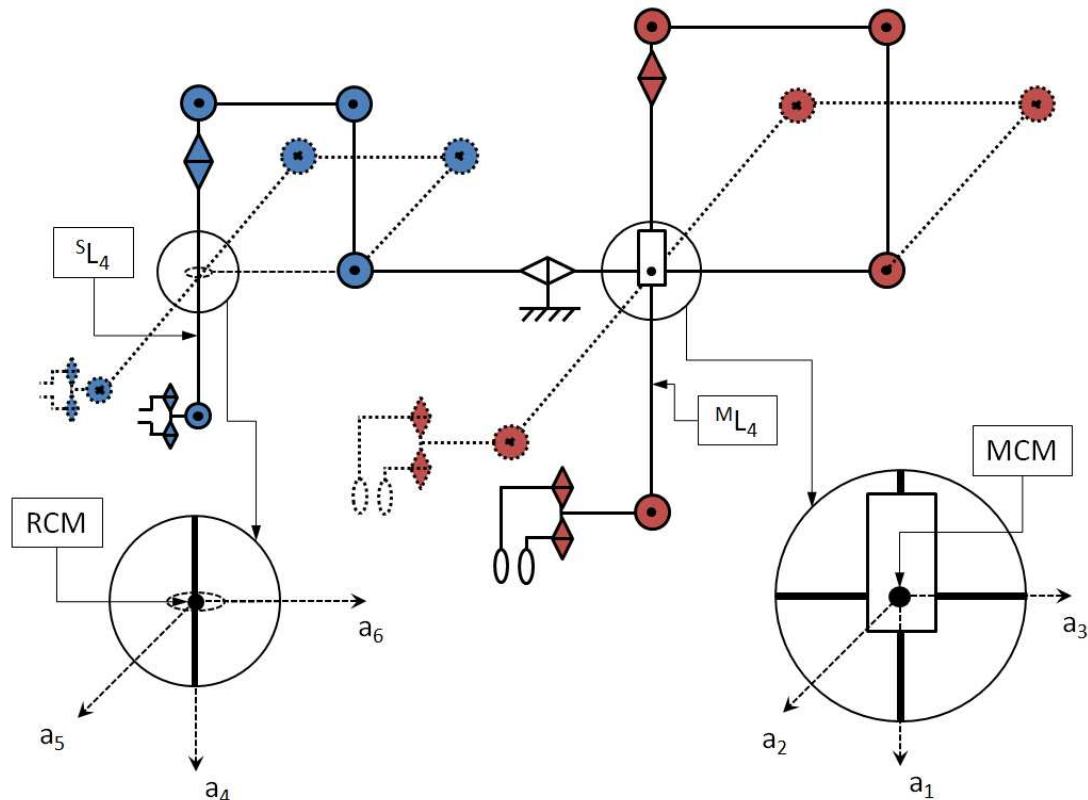
Figure 6-12: RCM induced by mechanical constraints

This configuration allows the corresponding slave link, $^{S}L_4$, to rotate about its longitudinal axis a_4, and about a fifth and a sixth virtual axis, a_5 and a_6, which are perpendicular to each other. The longitudinal axis a_4 of the link $^{S}L_4$ and the fifth and sixth virtual axes, a_5 and a_6, always intersect each other at a virtual stationary single point, in the vicinity of the remote manipulation - the Remote Center of Motion, RCM. During a minimally invasive surgical procedure, the RCM is brought in coincidence with the surgical incision point, reducing trauma to the patient and improving cosmetic outcomes of the surgery.

6.3.1.5 Gravity Compensation

In order to reduce, or eliminate, the effects of system's weight felt by the user, and increase the transparency of the telemanipulation, a mechanical gravity compensation system is implemented. For this propose, two solutions can be considered: spring and counterweight - based compensation. While the first solution may provide a more compact and lighter solution, by using a counterweight-based gravity compensation, the non-linear effects of the springs can be avoided and the movement of the distal links of the master and slave manipulators can be taken into account. Consequently, a counterweight-base gravity compensation was implemented, consisting of a set of counterweights, $^{M}m_1$, $^{M}m_2$, $^{M}m_3$, $^{S}m_1$, $^{S}m_2$ and $^{S}m_3$, which are connected to master and slave links, $^{M}L_1$, $^{M}L_2$, $^{M}L_4$, $^{S}L_1$, $^{S}L_2$ and $^{S}L_4$, bringing the center of gravity of each one of those kinks to a point coincident with its proximal joint, Figure 6-13. In this way, the overall center of gravity of the master

manipulator will be almost static, close to the intersection of axes of joints $^{MS}J_0$ and $^{M}J_1$. On the slave manipulator, the overall center of gravity will be statically placed on the intersection of axes of joints $^{MS}J_0$ and $^{S}J_1$.
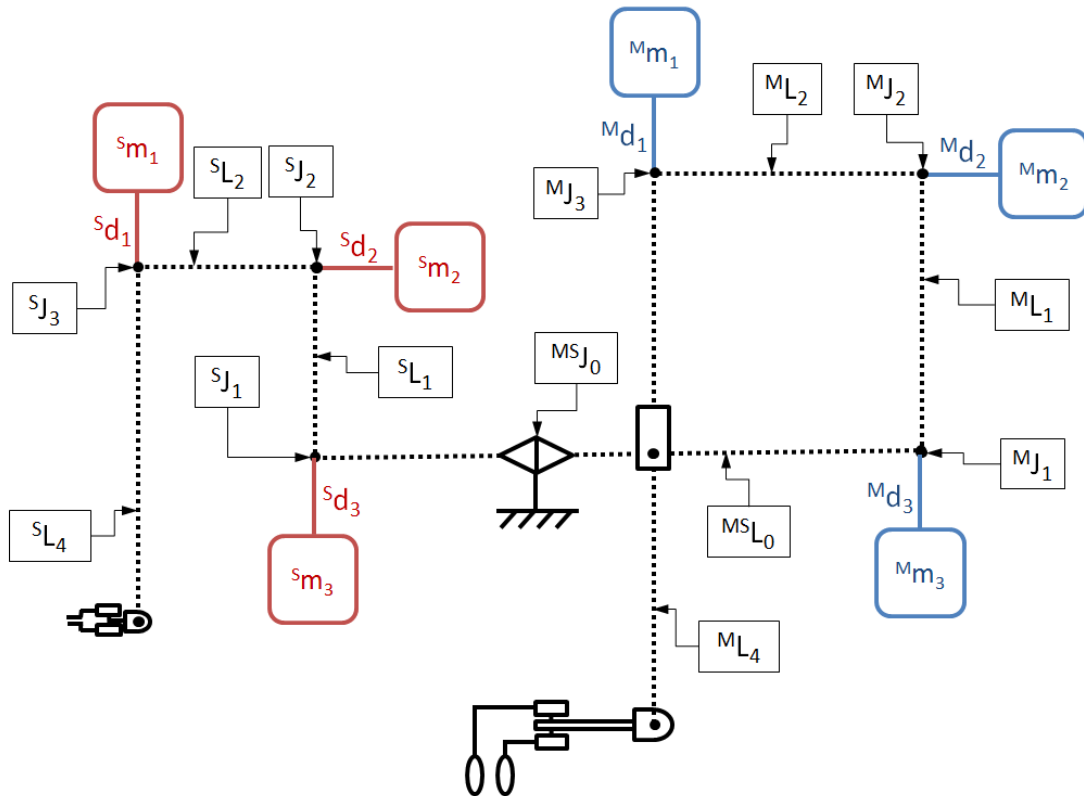
Figure 6-13: Mechanical Gravity Compensation System

6.4 Prototype Design and Realization

In order to evaluate the complete telemanipulator, a working prototype was designed and produced and its key mechanical performances were evaluated.

6.4.1 System Design

Figure 6-14a shows the full 3D model of the telemanipulator, being mounted on a reference base, which can be directly fixed to a Lab test bench.

The system's handle comprises a holding stick, configured to be held by the palm of the hand and to freely rotate about its longitudinal axis a_s, which is collinear with the axis of the second and third handle joints, $^{M}J_6$ and $^{M}J_7$, Figure 6-14b. This handle will be operated by the thumb and index of the user, in a grasping motion.

The handle is kinematically connected to the end-effector in a manner that the movement applied on the second and third handle links, $^ML_6$ and $^ML_7$, by the tips of the thumb and the index finger are reproduced by the two end-effector blades, $^SL_6$ and $^SL_7$, Figure 6-14c.

a)

b)

c)
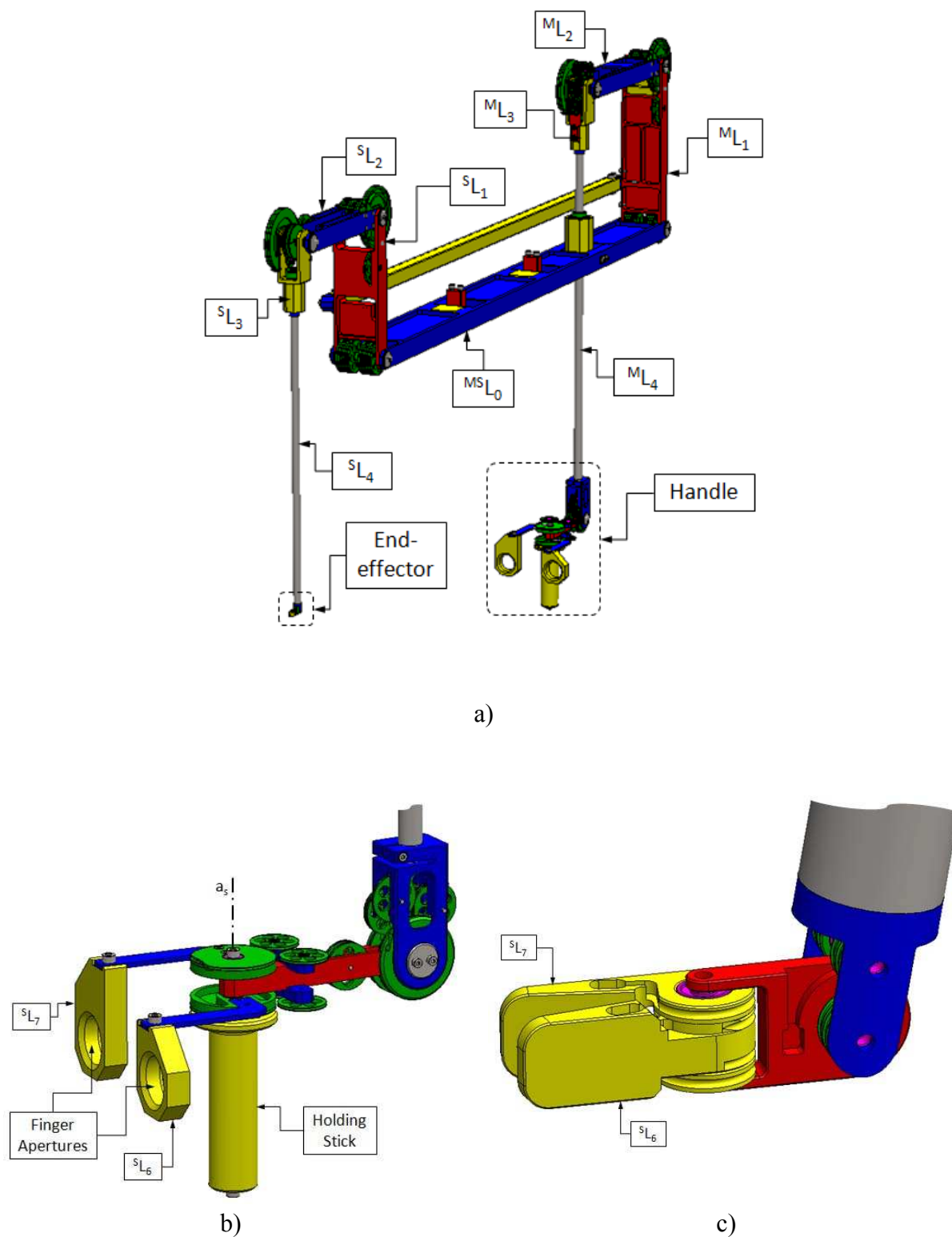
Figure 6-14: Perspective view of the a) full mechanical teleoperated surgical device b) handle and c) end-effector

Figure 6-15 shows the telemanipulator in different working positions. The amplitude of the movements applied on the handle by the surgeon is reproduced by the end-effector through system's mechanical transmission, with a down-scaling factor of 2/3.
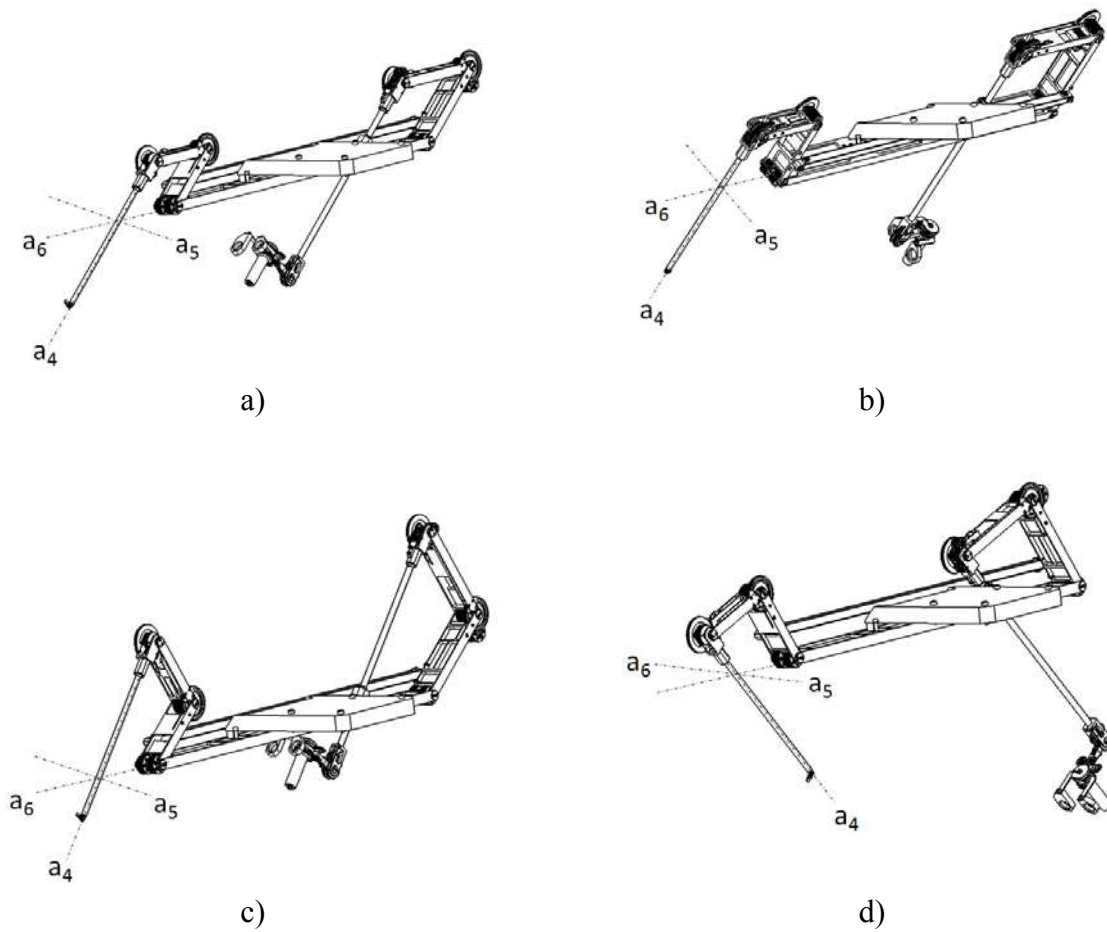
Figure 6-15: Different working configurations of the mechanical teleoperated surgical device

The mechanical constraints comprise a linear bearing that is mounted inside an articulated system, which enables the fourth master link, $^{M}L_4$, of the master manipulator, to rotatable about three different axes, θ_1, θ_2 , θ_3, intersecting at the stationary single point, MCM. Translation along θ_1 is provided by a sliding bearing at the MCM, Figure 6-16.

a)   b)
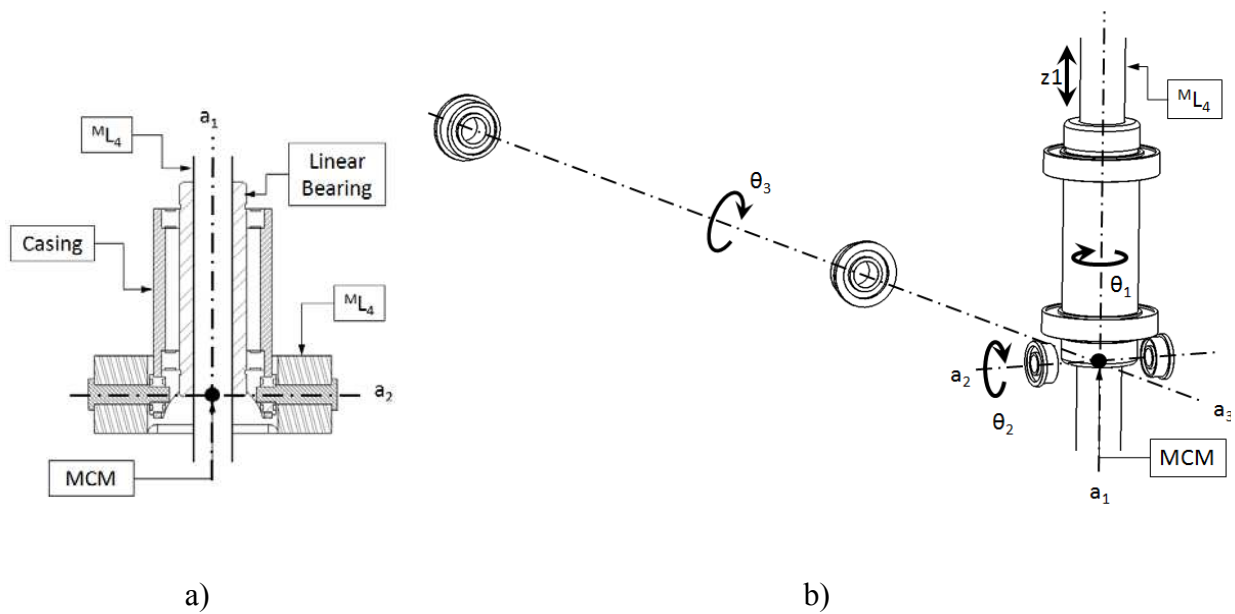
Figure 6-16: Mechanical constraints of the Mechanical Telemanipulator

6.4.2 Prototype

The working prototype of the telemanipulator can be seen in Figure 6-17, mounted on a stable reference base part. In order to reduce the weight, most of the components are made from an aluminum alloy (Al 7075-T6), which guarantees a fairly good trade-off stiffness/weight of the mechanical structure. The biocompatibility and capability of being sterilized are also assured by using this material.
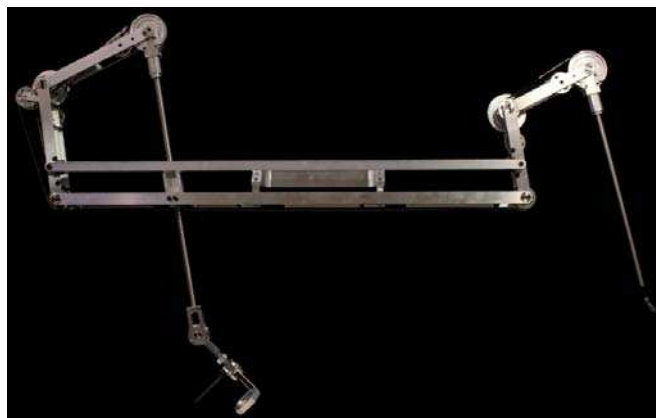
Figure 6-17: Working prototype

In order to minimize the frictional effects and avoid backlash, all joints are implemented with radial ball bearings and most of the components are produced by precise CNC machining process. The mechanical solutions, developed in this chapter, allow for smooth, backlash-free, high force and precise manipulation, being highly suitable for the performance of minimally

invasive surgical tasks. Figure 6-18, shows the prototype in four different working configurations.

a)

b)

c)

d)
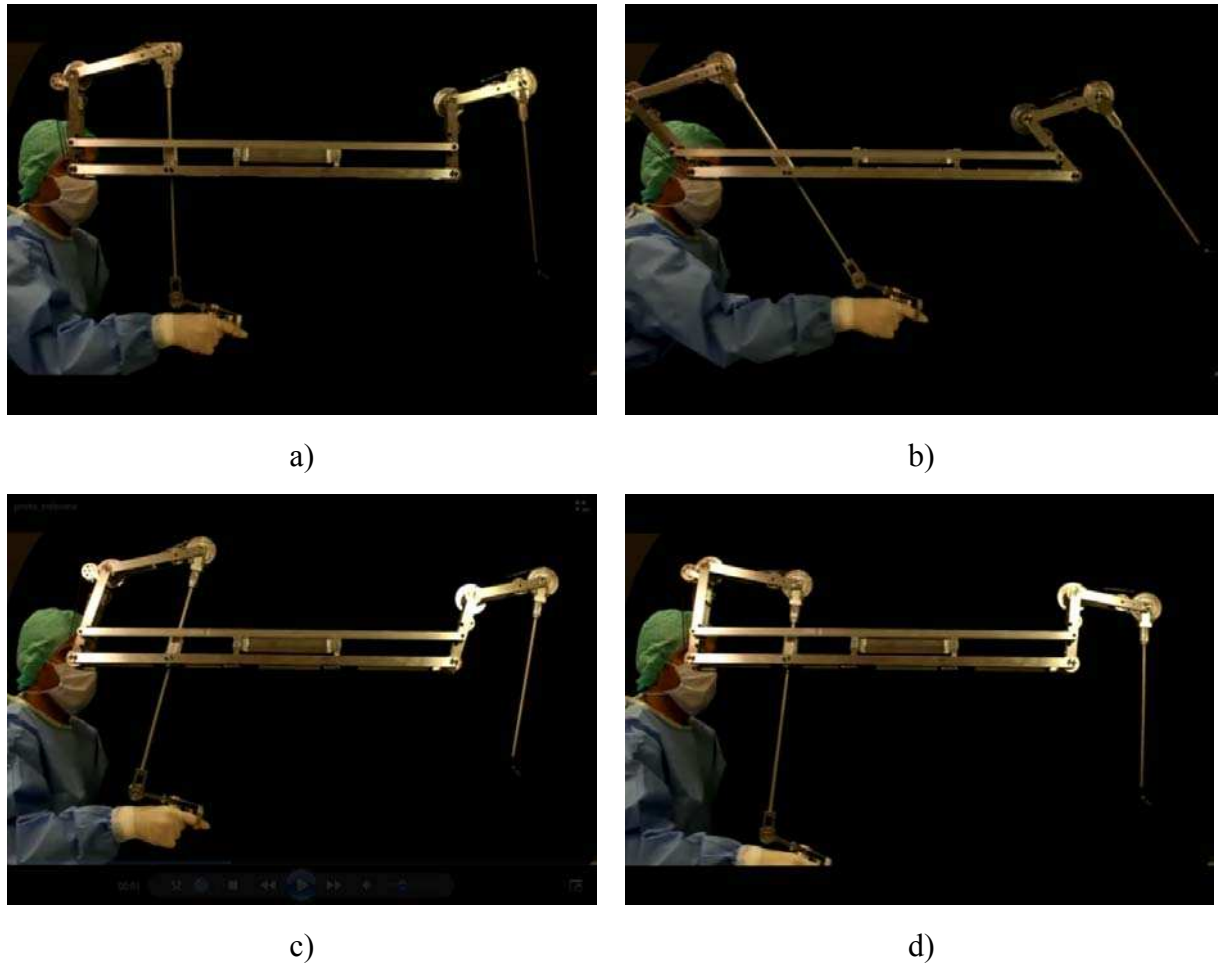
Figure 6-18: Prototype in different working configurations

6.5   Technical Evaluation

The evaluation of the telemanipulator is made through the following measurements: mechanical transparency and stiffness. These measurements assess the quality of the force interaction between the end-effector of the manipulator and the tissue inside the patient's body. The force sensors used are two *A XFTC320* load cells, one with a range of ±50 N and the other with ±10 N, both from the company *Measurement Specialties*^{TM}. The deformations were measured by using a standard dial gauge.

6.5.1   Stiffness

In order to measure the stiffness of the system, the position of the handle was locked, while the applied force on the slave manipulator's end-effector was increased gradually by the user

and registered by the force sensor. This operation was repeated for the *x*, *y* and *z* directions, **Figure 6-19**.
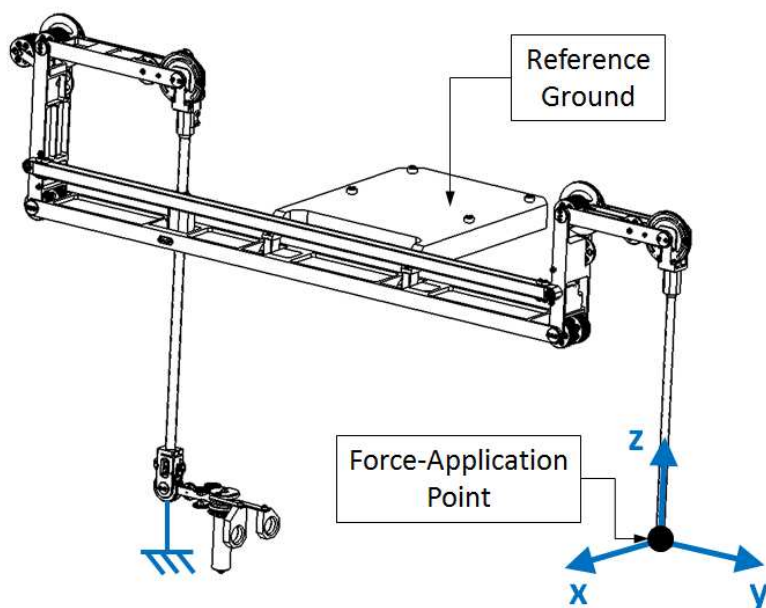
Figure 6-19: Test set-up for stiffness measurement on the tool end-effector

As shown in **Figure 6-20**, the relationship between the applied force and the displacements on the end-effector, along *x*, *y* and *z* directions, can be linearized within the measured range.
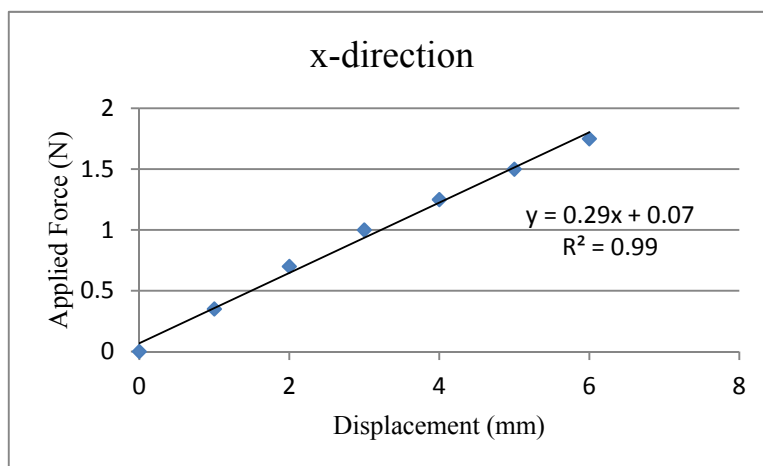
a)
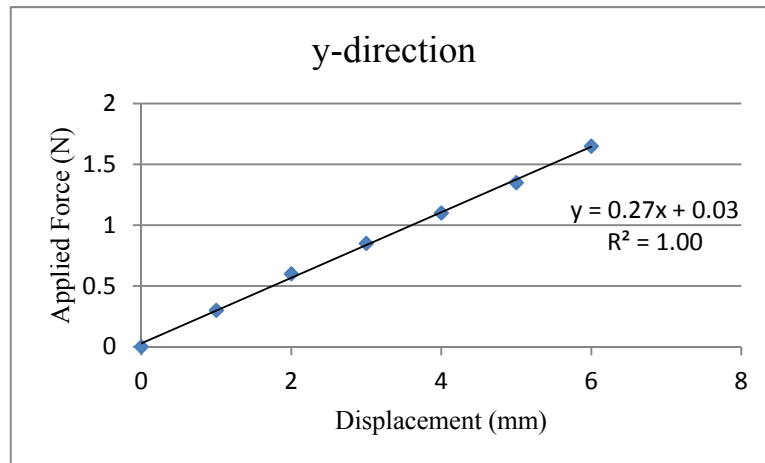
b)
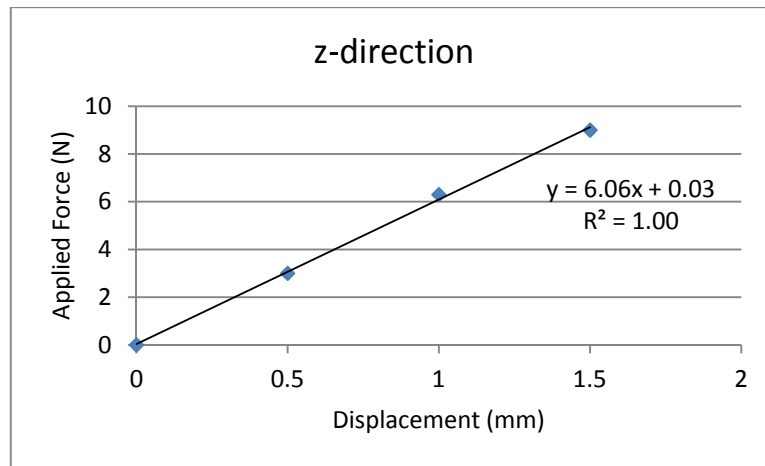
c)

Figure 6-20: Stiffness measurements on the tool end-effector, along x, y and z

Note that, on the x and y directions, a force of around 2N produces an end-effector displacement of about 5mm. Although this stiffness correspond to the values seen in standard laparoscopic and robotic tools, Figure 3-5, it can be considerably maximized if the stiffness of the tool shaft is increased, which can be achieved by increasing the thickness of the insertion tube. In this way, the stiffness at the tip of the instrument can be similar to the one felt at the proximal extremity of the tool shaft. Figure 6-21 shows the stiffness of the system on the proximal extremity of the tool shaft.
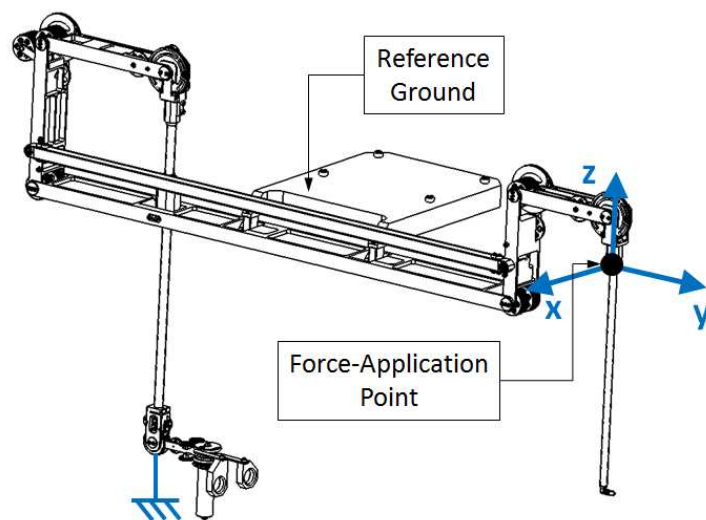
a)
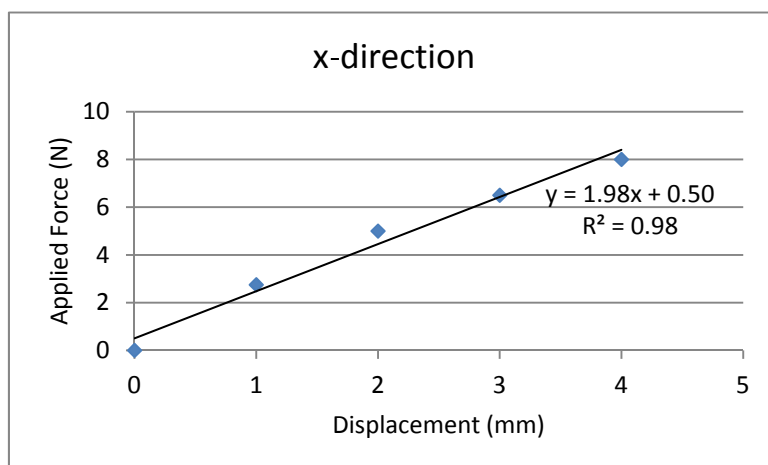
b)
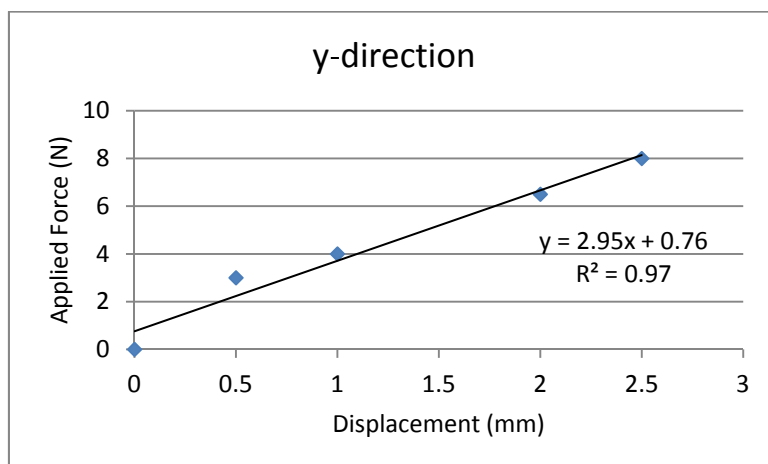
c)

Figure 6-21: Stiffness measurements on the proximal extremity of the tool shaft, along *x* and *y*

6.5.2 Mechanical Transparency

The mechanical transparency is related with the capacity of a system to appear mechanically invisible to the operator, not exerting any external forces on the user when used on the free space. Therefore, in order to access the transparent behavior of the system, different pairs of forces were applied on the system. For each direction, a force was applied one on the handle and an opposite force was on the tool end-effector, while both values were measured by the two force sensors (sensor 1 and sensor 2), **Figure 6-22**.
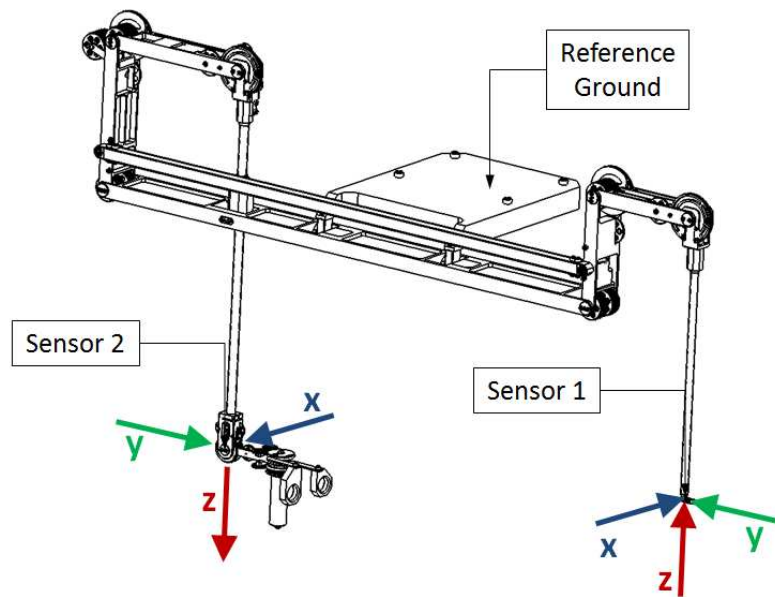
Figure 6-22: Test set-up for mechanical transparency assessment

The relationship between the two forces at the end-effector is shown in Figure 6-23, where the scaling factor was already considered. As can be seen, there is a significant matching for all the x, y and z directions.
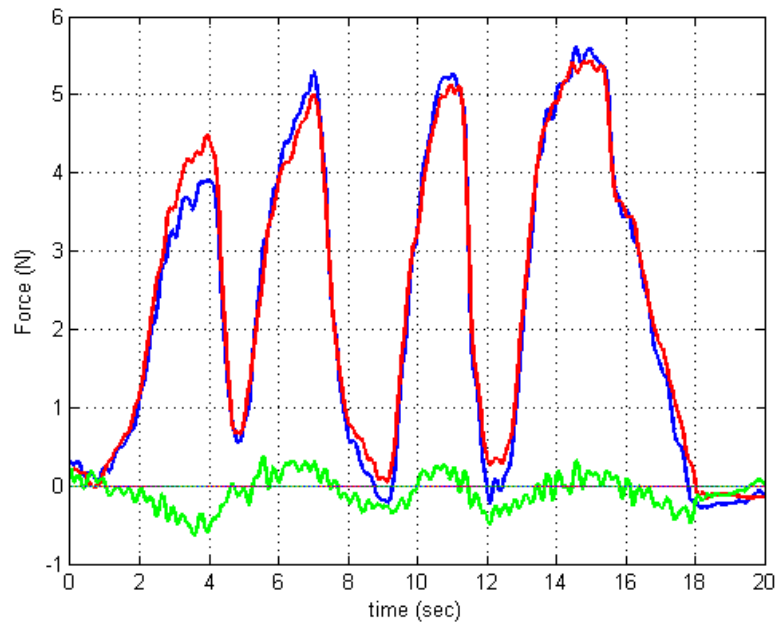
a)
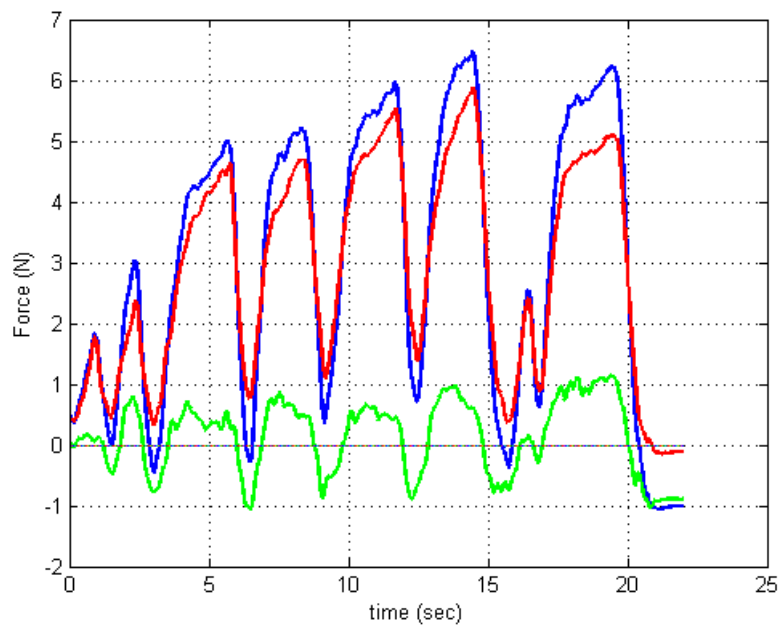
b)
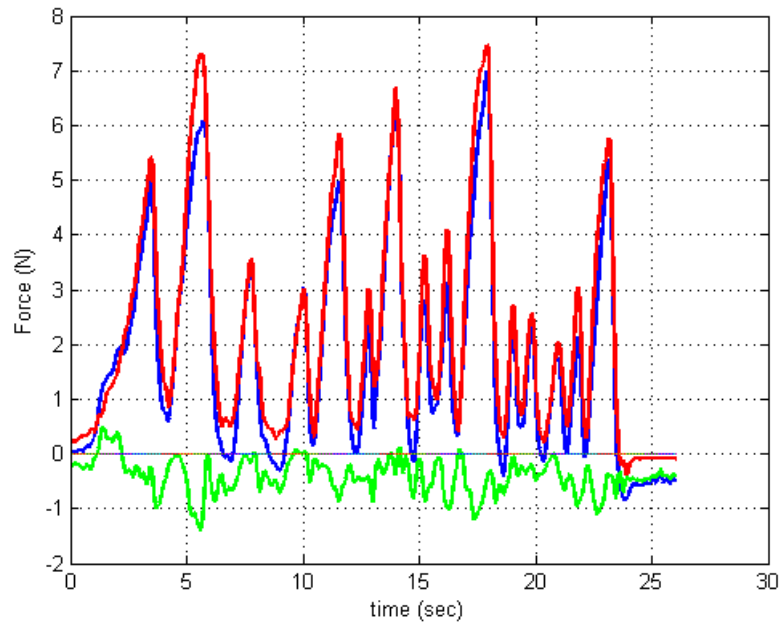
c)

Figure 6-23: Measurements of system's mechanical transparency, along x, y and z

6.6 Full Surgical Platform Overview

A general view of the full Surgical Platform, using the Mechanical Telemanipulator presented on this chapter is shown in Figure 6-24. It will be able to improve the ergonomy for surgeons, enabling them to position their hands in a natural orientation to each other, providing improved eye-hand coordination and intuitive manipulation with non-inversed movements. The comfort of the surgeons is also improved by elbows support.
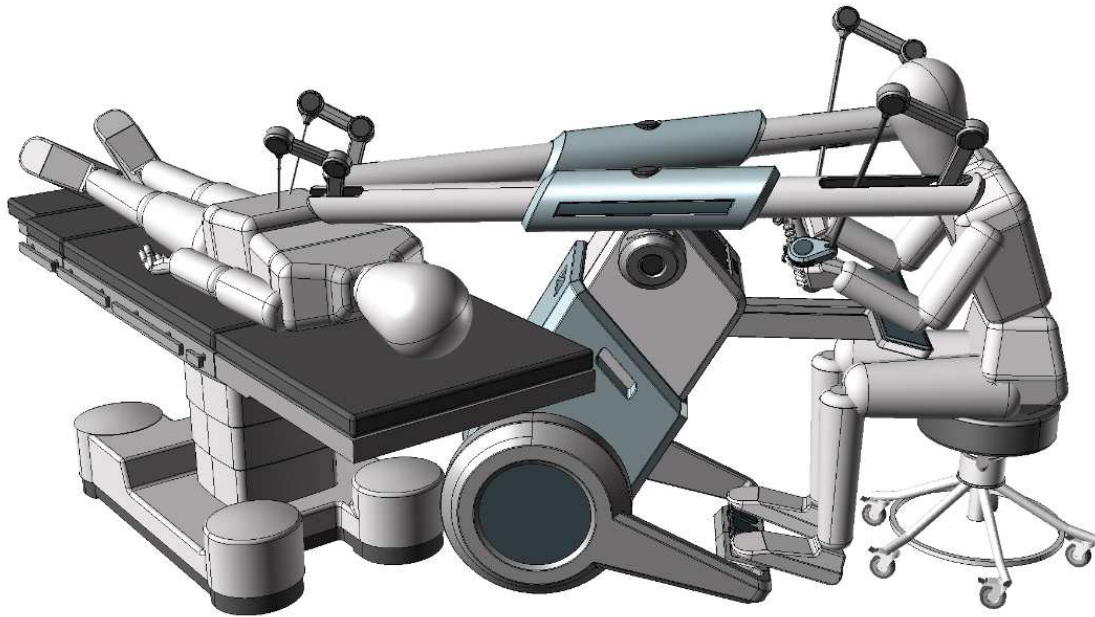
Figure 6-24: Surgical Platform, integrated in the operating environment

This Surgical Platform includes two identical mechanical telemanipulators, T_1 and T_2, configured to be operated independently from the other, providing a bi-manual manipulation (Figure 6-25).
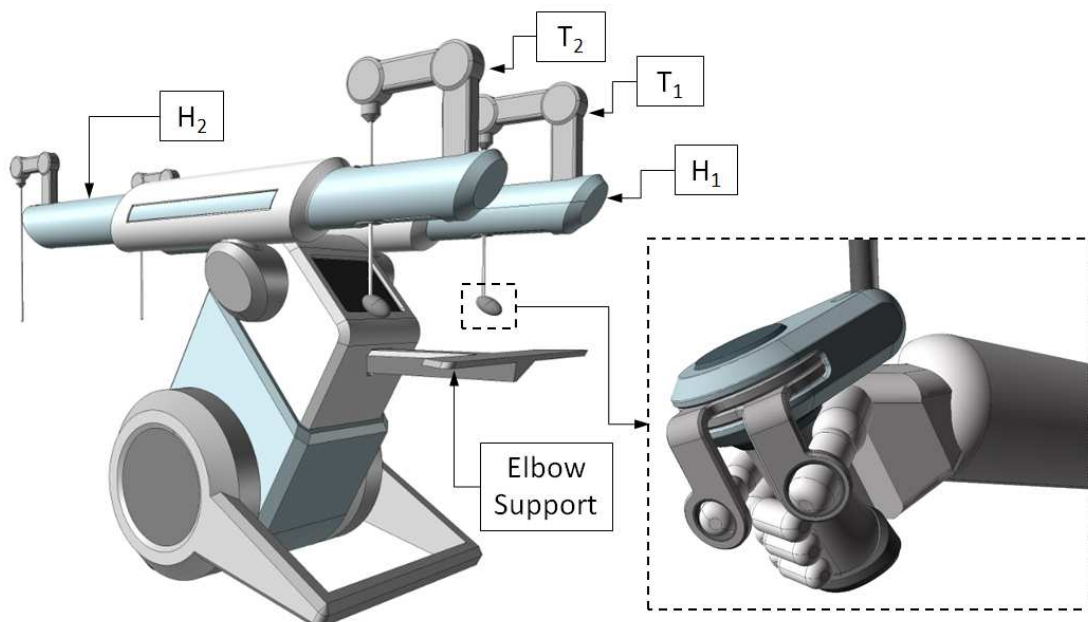
Figure 6-25: Perspective view of the full Surgical Platform

Being comfortably seated at the surgical platform, the surgeon will be able to have not only a direct view to the patient, but also a magnified view of the distal instrument inside the body on a 2D or 3D display monitor, Figure 6-26.
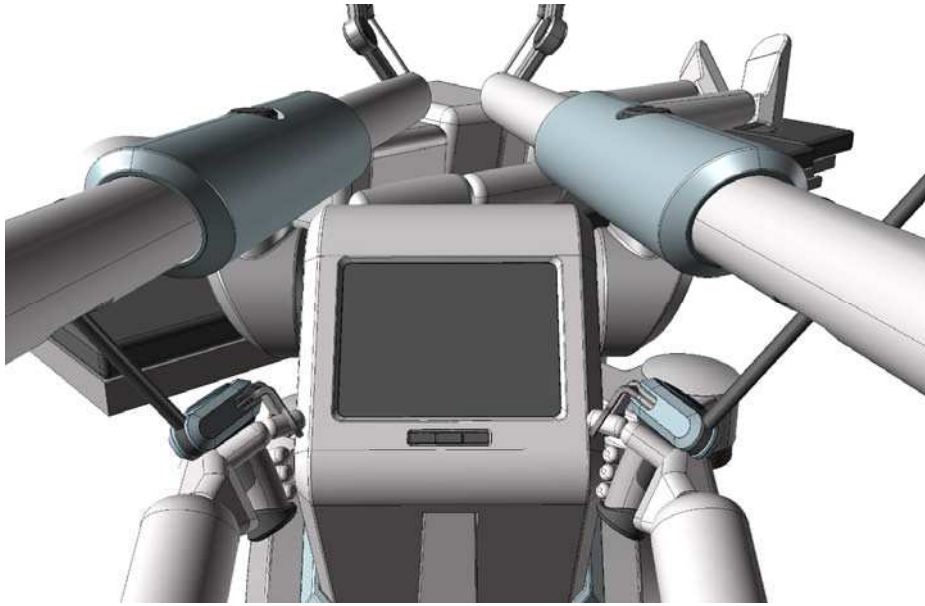
Figure 6-26: Surgeon perspective when manipulating the Surgical Platform

In order to accurately position the incision points (RCMs) and the two multi-articulated surgical tools in the vicinity of the abdominal cavity of the patient, the two telemanipulators are mounted on an articulated structure that enables the position of both systems to be independently adjusted in a total of 7DOF, Figure 6-27.
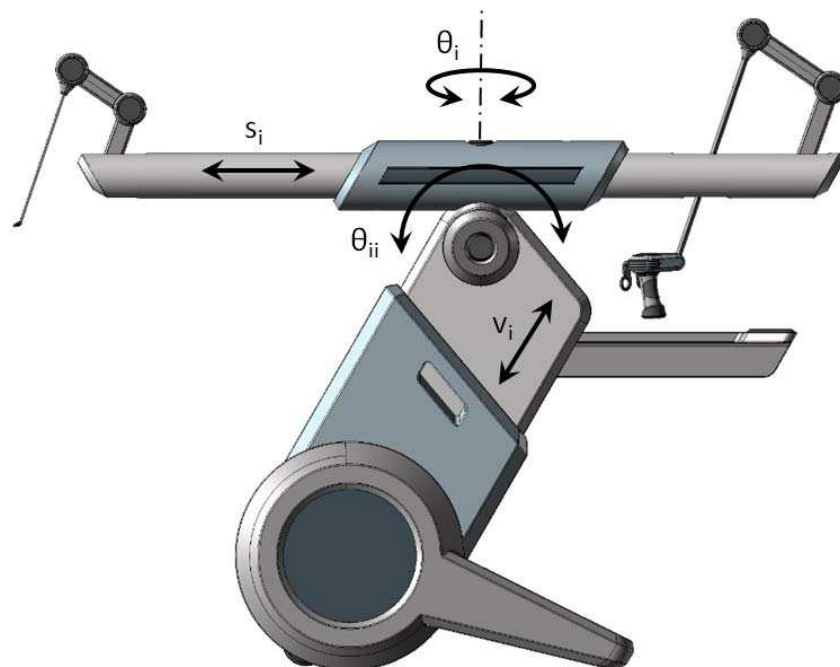
Figure 6-27: Adjustment means of the Surgical Platform for accurately positioning two distal tools in relation to the location of incision points realized on a patient

The two telemanipulators may also be are further rotatable about the moving base such that they can be inclined to a nearly vertical position, enabling the surgical platform to be easily transported and compactly stored within the operating room.
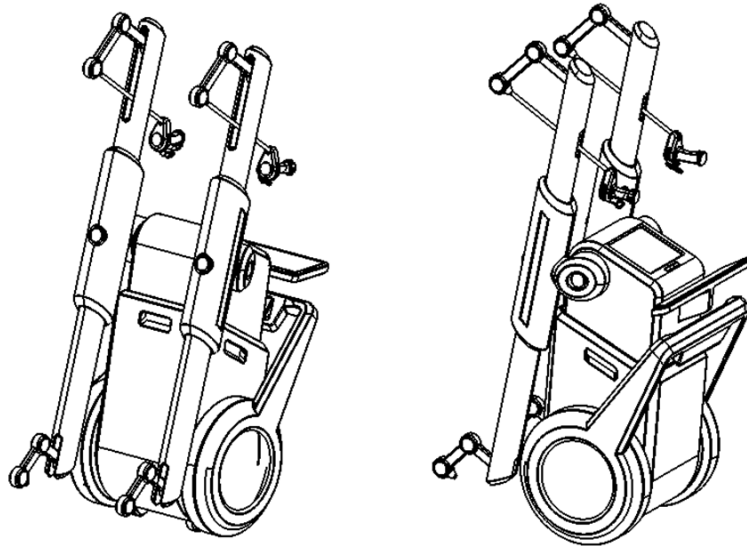
Figure 6-28: Front and back views of the Surgical Platform in a configuration to be easily transported and compactly stored within the operating room

6.7 Conclusions

In this chapter, a study of mechanical systems for MIS telemanipulators has been performed. From this work, an entirely novel concept for a mechanical telemanipulator system was developed. This system is able to deliver dexterous manipulations to remote and narrow places, like the human abdominal cavity. Its design and performance specifications were driven by surgical tasks requirements and its use on a surgical platform can contribute to increase the cost-effectiveness of minimally invasive surgical procedures, while providing better clinical outcomes to patients and reducing the overall cost to health care systems.

The mechanical system uses a technology able to actuate highly dexterous manipulators with complex kinematics while being able to deliver precision and high forces to remote and narrow places. Mechanical transmission means were developed to allow a perfect kinematic matching between the corresponding joints of a slave and a master manipulator. This master-slave relationship allows the movement of any of the joints of master manipulator to be transmitted to the analogous joint of a slave manipulator. Due to its kinematic design, the system allows two times seven degrees of freedom to the surgical instruments, providing great dexterity and intuitive manipulation to the surgeon. Thanks to a remote-center-of-motion, the surgical instrument can be controlled by the master manipulator, while respecting the constraints imposed by the incision point, reducing trauma to the patient and improving cosmetic outcomes.

The low inertia of the links of the master and slave units and the low-friction of the mechanical transmission means provide backlash and ripple-free movements, which gives to the surgeon a realistic feeling of the forces at the distal instruments.

The mechanical nature of the system simplifies not only sterilization, but also certification, legal and intellectual property issues as compared to robotic telemanipulators.

A financial case study was performed at the *Centre Hospitalier Universitaire Vaudois* (CHUV) in order to assess the financial advantages that this surgical platform could provide to the hospital. The study concluded that, by using this surgical platform for Prostatectomies, the CHUV could not only provide less invasive surgeries to their patients but also could achieve annual cost reductions up to 145'000 CHF, compared to Open Surgery and 576'000 CHF compared to Robotic Surgery. Moreover, by offering a more advantageous solution to their patients, the CHUV could also expect to increase their annual number of patients by 50-60%, which would also have a positive effect on the revenues of the hospital.

7 Conclusions

7.1 Introduction

A major progress in abdominal surgery has occurred during the last decades with the introduction of laparoscopic and minimally invasive techniques. These innovative procedures focused much attention due to several advantages: smaller abdominal incisions needed, resulting in faster recovery of the patient, improved cosmetics, and shorter stay in the hospital. However, surgical equipment for this kind of operations remains highly non-ergonomic for the surgeon and much more difficult to use than tools for open surgery. As a consequence, these minimally invasive techniques have only been used in fairly simple procedures, while the most complex case are still being performed through open approaches.

Nowadays, due to the landscape of medical reimbursement, there is a substantial push by insurance companies, health care organizations and hospitals to extend MIS to a wider range of surgical procedures in order to reduce hospital stays and therefore costs. In order to respond to these demands and technical challenges, medical device companies and research institutions have been working over the past years to develop improved minimally invasive technologies for MIS, mainly through the design of robotic systems. Robotic approaches significantly contribute to the improvement of the surgical performance by increasing the dexterity and user-friendliness of surgical manipulation through the use of robotic telemanipulators. However, despite years of research and the despite high potential of some systems, the field of surgical robotics is still only at the beginning of a very promising large scale development. Although a large number of robotic manipulators have been developed, some issues are not yet addressed, limiting a broader adoption of robotic systems by the majority of the hospitals. In this way, five major limitations can be indentified:

1. Surgical instruments should be provided with additional distal degrees of freedom to increase their internal dexterity and facilitate the execution of precise surgical tasks inside the abdominal cavity;
2. The surgical platforms should be more compact, enabling the patient to be easily reached if something goes wrong, being easily moved within the operating room;
3. Force feedback should be provided to surgeons, restoring theirs sense of touch to improve safety and speeding-up the surgical procedure;
4. The time required for set-up of surgical systems should be reduced;
5. The costs of acquisition, maintenance, disposable tools and training should be reduced.

While the nature of the three first limitations is essentially technical, the two last points are mainly concerned with economic aspects. Although bringing several technical advantages for surgeons, current robotic surgical systems are extremely expensive in acquisition, maintenance, disposable tools and training, representing much higher direct costs compared with open surgery and laparoscopic instrumentation. For this reason, access to Robotic

Surgery is limited to a minority of hospitals that can afford to purchase it and have enough patient volume to justify the acquisition. This tendency towards centralisation of complex minimally invasive surgeries draws patients from hospitals without surgical robots and places a significant burden on the health care system. In addition, these systems require a considerable amount of operating room time for the setting-up of the procedures, which, due to the presence of costly personnel and equipment, increases considerably the overall procedure costs.

Although, the solutions studied on this thesis have been applied in the context of surgical systems for MIS, the outcome of this research can be extended to several other application fields. From a general perspective, the ultimate goal of this thesis was to propose a document which may be useful and inspiring for machine designers, developers, or scientists who wish to create efficient and adapted remotely controlled manipulators for several applications involving multi-DOF manipulations.

In the frame of this work, two journal papers have been published and four patent applications filed, covering the systems studied in this thesis. A new start-up company, *DistalMotion Sàrl*, has also been created to further develop and commercialize a novel surgical device using the mechanical systems developed on this thesis.

7.2 Contributions and Originality

The research work developed in this thesis was motivated by the study of new mechanical systems to be used in different surgical telemanipulators, solving the limitations of existing robotic and manual surgical equipment. These objectives implied not only an investigation of technical aspects such as the performance requirements of surgical tools, but also the investigation of the different medical procedures and surgical tasks used by doctors during minimally invasive operations. The main contributions can be grouped into three categories: (1) positioning systems for surgical instruments, (2) dexterous endoscopic micro-manipulators and (3) mechanical telemanipulators for the remote manipulation of surgical tools for minimally invasive procedures.

7.2.1 Positioning Systems for MIS

A main contribution of this thesis was the development of a new mechanical system that can be applied in different external positioning robotic manipulators for minimally invasive surgical instruments. The proposed system provides enough dexterity to position MIS instruments at any location within the abdominal cavity, while respecting the mobility constraints imposed by the entry port. The implementation of a unique parallel kinematics results in a 4-DOF hybrid mechanism that provides three rotations and one translation, with a fixed remote center of motion. A significant advantage of this novel design is related to its compactness and light weight. It can be placed close to the operation table, allowing direct access to the patient without removing the manipulator. Consequently, safety is improved and

considerable space in the operating room is saved. This is a key advantage of the proposed design in comparison to existing solutions.

7.2.2 Dexterous Micro-manipulators for MIS

The second contribution of this thesis consists in the study of mechanical systems for MIS micro-manipulators. The development of multi-DOF robotic micro manipulators capable of reproducing complex human hand movements in minimally invasive procedures is one of the most important issues in the field of robotic systems for surgery. On one hand, it is important to increase the dexterity of the end-effectors inside the body, overcoming the issues of limited dexterity of conventional MIS tools in the abdominal cavity. On the other hand, the design should be kept as compact as possible. The final goal is to manage this trade-off, providing the surgeon with user-friendly aids, while keeping the procedure minimally invasive for the patient.

From this thesis' work, a new mechanical system was developed, being able to deliver multi-DOF complex kinematics to remote and narrow places, like the human abdominal cavity. The concept is based on the use of a cable driven transmission for miniature robot manipulators, with different types of revolute joints, making it possible to achieve high levels of dexterity and stiffness compared with existing solutions.

This system was integrated in the design of a new surgical platform for minimally invasive surgery, with requirements in terms of size, dexterity, force and precision, beyond the existing state of the art.

7.2.3 Mechanical Telemanipulators for MIS

The third contribution of this thesis is the development of a new fully mechanical telemanipulator system that is able to deliver dexterous manipulations to remote and narrow places, like the human abdominal cavity. By using a fully mechanical technology, this system is considerably more affordable to produce than existing robotic systems, being also more reliable, easier to sterilize and faster to set-up. The basic system is purely mechanical, highly simplifying not only sterilization, but also certification, legal and intellectual property issues as compared to a robotic system. As a consequence, it can significantly contribute to increase the cost-effectiveness of minimally invasive surgical procedures, while providing better clinical outcomes to patients and reducing the overall costs to health care systems.

In addition, the low inertia of its moving elements and the low-friction of its mechanical transmission are able to provide backlash and ripple-free movements, with natural force-feedback and motion scaling, which gives to the surgeon a realistic rendering of the forces at the distal instruments.

Although in the framework of this thesis this mechanical system has been designed for minimally invasive surgical procedures on the abdominal cavity, it may also be used for other

fields of surgery, like ophthalmology, brain surgery, orthopedics and dentistry, or outside the medical field.

7.3 Outlook

In recent years, the development of new medical devices has become an increasingly complex process. The advent of new technology concepts, complex regulatory requirements, and the ever increasing importance of reimbursement constraints require careful research and development planning.

While this thesis has proposed new mechanical systems to be used in different surgical devices, validated by the production of several working prototypes, the main challenge now lies in bringing these solutions from this thesis to the patient. Whereas research prototypes focus on providing the general feasibility concept, the immediate goal consists in developing a series of progressively advanced working models until all critical user requirements and core technical specifications have been met. Along the way, clinical studies have to be done to confirm that a product can be safely and effectively used in humans. The entire process will be lengthy and complicated. It will bring together broad engineering skills, surgeons from various specialties and legal, certification, marketing and financial experts. This is the subject of ongoing work by a newly created start-up company, DistalMotion (www.distalmotion.com).

Bibliography

Abbott DJ, Becke C, Rothstein RI, Peine WJ (2007) Design of an endoluminal NOTES robotic system. pp 410-416: IEEE.

Adhami L, Coste-Manière È (2003) Optimal planning for minimally invasive surgical robots. Robotics and Automation, IEEE Transactions on 19:854-863.

Arata J, Mitsuishi M, Warisawa S, Tanaka K, Yoshizawa T, Hashizume M (2005) Development of a dexterous minimally-invasive surgical system with augmented force feedback capability. pp 3207-3212: IEEE.

Bailey RW, Zucker KA, Flowers JL, Scovill WA, Graham SM, Imbembo AL (1991) Laparoscopic cholecystectomy. Experience with 375 consecutive patients. Annals of surgery 214:531.

Barbosa MVJ, Nahas FX, Ferreira LM (2008) A practical dressing to the umbilical stalk. Journal of Plastic, Reconstructive & Aesthetic Surgery 61:851-852.

Baumann R (1997) Haptic interface for virtual reality based laparoscopic surgery training environment. Unpublished doctoral dissertation 1734:43.

Beira R, Santos-Carreras L, Rognini G, Bleuler H, Clavel R (2011a) Dionis: A novel remote-center-of-motion parallel manipulator for Minimally Invasive Surgery. Applied Bionics and Biomechanics 8:191-208.

Beira R, Santos-Carreras L, Sengul A, Samur E, Clavel R, Bleuler H (2011b) An External Positioning Mechanism for Robotic Surgery. Journal of System Design and Dynamics 5:1094-1105.

Bejczy AK, Salisbury Jr J (1983) Controlling remote manipulators through kinesthetic coupling. COMP MECH ENG 2:48-58.

Berguer R (1998) Surgical technology and the ergonomics of laparoscopic instruments. Surgical endoscopy 12:458-462.

Berguer R (1999) Surgery and ergonomics. Archives of surgery 134:1011.

BRIAN AG, MARCUS GP (1999) A kinematic model of the upper limb based on the visible human project (vhp) image dataset. Computer methods in biomechanics and biomedical engineering 2:107-124.

Burdea G, Burdea C (1996) Force and touch feedback for virtual reality: John Wiley & Sons New York NY.

Burgner J, Swaney P, Rucker D, Gilbert H, Nill S, Russell P, Weaver K, Webster R (2011) A bimanual teleoperated system for endonasal skull base surgery. pp 2517-2523: IEEE.

Camberlin C, Senn A, Leys M, De Laet C (2009) Robot-assisted surgery: health technology assessment. Health Services Research (HSR).

Canes D, Desai MM, Aron M, Haber GP, Goel RK, Stein RJ, Kaouk JH, Gill IS (2008) Transumbilical single-port surgery: evolution and current status. european urology 54:1020-1030.

CARRERAS LS (2012) Increasing Haptic Fidelity and Ergonomics in Teleoperated Surgery. ÉCOLE POLYTECHNIQUE FÉDÉRALE DE LAUSANNE.

Cavusoglu MC (2000) Telesurgery and surgical simulation: Design, modeling, and evaluation of haptic interfaces to real and virtual surgical environments: University of California, Berkeley.

Cepolina F, Michelini R (2004) Review of robotic fixtures for minimally invasive surgery. The International Journal of Medical Robotics and Computer Assisted Surgery 1:43-63.

Chamberlain RS, Sakpal SV (2009) A comprehensive review of single-incision laparoscopic surgery (SILS) and natural orifice transluminal endoscopic surgery (NOTES) techniques for cholecystectomy. Journal of Gastrointestinal Surgery 13:1733-1740.

Clavel R (1988a) DELTA, a fast robot with parallel geometry. pp 91-100.

Clavel R (1988b) DELTA, a fast robot with parallel geometry. In: 18 International Symposium on Industrial Robots, pp 91-100.

Cui J, Tosunoglu S, Roberts R, Moore C, Repperger DW (2003) A review of teleoperation system control. In: Proceedings Florida Conference on Recent Advances in Robotics, FCRAR.

Curcillo 2nd P, King S, Podolsky E, Rottman S (2009) Single Port Access (SPA™) Minimal Access Surgery Through a Single Incision. Surgical technology international 18:19.

Dasgupta B, Mruthyunjaya T (1998) Force redundancy in parallel manipulators: theoretical and practical issues. Mechanism and Machine Theory 33:727-742.

Davies BL (1995) 19 A Discussion of Safety Issues for Medical Robots. Computer-integrated surgery: technology and clinical applications 287.

de Sousa LH, de Sousa JAG, de Sousa Filho LH, de Sousa MM, de Sousa VM, de Sousa APM, Zorron R (2009) Totally NOTES (T-NOTES) transvaginal cholecystectomy using two endoscopes: preliminary report. Surgical endoscopy 23:2550-2555.

Delaney CP, Pokala N, Senagore AJ, Casillas S, Kiran RP, Brady KM, Fazio VW (2005) Is laparoscopic colectomy applicable to patients with body mass index> 30? A case-matched comparative study with open colectomy. Diseases of the colon & rectum 48:975-981.

Dini GM, Ferreira LM (2007) A simple technique to correct umbilicus vertical malposition. Plastic and reconstructive surgery 119:1973-1974.

Dombre E, Michelin M, Pierrot F, Poignet P, Bidaud P, Morel G, Ortmaier T, Sallé D, Zemiti N, Gravez P (2004) MARGE Project: design, modeling and control of assistive devices for minimally invasive surgery. Medical Image Computing and Computer-Assisted Intervention–MICCAI 2004 1-8.

Faust RA, Kant AJ, Lorincz A, Younes A, Dawe E, Klein MD (2007) Robotic endoscopic surgery in a porcine model of the infant neck. Journal of Robotic Surgery 1:75-83.

Fei B, Ng WS, Chauhan S, Kwoh CK (2001) The safety issues of medical robotics. Reliability Engineering & System Safety 73:183-192.

Filipović Čugura J, Kirac I, Kuliš T, Janković J, Bekavac Bešlin M (2008) First case of single incision laparoscopic surgery for totally extraperitoneal inguinal hernia repair. Acta Clinica Croatica 47:249-252.

Gettman MT, Box G, Averch T, Cadeddu JA, Cherullo E, Clayman RV, Desai M, Frank I, Gill I, Gupta M (2008) Consensus statement on natural orifice transluminal endoscopic surgery and single-incision laparoscopic surgery: heralding a new era in urology? european urology 53:1117.

Ghafoor A, Dai JS, Duffy J (2000) Fine motion control based on constraint criteria under pre-loading configurations. Journal of Robotic Systems 17:171-185.

Ghodoussi M, Butner SE, Wang Y (2002) Robotic surgery-the transatlantic case. vol. 2, pp 1882-1888: IEEE.

Goertz RC (1952) Fundamentals of general-purpose remote manipulators. Nucleonics 10:36-42.

Goertz RC, Thompson WM (1954) Electronically controlled manipulator. Nucleonics (US) Ceased publication 12.

Gosselin C, Angeles J (1990) Singularity analysis of closed-loop kinematic chains. Robotics and Automation, IEEE Transactions on 6:281-290.

Green P, Piantanida T, Hill J, Simon I, Satava R (1991) Telepresence: dexterous procedures in a virtual operating field. Am Surg 57:192.

Guo W, Zhang Z, Han W, Li J, Jin L, Liu J, Zhao X, Wang Y (2008) Transumbilical single-port laparoscopic cholecystectomy: a case report. Chinese Medical Journal (English Edition) 121:2463.

Guthart GS, Salisbury Jr JK (2000) The Intuitive< sup> TM</sup> telesurgery system: overview and application. vol. 1, pp 618-621: IEEE.

Hagen ME, Wagner OJ, Thompson K, Jacobsen G, Spivack A, Wong B, Talamini M, Horgan S (2010) Supra-pubic single incision cholecystectomy. Journal of Gastrointestinal Surgery 14:404-407.

Hagn U, Konietschke R, Tobergte A, Nickl M, Jörg S, Kübler B, Passig G, Gröger M, Fröhlich F, Seibold U (2010) DLR MiroSurge: a versatile system for research in endoscopic telesurgery. International journal of computer assisted radiology and surgery 5:183-193.

Hong TH, You YK, Lee KH (2009) Transumbilical single-port laparoscopic cholecystectomy. Surgical endoscopy 23:1393-1397.

Hunter IW, Hollerbach JM, Ballantyne J (1991) A comparative analysis of actuator technologies for robotics. Robotics Review 2.

Ikuta K, Sasaki K, Yamamoto K, Shimada T (2002) Remote microsurgery system for deep and narrow space-development of new surgical procedure and micro-robotic tool. Medical Image Computing and Computer-Assisted Intervention—MICCAI 2002 163-172.

Jacobs M, Verdeja J, Goldstein H (1991) Minimally invasive colon resection (laparoscopic colectomy). Surgical laparoscopy & endoscopy 1:144.

Kaouk JH, Haber GP, Goel RK, Desai MM, Aron M, Rackley RR, Moore C, Gill IS (2008) Single-port laparoscopic surgery in urology: initial experience. Urology 71:3-6.

Kaya OI, Moran M, Ozkardes AB, Taskin EY, Seker GE, Ozmen MM (2008) Ergonomic problems encountered by the surgical team during video endoscopic surgery. Surgical Laparoscopy Endoscopy & Percutaneous Techniques 18:40-44.

Kübler B, Seibold U, Hirzinger G (2005) Development of actuated and sensor integrated forceps for minimally invasive robotic surger. The International Journal of Medical Robotics and Computer Assisted Surgery 1:96-107.

Lum MJH, Friedman DCW, Sankaranarayanan G, King H, Fodero K, Leuschke R, Hannaford B, Rosen J, Sinanan MN (2009) The raven: Design and validation of a telesurgery system. The International Journal of Robotics Research 28:1183-1197.

Lum MJH, Rosen J, Sinanan MN, Hannaford B (2004) Kinematic optimization of a spherical mechanism for a minimally invasive surgical robot. vol. 1, pp 829-834: IEEE.

Madhani AJ, Niemeyer G, Salisbury Jr JK (1998) The black falcon: a teleoperated surgical instrument for minimally invasive surgery. vol. 2, pp 936-944: IEEE.

Millman P, Stanley M, Colgate JE (1993) Design of a high performance haptic interface to virtual environments. pp 216-222: IEEE.

Minor M, Mukherjee R (1999) A dexterous manipulator for minimally invasive surgery. vol. 3, pp 2057-2064: IEEE.

Montz F, Holschneider C, Munro M (1994) Incisional hernia following laparoscopy: a survey of the American Association of Gynecologic Laparoscopists. The Journal of the American Association of Gynecologic Laparoscopists 1:S23.

Moorthy K, Munz Y, Dosis A, Hernandez J, Martin S, Bello F, Rockall T, Darzi A (2004) Dexterity enhancement with robotic surgery. Surgical endoscopy 18:790-795.

Morrey B, An K (1998) Biomechanics of the shoulder. The shoulder 1:208-245.

140

Ortmaier T, Weiss H, Falk V (2004) Design requirements for a new robot for minimally invasive surgery. Industrial Robot: An International Journal 31:493-498.

Perissat J, Collet D, Belliard R, Desplantez J, Magne E (1992) Laparoscopic cholecystectomy: the state of the art. A report on 700 consecutive cases. World journal of surgery 16:1074-1082.

Phee S, Low S, Sun Z, Ho K, Huang W, Thant Z (2008) Robotic system for no-scar gastrointestinal surgery. The International Journal of Medical Robotics and Computer Assisted Surgery 4:15-22.

Piccigallo M, Scarfogliero U, Quaglia C, Petroni G, Valdastri P, Menciassi A, Dario P (2010) Design of a novel bimanual robotic system for single-port laparoscopy. Mechatronics, IEEE/ASME Transactions on 15:871-878.

Rao PP, Bhagwat SM, Rane A (2008) The feasibility of single port laparoscopic cholecystectomy: a pilot study of 20 cases. HPB 10:336-340.

Rininsland H (1999) ARTEMIS. A telemanipulator for cardiac surgery. European Journal of Cardio-Thoracic Surgery 16:S106-S111.

Rosen J, Hannaford B, Satava RM (2010) Surgical Robotics: Systems Applications and Visions: Springer.

Sackier JM, Wang Y (1994) Robotically assisted laparoscopic surgery. Surgical endoscopy 8:63-66.

Salle D, Bidaud P, Morel G (2004) Optimal design of high dexterity modular MIS instrument for coronary artery bypass grafting. vol. 2, pp 1276-1281: IEEE.

Schenker P, Das H, Ohm T (1995) A new robot for high dexterity microsurgery. pp 115-122: Springer.

Schneider O, Troccaz J (2001) A six-degree-of-freedom passive arm with dynamic constraints (PADyC) for cardiac surgery application: Preliminary experiments. Computer aided surgery 6:340-351.

Schurr M, Breitwieser H, Melzer A, Kunert W, Schmitt M, Voges U, Buess G (1996) Experimental telemanipulation in endoscopic surgery. Surgical Laparoscopy and Endoscopy 6:167-175.

Seibold U, Kubler B, Hirzinger G (2005) Prototype of instrument for minimally invasive surgery with 6-axis force sensing capability. pp 496-501: IEEE.

Song H, Kim K, Lee J (2009) Development of the dexterous manipulator and the force sensor for Minimally Invasive Surgery. pp 524-528: IEEE.

Stylopoulos N, Rattner D (2003) Robotics and ergonomics. The Surgical clinics of North America 83:1321.

Sung GT, Gill IS (2001) Robotic laparoscopic surgery: a comparison of the DA Vinci and Zeus systems. Urology 58:893.

Sutherland GR, McBeth PB, Louw DF (2003) NeuroArm: an MR compatible robot for microsurgery. vol. 1256, pp 504-508: Elsevier.

Takahashi H, Warisawa S, Mitsuishi M, Arata J, Hashizume M (2006) Development of high dexterity minimally invasive surgical system with augmented force feedback capability. pp 284-289: IEEE.

Taylor G, Jayne D (2007) Robotic applications in abdominal surgery: their limitations and future developments. The International Journal of Medical Robotics and Computer Assisted Surgery 3:3-9.

Taylor RH, Funda J, Grossman DD, Karidis JP, Larose DA (1997) Improved remote center-of-motion robot for surgery. EP Patent 0,595,291.

Townsend WT (1988) The effect of transmission design on force-controlled manipulator performance.

Tsai LW (1999) Robot analysis: the mechanics of serial and parallel manipulators: Wiley-Interscience.

van den Bedem L (2010) Realization of a demonstrator slave for robotic minimally invasive surgery. PhD thesis, Technische Universiteit Eindhoven, 2010, ISBN 9789038623009.

Wang J, Gosselin CM (2004) Kinematic analysis and design of kinematically redundant parallel mechanisms. Journal of mechanical design 126:109-118.

Williams LF, Chapman WC, Bonau RA, McGee EC, Boyd RW, Jacobs JK (1993) Comparison of laparoscopic cholecystectomy with open cholecystectomy in a single center. The American journal of surgery 165:459-465.

Xu K, Goldman RE, Ding J, Allen PK, Fowler DL, Simaan N (2009) System design of an insertable robotic effector platform for single port access (spa) surgery. pp 5546-5552: IEEE.

Xu K, Simaan N (2008) An investigation of the intrinsic force sensing capabilities of continuum robots. Robotics, IEEE Transactions on 24:576-587.

Yagi A, Matsumiya K, Masamune K, Liao H, Dohi T (2006) Rigid-flexible outer sheath model using slider linkage locking mechanism and air pressure for endoscopic surgery. Medical Image Computing and Computer-Assisted Intervention–MICCAI 2006 503-510.

Zemiti N, Ortmaier T, Morel G (2004) A new robot for force control in minimally invasive surgery. vol. 4, pp 3643-3648: IEEE.

Zlatanov D, Fenton R, Benhabib B (1998) Identification and classification of the singular configurations of mechanisms. Mechanism and Machine Theory 33:743-760.

Zorrón R, Filgueiras M, Maggioni LC, Pombo L, Carvalho GL, Oliveira AL (2007) NOTES transvaginal cholecystectomy: report of the first case. Surgical Innovation 14:279-283.

List of Figures

144

146

148

List of Tables